Stony Brook University

Elucidation of RNase R Mediated Nonstop mRNA Decay on Stalled Ribosomes

A Dissertation Presented

by

Krithika Venkataraman

to

The Graduate School

in Partial Fulfillment of the

Requirements

for the Degree of

Doctor of Philosophy

in

Molecular and Cellular Biology

(Biochemistry and Molecular Biology)

Stony Brook University

May 2014

Stony Brook University

The Graduate School

Krithika Venkataraman

We, the dissertation committee for the above candidate for the

Doctor of Philosophy degree, hereby recommend

acceptance of this dissertation.

A. Wali Karzai – Dissertation Advisor
Associate Professor, Department of Biochemistry and Cell Biology

Miguel Garcia-Diaz - Chairperson of Defense
Associate Professor, Department of Pharmacological Sciences

Rolf Sternglanz
Distinguished Professor Emeritus, Department of Biochemistry and Cell Biology

Jingfang Ju
Associate Professor, Department of Pathology

James B. Bliska
Professor, Department of Molecular Genetics and Microbiology

This dissertation is accepted by the Graduate School

Charles Taber
Dean of the Graduate School

Abstract of the Dissertation

Elucidation of RNase R Mediated Nonstop mRNA Decay on Stalled Ribosomes

by

Krithika Venkataraman

Doctor of Philosophy

in

Molecular and Cellular Biology

(Biochemistry and Molecular Biology)

Stony Brook University

2014

Ribosomes are macromolecular machines that catalyze the fundamental process of protein synthesis in the cell. Proper proceeding of the translation process is essential for the fitness and survival of all cells. However, stalling of ribosomes occurs on aberrant mRNA transcripts that lack the necessary information for proper decoding. Persistence of such defective mRNAs leads to futile cycles of translation and sequestration of the ribosomal machinery. Bacteria have evolved a versatile translation quality control mechanism termed *trans*-translation. A chimeric transfer-messenger RNA (tmRNA) and its essential protein co-factor Small protein B (SmpB) are the pivotal components of this major ribosome-rescue system. As a result of the action of SmpB-tmRNA complex, stalled ribosomes undergo proper translation termination, thereby allowing recycling of the ribosomal subunits. A special hallmark of this system is the recruitment of a 3′ – 5′ exoribonuclease, RNase R, to degrade the defective mRNA on stalled ribosomes. Previous studies have shown that the distinctive C-terminal lysine-rich (K-rich) domain of RNase R is essential for defective mRNA degradation. In this thesis project, I investigated the necessary elements of the *trans*-translation system that are required for facilitating RNase R mediated nonstop mRNA decay. I have shown that conserved residues Glu740/Lys741 and Lys749/Lys750 present in the K-rich domain of RNase R are critical for *trans*-translation dependent defective mRNA decay. Through mutational analyses of tmRNA and SmpB, I have found that the decay of defective mRNA initiates after establishment of the tmRNA open reading frame (ORF) as the surrogate template, facilitated in part by the SmpB C-terminal tail. Furthermore, my investigations suggested that the putative contacts made by the ultimate and penultimate codons in the tmRNA ORF with the translation apparatus are necessary to enable RNase R to access the 3′ end of the defective mRNA. Finally, RNA-protein crosslinking and immunoprecipitation analysis revealed that RNase R binds near the mRNA exit-channel on the small ribosomal subunit for optimal capture of the emerging defective mRNA from stalled ribosomes.

Table of Contents

List of Figures and Tables

Acknowledgments

"Mata Pita Guru Deva" – an old Indian saying that translates to Mother, Father, and Teachers/Educators are held at a higher pedestal than God. I have been truly blessed in every aspect of life – for having such a supportive and encouraging family. I am indebted to my parents, Mr. K. Venkataraman and Mrs. V. Jayalakshmi, for inculcating values and principles, especially the importance of education. I thank all my family members, particularly my brother Swaminath and my grandfather Mr. K. Adinarayanan, for guiding me through my life.

I would like to thank my undergraduate advisor, Dr. V. Ponnusami, for showing me the right path, without which this thesis would not have been possible. My graduate school pursuit has been an enriching experience, and Dr. Wali Karzai played a pivotal role in it right from the beginning. I will always be grateful to him for he helped me crystallize from a novice science-lover into a scientist that I am today. He let me explore my passion, both at and outside of the bench. I am particularly thankful to him for being available to discuss science with me, even if it meant staying late in the lab to look at the blots, and going home after dinner time. I thank all past and present members of the Karzai lab for all the science and non-science activities that we did together which has made my graduate school experience a fun ride. Specifically, I'd like to thank Dr. Perry Woo who kept motivating me in every way. Bouncing off ideas and sharing the same level of enthusiasm in doing research helped me enjoy my graduate school, and also get past tough times at the bench without feeling low. I'd like to thank my collaborators Kip Guja, Marek Kudla and Dr. Robert Haltiwanger for assisting me in addressing key research questions, and being available to answer my queries at moment's notice. I must thank my committee members Drs. Garcia-Diaz, Bliska, Sternglanz, and Ju for giving insightful comments and guiding me through to the end of a successful graduate career.

My outside-of-graduate-school experience would not have been joyous if it wasn't for the unconditional support I received from Nikkhil Ramadurai and Kalpana Ramakrishnan. I thank all the friends I made here at Stony Brook, particularly Deepika Vasudevan, who have been with me through thick and thin.

Chapter 1: Introduction

1.1 Translation in bacteria

Protein synthesis is a vital process catalyzed by specialized macromolecular machines, called ribosomes, in all living cells. The bacterial ribosome is comprised of two subunits, the 50S large subunit and the 30S small subunit. A functional 70S ribosomal assembly has three tRNA binding sites for the incoming aminoacyl (A-site), peptidyl (P-site), and exiting (E-site) tRNAs. Normal translation proceeds in three different stages – initiation, elongation, and termination. Each of these stages has to occur with precision in order to ensure high fidelity and accuracy in the process. Canonical translation initiation involves binding of the 30S subunit to the Shine-Dalgarno sequence present near the 5' end of the mRNA template. Initiation factors IF1, IF2, and IF3 coordinate the assembly of the 70S ribosome on the mRNA template, with formyl-methionine initiator tRNA bound to the P-site wherein the start codon AUG is positioned. The next codon, downstream of the start codon, is positioned in the A-site of the 70S complex which is recognized by the incoming aminoacylated tRNAs. The elongation step involves building of the polypeptide chain via decoding of the mRNA template and corresponding extension of the chain by one amino acid. The accuracy of this step is ensured by several factors including EF-Tu, and EF-G. The incoming EF-Tu-GTP-aminoacyl tRNA ternary complex recognizes the complementary codon in the A-site.

Elements in the decoding center of the ribosome, which include the highly conserved A1492, A1493, and G530 residues, aid in the selection of proper incoming aminoacyl-tRNA by detecting the correct base pairing of the mRNA codon and anticodon present in the tRNA. Following the hydrolysis of GTP bound to EF-Tu, the polypeptide chain tethered to the peptidyl-tRNA in the P-site is transferred via a transpeptidation reaction onto the amino acid bound to the incoming A-site tRNA. This critical step is catalyzed at the peptidyl transferase center in the 50S subunit of the

ribosome. Another GTPase, EF-G, facilitates the translocation of the tRNAs and the mRNA. This places the deaminoacylated tRNA in the E-site, peptidyl tRNA in the P-site, and subsequent emptying of the A-site to allow the incoming cognate ternary complex to recognize the next codon. In this manner, the elongation cycle is repeated until the ribosomes reach an in-frame stop codon [1] .

Translation termination is as important an event as translation initiation and elongation. This step signals the end of the coding sequence, permitting the release of the nascent polypeptide and enabling the subsequent disassembly and recycling of the ribosomal subunits for future translation events. Unlike sense codons recognized by the corresponding cognate tRNAs, stop codons are recognized by special protein factors termed Release Factors (RF). RF1 recognizes amber (UAG) and ochre (UAA) codons whereas RF2 recognizes opal (UGA) and ochre (UAA) codons. Stop codon recognition by release factors in the decoding center of the A-site positions the universally conserved GGQ motif, present in both release factors, in the peptidyl transferase center to aid in the hydrolysis of the peptidyl tRNA. This step is critical for the release of the polypeptide chain from the ribosome. Following this step, RF1/2 is released from the ribosome, facilitated in part by GTP binding and hydrolysis on RF3. The departure of RF3 allows the subsequent binding of ribosome recycling factor (RRF) and the EF-G-GTP complex, which results in the disassembly of the 70S ribosome. An overview of bacterial translation process is depicted in Figure 1.1 [2].

There are several scenarios wherein the translation machinery stalls on mRNA transcripts. Such sequestration of the translation components is deleterious to the cell as it severely impacts the protein production capacity, and the fitness of the cell. Therefore, rescue of stalled ribosomes is an important metabolic requirement to steer the complex to undergo proper termination. I will next discuss the details of the various bacterial ribosome rescue pathways.

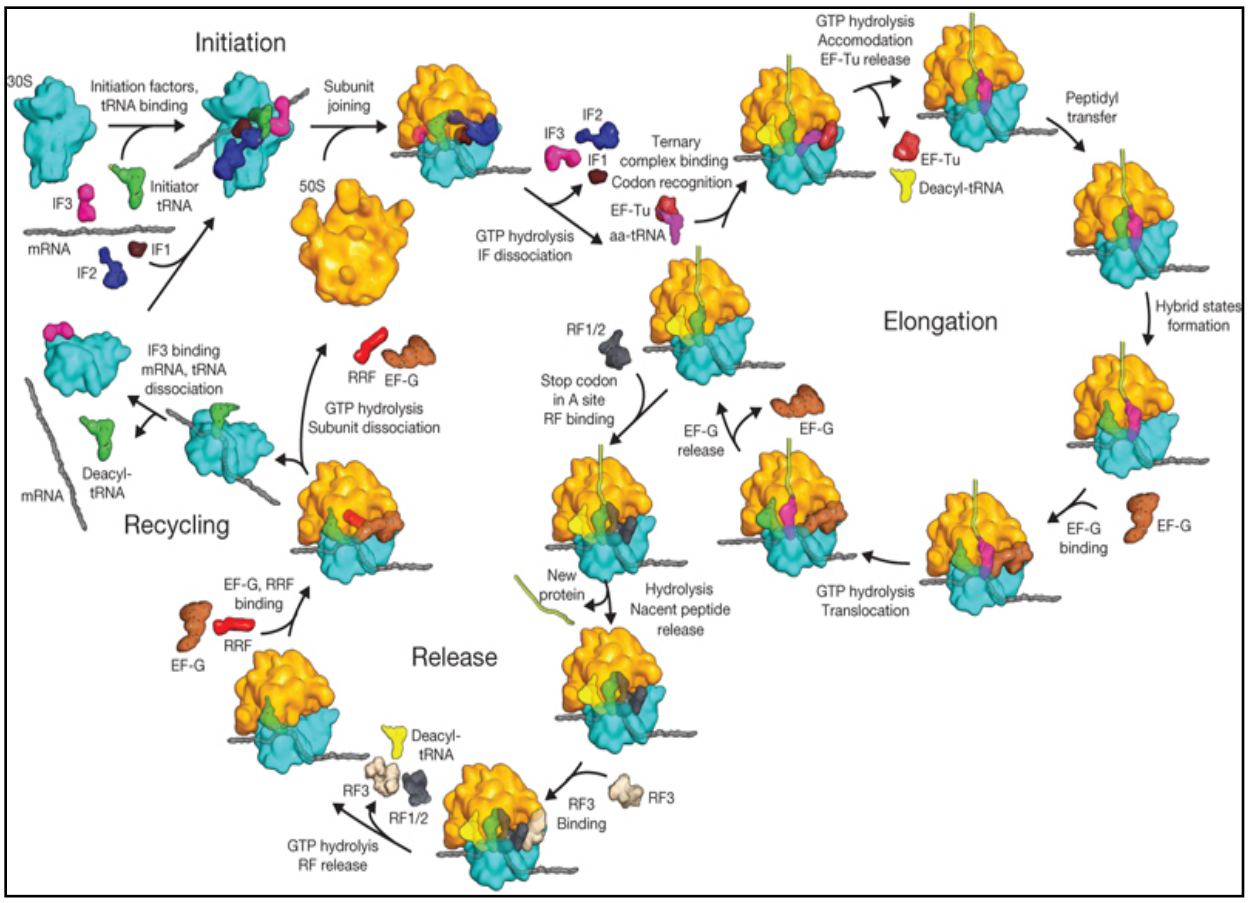

Figure 1.1 Overview of bacterial translation. For simplicity, not all intermediate steps are shown. aa-tRNA, aminoacyl-tRNA; EF elongation factor; IF, initiation factor; RF, release factor. This figure is adapted from TM Schmeing & V Ramakrishnan *Nature* **000**, 1-9 (2009) doi:10.1038/nature08403 [2]

1.2 Translational quality control in bacteria

Translational quality control is crucial to maintain high fidelity in gene expression. Ribosomes are known to pause transiently on translation attenuation sites encoded within transcripts. This is thought to temporally disengage decoding of the transcript and other co-translational events [3]. Discontinuous elongation of the polypeptide chain is hypothesized to assist in the ensuing processes such as proper folding of the emerging

protein domain by chaperones, binding of cofactors, etc. However, prolonged translational arrest often occurs when ribosomes decode mRNA templates that are devoid of necessary signals to proceed to completion. For example, translation of an mRNA containing a string of rare codons results in stalling of ribosomal complex due to limited availability of cognate tRNAs in the cellular pool. This situation is analogous to 'no-go' scenario in eukaryotes [4]. Similarly, mRNAs that lack an in-frame 3' termination codon (nonstop mRNA) elicit ribosome stalling with an empty A-site at the end of the message. Such transcripts arise routinely in the cell due to several reasons, which include premature transcriptional termination, action of ribonucleases, and chemical and environmental damage. Other instances include erroneous frame-shifting, miscoding antibiotics such as Kanamycin, and presence of nonsense suppressor tRNAs [5, 6]. Such unproductive translational complexes become substrates for bacterial ribosome-rescue systems. However, it is not clear how these rescue systems discern between transiently paused ribosomes and ribosomes undergoing prolonged translational arrest.

In *E. coli*, three distinct pathways have been discovered to engage in the rescue of unproductively stalled ribosomes. The principal rescue mechanism that has been well characterized is *trans*-translation. The t*rans*-translation pathway is dispensable in *E. coli* whereas it is necessary for survival of several bacteria such as *Mycoplasma,* and *Neisseria* [7, 8]. This suggested that the mechanisms for resolving stalled ribosomes are critical for survival of all bacteria, and that *E. coli* has alternative means to promote stalled ribosomes to undergo translation termination and recycling. This led to the discovery of alternative ribosome rescue factors ArfA, and ArfB [9, 10]. The alternative pathways, as the name suggests, seem to be deployed when cells do not have a functional *trans*-translation system. Unlike *trans*-translation, wherein RNA and protein cofactors tightly orchestrate the event, alternative rescue pathways seem to be primarily coordinated by protein factors. The common prerequisite for all these pathways is the presence of a vacant A-site in the stalled ribosomes. However, it is unclear how these surveillance factors initially recognize stalled ribosomes.

1.2.1 *trans*-Translation

trans-Translation is the first dedicated ribosome rescue pathway identified in bacteria. The two key components of this highly conserved system are transfer-messenger RNA (tmRNA) encoded by the *ssrA* gene and its essential protein partner Small protein B (SmpB). The genes encoding SmpB (*smpB*) and tmRNA (*ssrA*) have been found in all bacteria sequenced till date.

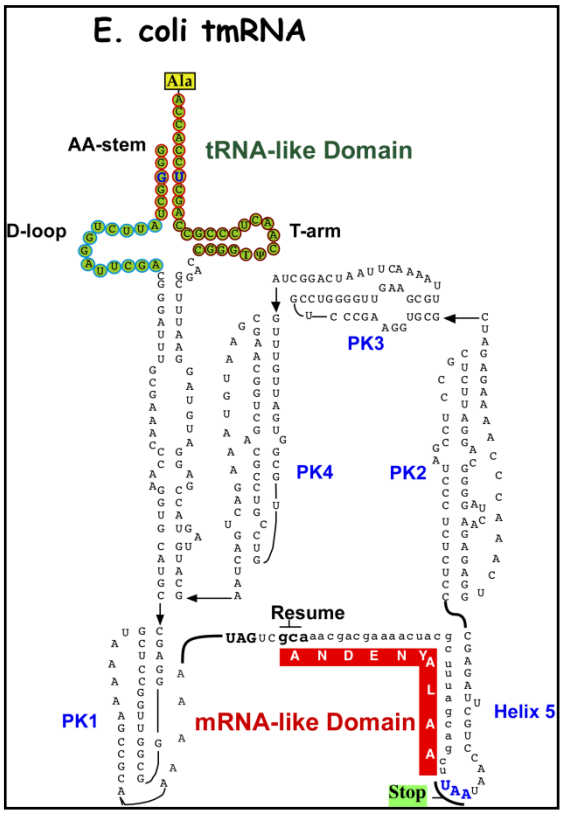

Figure 1.2 A schematic representation of *E. coli* tmRNA. tmRNA has features of both tRNA and mRNA. The tRNA-like domain (TLD) consists of T-arm, D-loop, and the canonical amino acid acceptor stem. Alanyl tRNA-synthetase charges the tmRNA with alanine residue. The mRNA-like domain (MLD) codes for 10 amino acids in *E. coli* (red). The MLD is flanked by pseudoknot (PK) 1 and 2, and encompasses helix 5 region. Courtesy: Dr. Wali Karzai

The bi-functional tmRNA is 363 nucleotides long in *E. coli* (Figure 1.2). The 3' and 5' ends of tmRNA fold to form a tRNA-like domain (TLD), consisting of amino acid acceptor stem, TΨC stem and D loop. Similar to tRNAs, tmRNA TLD terminates with the canonical CCA sequence at its 3' end, and is recognized and aminoacylated by alanyl-tRNA synthetase. In lieu of the anticodon loop, tmRNA contains an mRNA-like domain (MLD) with a short open reading frame (ORF) followed by termination codon (UAA). Additionally, there are four pseudoknots (PK1-4) present in the predicted secondary structure of tmRNA, whose functions have not been identified yet. The MLD is located between PK1 and PK2, and it encompasses the helix 5 region. Disruption of helix 5 incapacitates tmRNA mediated tagging and subsequent rescue of ribosomes. Additionally, the non-canonical resume codon (GCA in case of *E. coli*) seems to be essential for accurate establishment of the reading frame and resumption of translation by stalled ribosomes, indicating a species-specific nature of tmRNA-mediated rescue of ribosomes [11].

SmpB is a highly basic globular protein, with an RNA-binding core capable of selectively binding to the tRNA-like domain of tmRNA with high affinity. It also has an unstructured C-terminal tail that becomes ordered upon occupying the mRNA entry channel of the ribosome [12]. The tmRNA-binding core of SmpB has the capacity to deliver tmRNA to stalled ribosome. Previous studies have shown that the C-terminal tail of SmpB is critical for proper accommodation and accurate decoding of the tmRNA ORF [11, 13]. A recently solved crystal structure of ribosome-bound SmpB-tmRNAΔMLD supports this observation (Figure 1.3). The amino acid residues in the C-terminal tail (magenta) seem to be making putative contacts with the elements in the mRNA entry channel of the ribosome and the decoding center, thus mimicking an mRNA. This step is hypothesized to be essential for the ensuing accommodation of the tmRNA MLD.

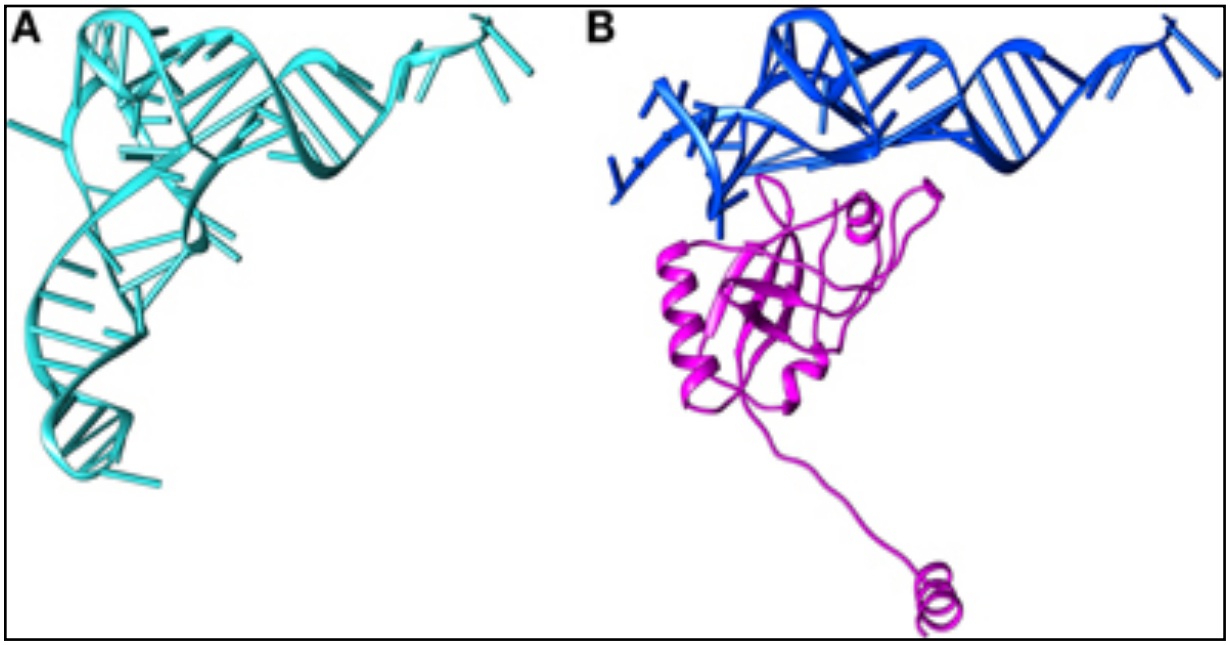

Figure 1.3 Structural comparison between tRNA and the tRNA-like domain of tmRNA bound to SmpB. (A) The structure of tRNA (PDB entry 2WRN). **(B)** The structure of TLD-SmpB (PDB entry 4ABR). The TLD is blue and SmpB is magenta. The TLD resembles the upper part of a tRNA, with SmpB replacing the tRNA anticodon stem-loop. This figure is adapted from Giudice E et.al. *Front. Microbiol.* **2004**. doi: 10.3389/fmicb.2014.00113 [14]

Together with elongation factor Tu (EF-Tu) and GTP, alanine-charged tmRNA and SmpB form a quaternary complex that recognizes stalled ribosome with an empty A-site, devoid of coding information. Once $tmRNA^{Ala}$ is accommodated in the A-site, the nascent polypeptide chain is transferred to the alanine residue on the tRNA-like domain of tmRNA. By a mechanism that is facilitated in part by amino acid residues in the C-terminal tail of SmpB, the lead ribosome switches from the defective mRNA template, and starts decoding the tmRNA ORF as a surrogate template. The tmRNA ORF also encodes for an in-frame stop codon that ensures proper termination of protein synthesis, ribosome rescue, and recycling of components of the translation machinery [6, 15, 16]. As a consequence, the nascent polypeptide is co-translationally appended with the short peptide sequence (the ssrA tag or degron) encoded by the tmRNA ORF. In *E. coli*, together with the alanine residue supplied by the alanyl-tmRNA, the ssrA degron contains 11 amino acids, AANDENYALAA, that contain the recognition motifs

for various proteases and substrate adaptors, thus marking the nascent polypeptide for rapid clearance from the cell (Figure 1.4).

tmRNA is one of the most abundant RNAs in bacteria. The importance of this system is exemplified by the fact that it is essential for survival and/or virulence of several pathogenic bacterial species [17-19]. For instance, it has been shown that *Yersinia pseudotuberculosis* strains with disruption in SmpB and/or tmRNA are unable to proliferate in macrophages, and are avirulent. Other phenotypes manifested by SmpB-tmRNA deficient bacteria include heightened sensitivity to environmental stress and antibiotics, and slow recovery from carbon starvation [6]. The SmpB-tmRNA rescue system is used not only to help stalled ribosomes undergo recycling but also as a tool for modulating gene expression.

1.2.2. Alternative ribosome rescue factors

As mentioned earlier, unlike in certain bacteria, the tmRNA-SmpB system is not essential for survival in *E. coli* indicating that it might have back-up rescue systems. The Chadani and Abo group systematically performed experiments to look for synthetically lethal mutants of *ssrA* [10, 20]. This led to the identification of a previously uncharacterized protein, YhdL, that partially substitutes for tmRNA-mediated ribosome rescue. This factor, renamed ArfA, indeed functions in the predicted manner. Like *ssrA*, the *arfA* gene is dispensable in *E. coli*. Interestingly, *arfA* expression is tightly controlled by the *trans*-translation system suggesting that ArfA is utilized as a second line of rescue pathway. *arfA* transcript contains a predicted hairpin structure, which is recognized and cleaved by RNase III [21]. As a result, this truncated mRNA (nonstop mRNA) becomes a substrate for *trans*-translation. However, in the absence of tmRNA, the truncated ArfA polypeptide is stabilized, and is fully capable of rescuing stalled ribosomes. A unique property of this alternative pathway is, unlike normal translation termination, ArfA recruits Release Factor 2, and helps in the accommodation of RF2 in the A-site of the stalled ribosomes in a termination codon-independent manner. This

facilitates the hydrolysis of peptidyl-tRNA and hence promotes ribosomal disassembly. Availability of a crystal structure of ribosome bound to ArfA/RF2 will provide finer details of this mode of ribosome rescue.

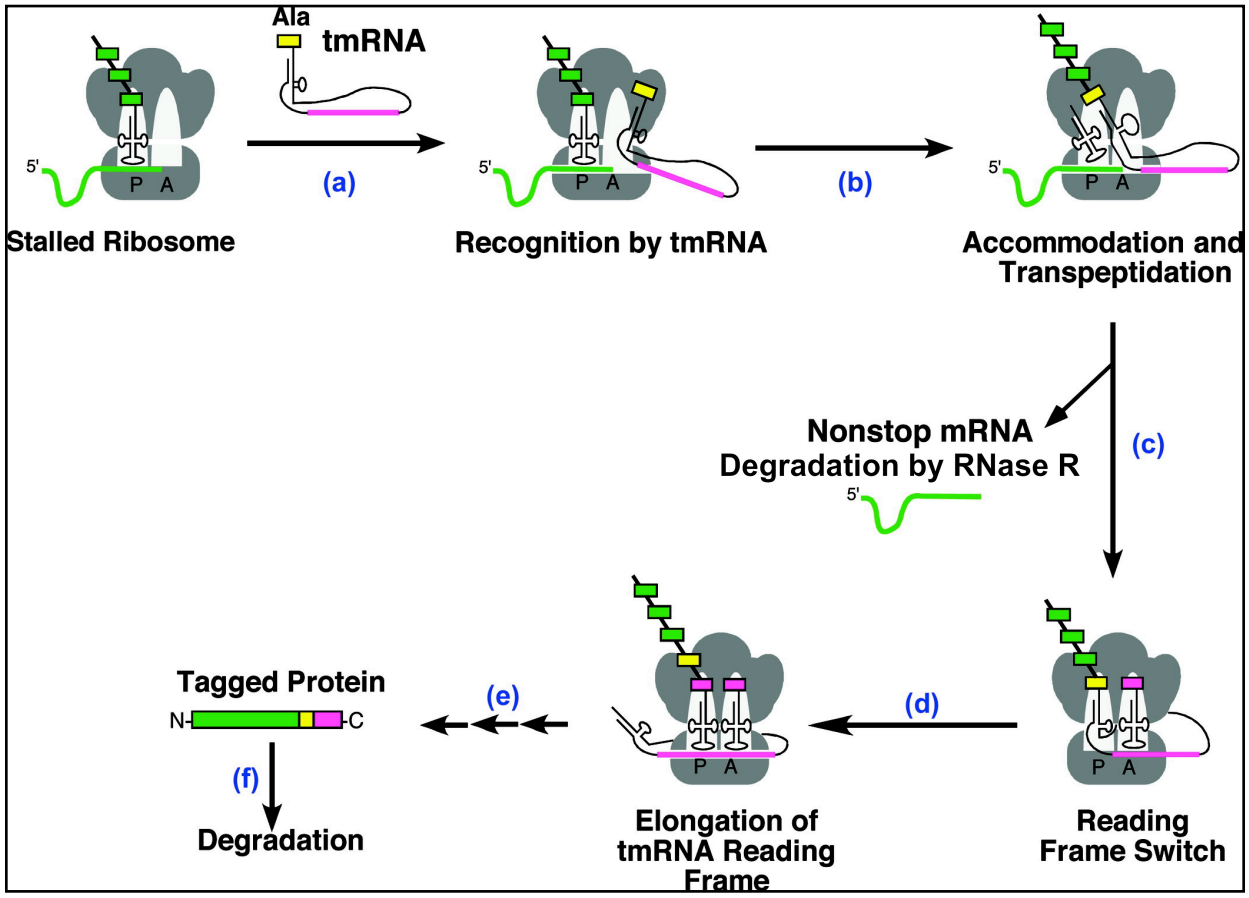

Figure 1.4 *Trans*-translation model for tmRNA-mediated protein tagging and ribosome rescue. A ribosome stalls on an incomplete or untranslatable message, leading to (a) the recruitment of aminoacylated tmRNA to the ribosomal A site and (b) transfer of the nascent chain to the alanine-charged tRNA-like domain of tmRNA. A message-switching event (c) then replaces the faulty mRNA with an open reading frame within tmRNA (d), which is translated until a stop codon is reached (e) and the tagged protein is released and degraded by C-terminal specific proteases (f). This figure is adapted from Dulebohn DP et. al. *Biochemistry* **2007** *46* (16), 4681-4693.[22]

Yet another ribosome rescue pathway was identified, primarily mediated by ArfB (formerly known as YaeJ). However, it does not seem to fully compensate for the lack of tmRNA and ArfA unless it is overexpressed in *ssra/arfA* double knockout *E. coli* strain. ArfB is a globular protein with a flexible C-terminal tail. A crystal structure of ArfB bound to ribosome shows that its unstructured C-terminal tail occupies the empty mRNA entry channel, which is thought to act as a sensor that help ArfB identify stalled ribosomes with vacant A-site. Unlike ArfA, ArfB promotes aminoacyl ester hydrolysis of peptidyl-tRNA by itself because it has the universally conserved GGQ motif similar to that of release factors. This facilitates the subsequent dissociation of ribosomal subunits. Because of these distinct properties, ArfB is classified as a ribosome-dependent, codon-independent peptidyl-tRNA hydrolase [9, 23].

Overall, the three distinct ribosome-rescue pathways discussed here underscore the importance of resolving stalled ribosome complexes. Regardless of the nature of the mRNA that elicits ribosome stalling (no-go mRNA/nonstop mRNA), A-site cleavage of mRNA seems to be an important criterion for all the three pathways. This turns all the mRNA templates into nonstop mRNAs. The empty A-site created as a result might serve as a signal for the rescue systems to take the stage. However, the factor responsible for mRNA cleavage in the A-site in this case is yet to be identified.

1.3 Messenger RNA turnover in bacteria

RNA degradation is one of the key modes of controlling gene expression at a post-transcriptional level. Modulation of gene expression at a post-transcriptional stage helps in rapid adaptation to changing environmental changes, regulating levels of proteins required for survival in the new environment [24]. Presence of over 20 ribonucleases (RNases) in *E. coli* suggests that RNA metabolism is an important aspect of cell survival and fitness. Some of the RNases have evolved to carry out specialized

functions, and do not ubiquitously or nonspecifically degrade all RNAs. For example, RNase III, which specifically cleaves double stranded RNAs, has been implicated in the complex pathway of ribosomal RNA maturation [25]. Several bacterial toxins have been identified as ribonucleases. Bacterial toxin RelE is characterized as a ribosome-dependent endoribonuclease that is activated especially under stress condition [26]. On the other hand, some RNases (RNase II, RNase R, etc.) do not seem to exhibit sequence specificity. These RNases are often associated with general RNA degradation in the cell.

RNA degradosome is a multi-enzyme scaffold that is primarily dedicated for cellular mRNA degradation. The indispensable enzyme involved in the formation of this membrane-bound scaffold in *E. coli* is endoribonuclease RNase E (Figure 1.5). RNase E has been shown to cleave mRNAs preferentially at single stranded regions enriched in A/U bases. Although RNase E does not seem to require the presence of monophosphate at the 5' end of the substrate RNA, such processed RNAs, generated mainly by pyrophosphohydrolase RppH, have been shown to be potent activators of RNase E. The N-terminus of RNase E contains the membrane-anchoring segment followed by the catalytic domain that is crucial for cell survival. The C-terminal domain of RNase E acts as the platform for the scaffold assembly [27-29].

Other components of the RNA degradosome are known to interact with the non-catalytic C-terminal domain of RNase E in a cell phase-dependent manner [30]. These include DEAD-box RNA helicase RhlB, Poly (A) Polymerase I (PAP I), Polynucleotide Phosphorylase (PNPase), and RNA chaperone Hfq. RNA helicase like B (RhlB) has the ability to unwind complex secondary structures in the mRNA by deriving energy from ATP hydrolysis. It has also been shown to directly interact with PNPase. In contrast to eukaryotes, PAP I-mediated addition of Poly (A) tail at the 3' end destabilizes the mRNA. It has been shown that general cellular ribonucleases, RNase II and RNase R, bind to Poly (A) RNA sequence with high affinity *in vitro*. However, the presence of a Poly (A) tail is not essential to trigger nucleolytic activity of the enzymes. Unlike other RNases, the highly conserved reversible PNPase is a 3'-5' phosphorylitic enzyme that uses inorganic phosphate moiety for its activity, and can synthesize RNA using

nucleotide diphosphate precursors [31]. It has been shown that double deletion of genes encoding PNPase and RNase R or PNPase and RNase II is synthetically lethal. This signifies the functional redundancies of RNases in the cell [32]. Overall, dynamic interactions of a diverse array of RNA processing enzymes with the RNA degradosome contributes to fine-tuning its activity based on the cellular needs.

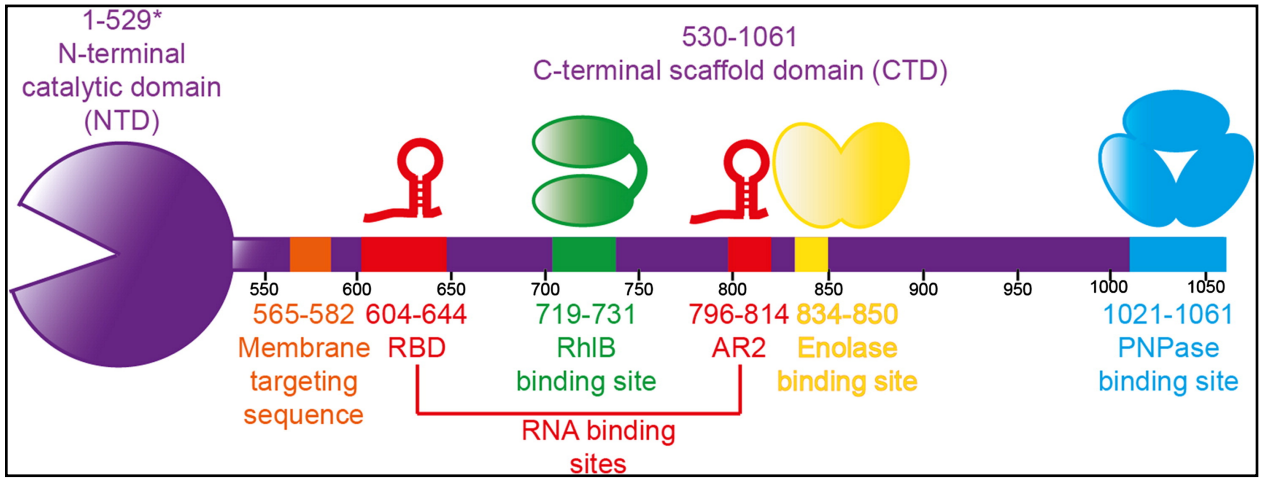

Figure 1.5 Components of the canonical RNA degradosome. The asterisk marks the predicted size of the catalytic domain of RNase E; the amino acids 511–529 were not visible in the crystal structure. This figure is adapted from Bandyra KJ et.al. *Biochimica et Biophysica Acta* **2013** Vol 1829,Issues 6–7,514–522. http://dx.doi.org/10.1016/j.bbagrm.2013.02.011 [28]

Regulation of mRNA stability through small noncoding RNAs has garnered attention in recent years. This pathway requires the function of RNA chaperone Hfq. These small RNAs range from 50 to 300 nucleotides, and are expressed either in *cis*- or in *trans*-. The sRNAs expressed in *cis* with their target mRNAs hybridize with extended complementarity whereas *trans*-expressed sRNAs seem to have mismatches leading to limited complementarity with their targets [33, 34]. Nevertheless, both types of sRNAs require the assistance of Hfq to find their target mRNAs. Additionally, Hfq plays a protective role and helps in stabilization of sRNAs *in vivo*. Hybridization of sRNAs with

their targets has three possible outcomes – (i) Hybridization of sRNAs with the ribosome-binding site (RBS) or 5' UTR of the target mRNAs can occlude and prevent translation initiation. This makes the mRNAs susceptible to degradation by ribonucleases (ii) By binding to inhibiting secondary structures in the target mRNAs (e.g., structures sequestering the RBS) sRNAs can enhance their translatability (iii) sRNA-mRNA duplex can in turn recruit RNases or RNA degradosome; 5' phosphate can trigger the endonucleolytic activity of RNase E leading to the clearance of the mRNA. RNase III has also been implicated in cutting the sRNA-mRNA duplex (Figure 1.6). [35]

Evolution of different approaches designed for RNA metabolism in the cell reinforces the notion that it is a fundamental aspect of gene regulation. The examples quoted above predominantly focus on the regulation of intact mRNAs. The special scenario of defective mRNA decay pathway in bacteria is discussed extensively in this thesis.

1.4 Coupling of translational quality control and mRNA degradation

A major factor contributing to transcript stability is ribosome-mediated protection of potential cleavage sites from the endonucleolytic activity of RNase E. Translating ribosomes are thought to sterically hinder ribonucleases from accessing cleavage sites present in mRNAs, leading to their increased stability. However, the stability of defective or nonstop mRNAs, which promote the accumulation of unproductively stalled ribosomes, is dramatically reduced [27]. Bacteria have evolved an elegant pathway to connect translational quality control with counteracting the persistence of defective mRNA. Aberrant mRNA degradation is a distinguishing feature of *trans*-translation mediated ribosome rescue - an equivalent mRNA decay process has not been identified for the alternate ArfA and ArfB ribosome rescue pathways. Such a combination of

translational quality control mechanism and defective mRNA decay might be energetically economical for the cell. It also suggests that ribosomes are not mere protein synthesis machineries rather they have the exceptional capacity to serve as a dynamic platform for assorted co-translational, and quality control measures.

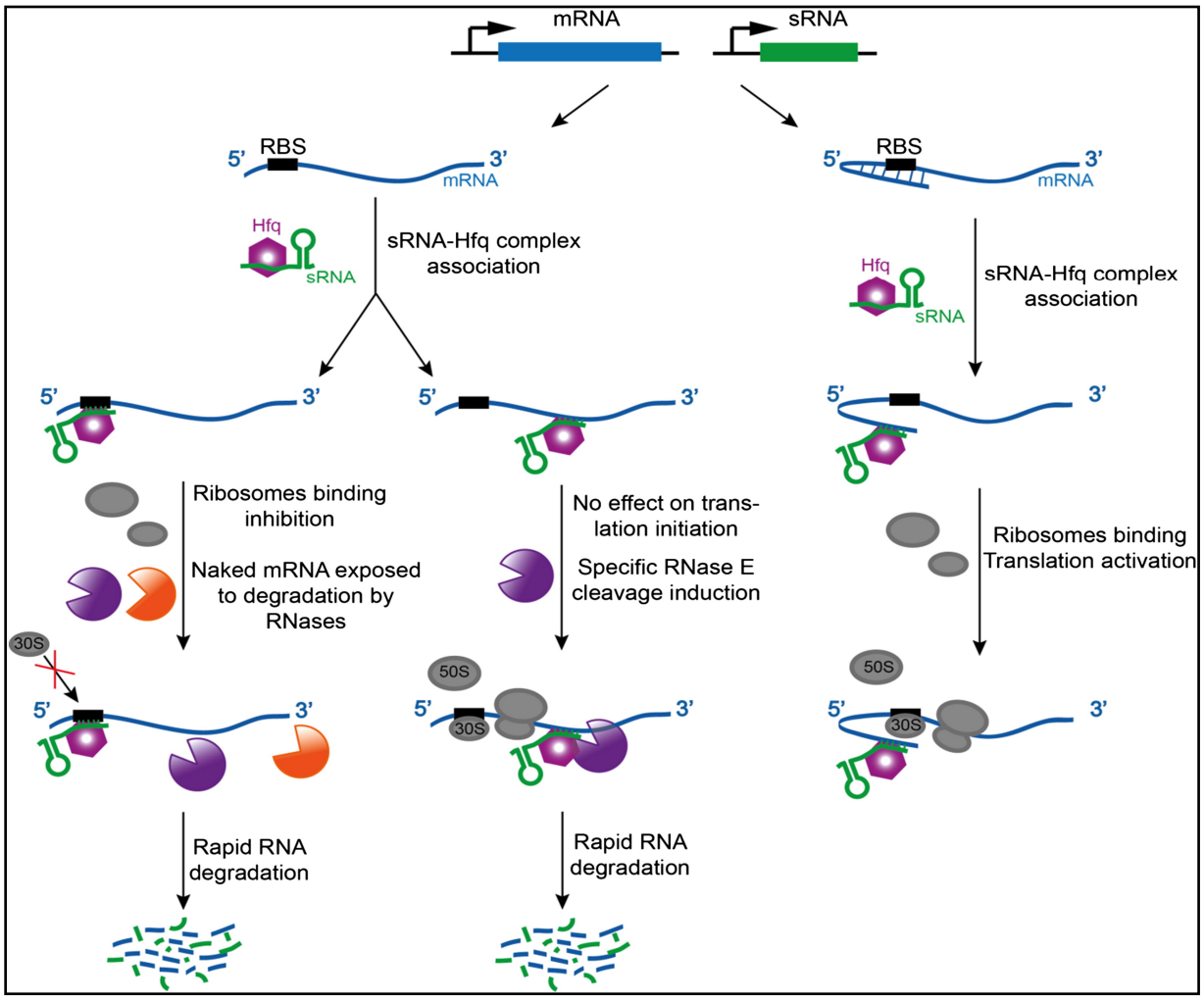

Figure 1.6 RNase E, the degradosome and sRNA mediated post-transcriptional regulation. Cartoon schematic of the sRNA mediated pathways for degradation (left and central panels) and translational activation (right panel). The purple body represents RNase E and the orange body is an exoribonuclease. This figure is adapted from Bandyra KJ et.al. *Biochimica et Biophysica Acta* **2013** Vol 1829, Issues 6–7,514–522. http://dx.doi.org/10.1016/j.bbagrm.2013.02.011 [28]

The highly conserved RNase R is the lone 3′-5′ exoribonuclease that carries out selective degradation of nonstop and defective mRNAs. RNase R co-purifies with the stalled ribosomal complex indicating that it is recruited to the site of rescue to capture the defective mRNA. This exclusive function of RNase R is dependent on the action of SmpB-tmRNA complex on stalled ribosome. Of all the ribonucleases present in the cell, why is RNase R chosen to perform this task? The C-terminal lysine-rich (K-rich) domain of RNase R, not shared by other members of the RNase II family of exoribonucleases, plays an important role in productive engagement of RNase R on stalled ribosomes (Figure 1.7). Putative contacts made by the K-rich domain with the *trans*-translation apparatus helps RNase R access the aberrant mRNA for degradation [36, 37].

Figure 1.7 Schematic representation of the domain architecture of RNase R and RNase II. RNase R and RNase II share extensive similarity in the N-terminal cold-shock, central nuclease and C-terminal S1 domains. RNase R has two additional domains, a N-terminal putative helix-turn-helix (HTH) domain and a C-terminal lysine-rich (K-rich) domain. This figure is adapted from Ge Z et.al. *Mol. Microbiol.* **2010** 78(5): 1159–1170 [36]

There are several outstanding questions to be addressed in order to fully understanding this unusual mode of defective mRNA decay. The critical amino acid residues and the structure of RNase R K-rich domain are not known. Although the key players involved in engaging RNase R on stalled ribosomes have been identified, namely SmpB and tmRNA, it is not clear how they coordinate in activating RNase R to degrade the defective mRNA. The mechanistic time-frame of when RNase R captures the aberrant mRNA has to be elucidated. Finally, it has been shown that the defective mRNA decay initiates on the ribosome. However, the interacting partners on ribosomes critical for RNase R function have remained unexplored.

1.5 Outline of dissertation

In Chapter 2, I have detailed the biochemical assays that I conducted to identify crucial residues in the K-rich domain of RNase R that play a role in *trans*-translation mediated nonstop mRNA decay. In collaboration with Kip E. Guja, I have obtained the SAXS structural model of *Escherichia coli* RNase R (full length and C-terminal domain truncation variant). In Chapter 3, I present work that sheds light on the mechanistic details of RNase R-mediated nonstop mRNA degradation. In particular, I explored the role of the C-terminal tail of SmpB and the open reading frame of tmRNA in this process. In Chapter 4, I performed RNA CLIP and high throughput sequencing studies, which were performed in collaboration with Dr. Marek Kudla. This work highlights the key ribosomal and non-ribosomal proteins essential for the nonstop mRNA degradation by RNase R. Also, I discuss the mass spectrometric analyses of S6 C-terminal tail modification under various conditions. This work was performed with some assistance from Dr. Deepika Vasudevan, and Dr. Robert Haltiwanger.

Chapter 2: Non-stop mRNA decay: a special attribute of *trans*-translation mediated ribosome rescue

* The work contained within this chapter was published in Frontiers in Microbiology (2014) doi: 10.3389/fmicb.2014.00093

2.1 Abstract

Decoding of aberrant mRNAs leads to unproductive ribosome stalling and sequestration of components of the translation machinery. The SmpB-tmRNA mediated *trans*-translation pathway, in addition to re-mobilizing stalled translation complexes, co-translationally appends a degradation tag to the associated nascent polypeptides, marking them for proteolysis by various cellular proteases. Another unique feature of *trans*-translation, not shared by the alternative rescue pathways, is the facility to recruit ribonuclease R (RNase R) for targeted degradation of non-stop mRNAs, thus preventing further futile cycles of translation. The distinct C-terminal lysine-rich (K-rich) domain of RNase R is essential for its recruitment to stalled ribosomes. To gain new insights into the structure and function of RNase R, we investigated its global architecture, the spatial arrangement of its distinct domains, and the identities of key functional residues in its unique K-rich domain. Small-angle X-ray scattering models of RNase R reveal a tri-lobed structure with flexible N- and C-terminal domains, and suggest intimate contacts between the K-rich domain and the catalytic core of the enzyme. Alanine-scanning mutagenesis of the K-rich domain, in the region spanning residues 735 and 750, has uncovered the precise amino acid determinants required for the productive engagement of RNase R on tmRNA-rescued ribosomes. Theses analyses demonstrate that alanine substitution of conserved residues E740 and K741 result in profound defects, not only in the recruitment of RNase R to rescued ribosomes but also in the targeted decay of non-stop mRNAs. Additionally, an RNase R variant with alanine substitution at residues K749 and K750 exhibits extensive defects in ribosome enrichment and non-stop mRNA decay. In contrast, alanine substitution of

additional conserved residues in this region has no effect on the known functions of RNase R. *In vitro* RNA degradation assays demonstrate that the consequential substitutions (RNase $R^{E740A/K741A}$ and RNase $R^{K749A/K750A}$) do not affect the ability of the enzyme to degrade structured RNAs, indicating that the observed defect is specific to the *trans*-translation related activities of RNase R. Taken together, these findings shed new light on the global architecture of RNase R and provide new details of how this versatile RNase effectuates non-stop mRNA decay on tmRNA-rescued ribosomes.

2.2 Introduction

Controlling mRNA stability is one of the key means of post-transcriptional regulation of gene expression. A major factor contributing to transcript stability is ribosome-mediated protection of potential cleavage sites from the endonucleolytic activity of RNase E, an essential component of the RNA degradosome. Translating ribosomes are thought to sterically hinder ribonucleases from accessing cleavage sites present in mRNAs, leading to their increased stability [27, 29]. However, the stability of defective or non-stop mRNAs, which promote the accumulation of unproductively stalled ribosomes, is dramatically reduced. In bacteria, a universally conserved ribosome rescue mechanism called *trans*-translation facilitates the selective increase in non-stop mRNA decay [6, 15, 22, 38-41]. The central components orchestrating the *trans*-translation process are the hybrid transfer-messenger RNA (tmRNA) and its requisite protein cofactor SmpB [16, 42]. The biological significance of salvaging unproductively stalled ribosomes is highlighted by the fact that three independent ribosome rescue mechanisms have evolved in *E. coli* and many related bacterial species. However, selective non-stop mRNA decay is a unique consequence of the SmpB-tmRNA mediated *trans*-translation process [11, 22, 36, 37] – an equivalent mRNA decay process has not been identified for the alternate ArfA and ArfB ribosome rescue pathways [9, 10, 20].

The highly conserved ribonuclease R (RNase R) is the sole 3′–5′ exoribonuclease responsible for the selective degradation of non-stop and defective mRNAs [37]. RNase R belongs to the RNB family of exoribonucleases and shares ~45% sequence similarity with RNase II. Based on sequence analysis, it was inferred that RNase R and RNase II have similar overall organization of the cold shock, catalytic RNB, and S1 domains [43]. In addition to these core domains, RNase R has distinctive N-terminal helix-turn-helix and C-terminal lysine-rich (K-rich) domains that are not present in RNase II. Recent data have made it abundantly clear that the activities of RNase R are intimately linked with the SmpB-tmRNA system. While RNase R is known to participate in the *trans*-translation process and play a decisive role in the cell-cycle dependent degradation of circularly permuted tmRNA, the SmpB-tmRNA complex also somehow regulates the stability of RNase R [44, 45]. Despite the high degree of similarities between RNase II and RNase R, the SmpB-tmRNA system does not appear to affect the function or stability of RNase II, suggesting the unique N- and C-terminal domains of RNase R are involved in the specialized functions of this versatile enzyme. Indeed, we recently demonstrated that the K-rich C-terminal domain of RNase R is required for the tmRNA-mediated ribosome enrichment and non-stop mRNA decay activities of RNase R.

While the crystal structure of RNase II has revealed its structural organization at atomic resolution, information on the three-dimensional (3D) shape and domain architecture of RNase R is not available [46, 47]. Thus, it is of great interest to gain new insights into the overall 3D shape and spatial domain organization of RNase R and identify key functional residues that are required for its *trans*-translation related activities. In this study, we used small-angle X-ray scattering (SAXS) techniques to determine the global solution structure of RNase R. Our analysis reveals the overall architecture of RNase R, the high degree of similarity of its core domain to RNase II, and the relative spatial positioning of the flexible N- and C-terminal domains with respect to its catalytic core. Additionally, systematic mutational and biochemical analyses of the K-rich domain of RNase R highlight the importance of residues E740–K741 and K749–K750 in engaging tmRNA-rescued ribosomes and facilitating selective degradation of non-stop mRNAs.

2.3 Materials and Methods

2.3.1 Strains and Plasmids

Escherichica coli strain MG1655 *rnr::kan* was obtained by P1 transduction using the Keio *rnr::kan* disruption strain as a donor [48]. A plasmid expressing the coding region of N-terminal domain of λ-cI protein (pλ-cI-NS), which encodes for an N-terminal His6 epitope but lacks in-frame stop codons, served as the source of the non-stop reporter mRNA. A control reporter plasmid (pλ-cI-S), which encodes for an N-terminal His6 epitope and has two tandem in-frame stop codons, served as the source of the "normal" or stop codon containing reporter mRNA. A pACYCDuet-1 plasmid (p*rnr*) harboring the *E. coli rnr* gene under the control of the arabinose inducible P_{BAD} promoter was used as a template to synthesize RNase R variants by site directed mutagenesis. For purification of RNase R and its variants, the coding region of *E. coli rnr* gene was cloned into the MCS of pET15b under the control of isopropyl β-D-thiogalactoside (IPTG)-inducible T7 promoter. This plasmid was used as a template to synthesize RNase R variants by site directed mutagenesis. The plasmids were transformed into W3110 (DE3) *rnr rnb* strain for over-expression and purification of the corresponding RNase R variants, as previously described [36].

2.3.2 SAXS Measurements

Purified RNase R samples were prepared in 50 mM Tris-HCl (pH 7.5), 250 mM KCl, and 1 mM DTT within 24 h of data acquisition and stored at 4°C. Scattering data were collected at beamline X9 of the National Synchrotron Light Source (NSLS, Upton, NY, USA) using a Pilatus 300K located 3.4 m from the sample for small-angle X-ray data. Wide-angle X-ray scattering data were collected simultaneously with SAXS data using a Photonic Science CCD camera located 0.47 m from the sample. Twenty microliters of sample were continuously flowed through a 1 mm diameter capillary and exposed to a 400 μm × 200 μm X-ray beam with a wavelength of 0.9184 Å for 30 s of total measurement time. Scattering data were collected at concentrations of 2.2, 3.7,

4.2, 5.0, and 10 mg/mL for RNase R^{WT} and at concentrations of 0.7, 2.8, 3.0, 3.5, and 6.0 mg/mL for RNase R^{723}. Each concentration was measured in triplicate. Normalization for beam intensity, buffer subtraction, and merging of data from both detectors were carried out using PRIMUS [49]. The radius of gyration (R_g) was calculated using a Guinier approximation, $I(q)=I(0)\exp(-q^2 R_g^2/3)$, where a plot of $I(q)$ and q^2 is linear for $q < 1.3/R_g$ [50]. Three independent scattering trials were averaged. GNOM was used to determine the pair distribution function, $P(r)$, and maximum particle dimension, D_{max} [51]. The linearity of the Guinier region and the forward scattering intensity were used to validate that the samples were monodisperse in solution. The forward scattering intensity, *I(0)*, is the theoretical scattering at a *q*value of 0 and is proportional to the molecular weight of the sample [52]. *I(0)*/*c*, where *c* is sample concentration, was identical for all RNase R measurements. For RNase R^{723}, ten independent *ab initio* beads models that describe the experimental data were calculated using DAMMIN [53]. The resulting models, which had an average χ^2 of 0.65 ± 0.16, and a normalized spatial discrepancy (NSD) of 0.71 Å, were subsequently aligned, averaged, and filtered by occupancy using the DAMAVER suite of programs [54]. An electron density map was calculated from the filtered average model using SASTBX [55]. For RNase R^{WT}, the crystal structure of RNase II was modeled against the solution structure data by combined rigid body fitting and *ab initio* bead modeling, using BUNCH [56].

2.3.3 Reporter mRNA Stability and Ribosome Enrichment Analysis

Escherichica coli strain MG1655 *rnr::kan* harboring the reporter plasmid pλ-cI-NS and the various p*rnr* variants were grown at 37°C in Luria-Bertani (LB) broth containing 0.01% arabinose, 100 µg/ml of Ampicillin, and 30 µg/ml of Chloramphenicol. At an optical density at 600 nm (OD_{600}) of ~0.6, expression of the λ-cI-NS reporter mRNA was induced with a final concentration of 1 mM IPTG for 1 h. Equal number of cells were harvested and total RNA was isolated using TRI Reagent (MRC Inc.). To test the activity of RNase R variants, *in vitro* RNA degradation assays were performed as previously described [36]. The oligoribonucleotide substrate used was a single stranded

RNA with an internal step-loop structure and a 3′ poly A overhang (*trp*At-A_{10}: 5′-GCAGCCCGCCUAAUGAGCGGGCAAAAAAAAAA-3′). Reaction mixtures containing the 32P-labeled *trp*At-A_{10} substrate and the desired RNase R variants were assembled and incubated at 37°C. Aliquots of 5 µl were taken at indicated time points and quenched by the addition of 5 µl of the formaldehyde gel-loading dye. Full-descriptions of the *in vivo* reporter mRNA stability and ribosome enrichment assays have been described elsewhere [36, 57]. A brief description of the ribosome enrichment assay is provided here. Non-stop or stop reporter mRNAs were expressed in MG1655 *rnr::kan* strain complemented with designated plasmid borne RNase R variant, under a P_{BAD} promoter. Cells were grown in media containing 0.01% arabinose to OD_{600} of 1.0 and the expression of reporter constructs was induced by the addition of IPTG to a final concentration of 1 mM. Cells were allowed to grow for another 45 min, harvested, resuspended in Buffer E (50 mM Tris-HCl pH 7.5, 300 mM NH_4Cl, 20 mM $MgCl_2$, 2 mM β-ME, and 10 mM Imidazole) and lysed by French Press. Ribosomes were pelleted from cleared cell lysates by centrifugation at 29,000 rpm for 16–18 h through a 32% sucrose cushion in Buffer E. Ribosomes translating the reporter mRNAs were purified from tight-coupled ribosomes by Ni^{2+}-NTA affinity chromatography. The ribosome-associated RNase R was detected by Western blot analysis using polyclonal anti-RNase R antibody. Protein bands were quantified using ImageJ.

2.4 Results

2.4.1 Global Architecture and Domain Orientation of RNase R in Three-Dimensional Space

To gain insight into the overall 3D architecture and relative domain positioning of RNase R, we determined its solution structure at low resolution using SAXS techniques. As a preliminary step, and as a complement to the low resolution SAXS data, we used the I-TASSER platform [58], employing the entire protein data bank (PDB) as the search space, to generate a homology model of full-length RNase R (RNase R^{WT}). Our results

provide secondary structure predictions for the N- and C-terminal domains of RNase R (Figure 2.1A) that are in good agreement with previous studies [59]. The three top scoring models from I-TASSER (Figure 2.1B) support the notion that RNase R has a structurally conserved core domain that is highly similar to the known crystal structure of RNase II [46, 47]. The I-TASSER models predicted that the unique N- and C-terminal domains, which do not share significant homology to any known structures, flank the core catalytic domain of RNase R. Notably, the C-terminal K-rich domain is predicted to contain an extensive loop segment that likely imparts significant flexibility to this domain. To further characterize the 3D shape and spatial arrangement of the N- and C-terminal domains, we collected SAXS data on RNase R^{WT} and RNase R^{723}, an RNase R variant lacking the entire K-rich domain. The SAXS envelope for RNase R^{723} has a shape that is highly similar to RNase II. Docking of the conserved core domain into the SAXS envelope using SITUS resulted in a robust fit with a correlation coefficient of 0.88 (Figure 2.1C). Additional density is apparent near the N-terminus that most likely corresponds to residues 1–65 of RNase R. Having confirmed that the solution structure of RNase R displays a conserved molecular shape with RNase II, we collected SAXS data on RNase R^{WT}, and carried out rigid-body modeling with the conserved core domain of RNase R. We combined the core domain modeling with *ab initio* C-α bead modeling for the missing N- and C-terminal domains using BUNCH (Figure 2.1D). The resulting SAXS model of RNase R^{WT} reveals a tri-lobed structure that is somewhat elongated, and is consistent with the presence of extensive flexible loops, as predicted by homology modeling. The scattering patterns from RNase R^{723} and RNase R^{WT} (Figure 2.1E) were quite similar, reflecting their largely analogous topologies, and the SAXS model of the N-terminal and core domains of RNase R^{WT} correlated well with the overall shape of the RNase R^{723} envelope. Both models demonstrate an excellent fit to the raw scattering data (Figure 2.1E), with discrepancies (χ^2) of 0.68 for RNase R^{723} and 1.43 for RNase R^{WT}. Visual comparison of the two models reveals the relative positioning of the K-rich C-terminal lobe with respect to the core and N-terminal domains. Both the I-TASSER and SAXS models imply intimately close links between the catalytic core and the K-rich domains of RNase R, suggesting a potential regulatory role for the K-rich domain. However, the extent of such contacts and the identity of

functionally important amino acid residues in the K-rich domain that participate in any potential intra- or inter-molecular interactions have not been determined.

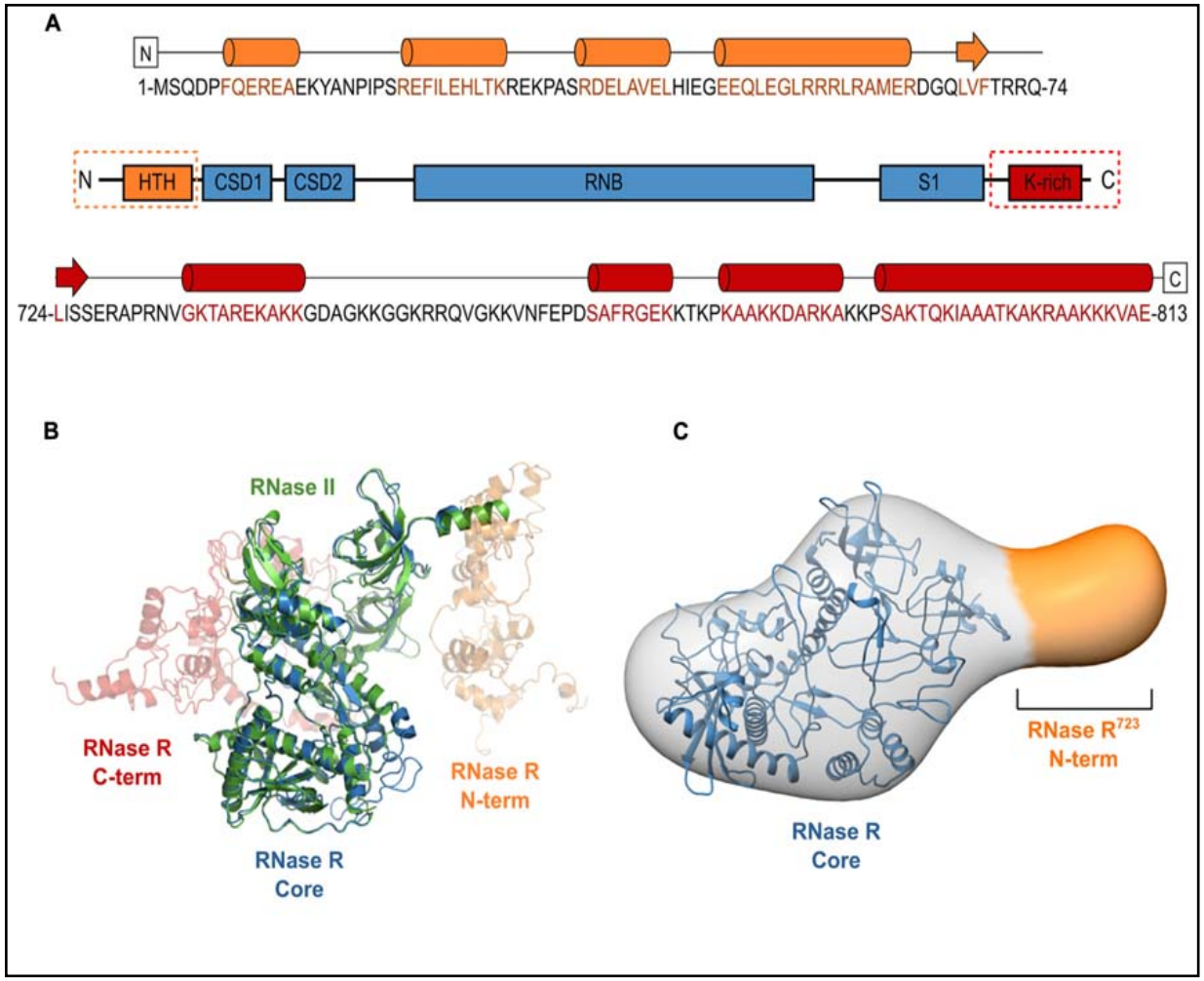

Figure 2.1 The overall shape and relative domain orientation of full-length RNase R. (A) Secondary structure prediction from I-TASSER for the N-terminal domain (orange), the catalytic core (blue), and the C-terminal domain (red) of RNase R. Predicated helical regions are shown as cylinders, β-strands as arrows, and random coil regions as black lines. **(B)** Super-position of the crystal structure of RNase II (PDB ID 2ID0) and the three top-scoring homology models of full-length RNase R generated with I-TASSER. RNase II is shown as a green cartoon, the conserved core of RNase R is shown as a blue cartoon. **(C)** SAXS envelope showing the 3D molecular shape of RNase R^{723}. The I-TASSER model of the conserved core domain (shown in panel **B**) has been docked into the SAXS envelope using SITUS, with a resulting correlation coefficient of 0.88. The additional density seen in the SAXS envelope (indicated in orange) corresponds to residues 1–65 of RNase R^{723}. The C-terminal residue in the I-TASSER model of the core domain is indicated with an asterisk.

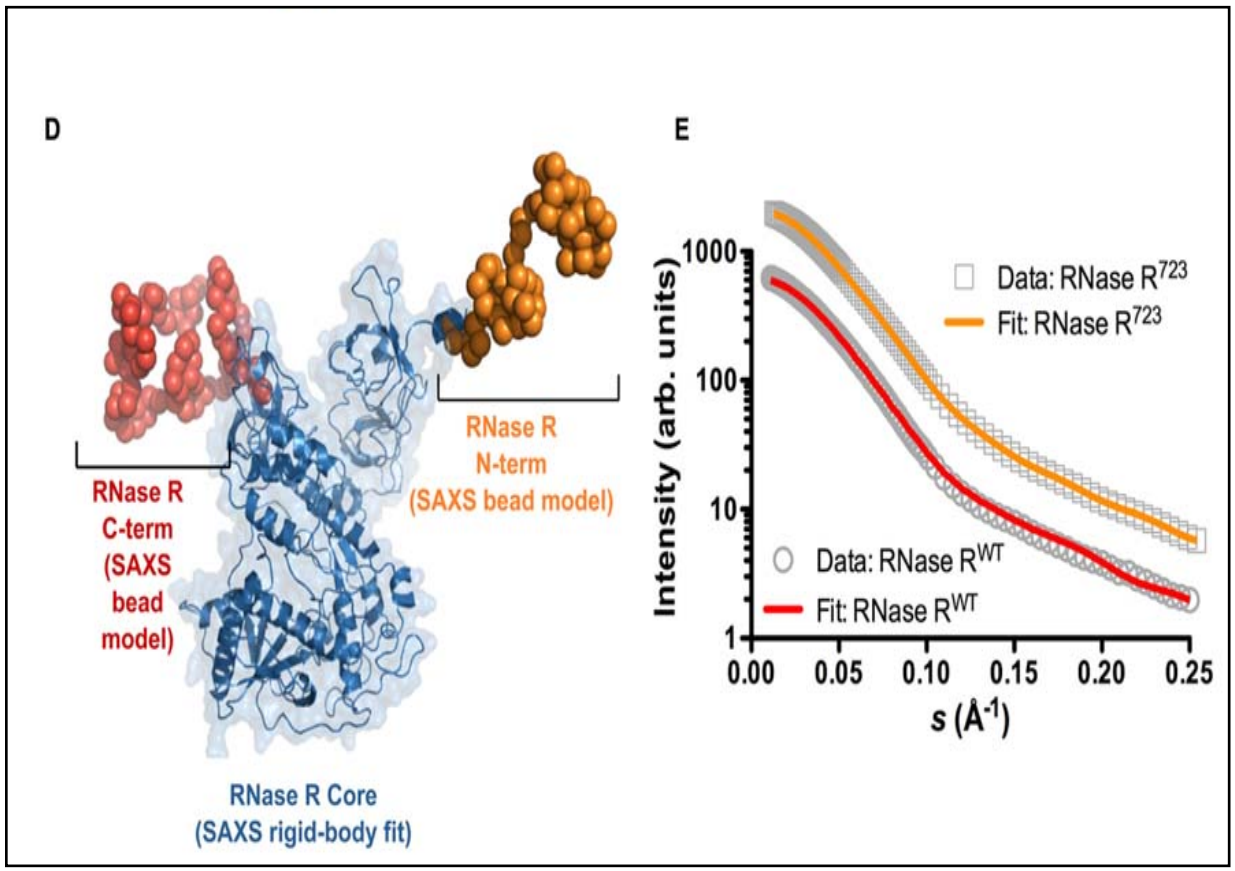

Figure 2.1 Cont'd - **The overall shape and relative domain orientation of full-length RNase R (D)** SAXS model of RNase R^{WT} shows the 3D shape and relative orientations of the C- and N-terminal domains. The core domain was fit to the SAXS data as a rigid body (shown as a blue cartoon with transparent surface), and the missing terminal regions were modeled as C-α beads using the BUNCH program of the ATSAS suite. **(E)** The experimental scattering profiles of RNase R^{WT} and RNase R^{723}. The relative scattering intensity (*I*) is plotted as a function of the momentum transfer, or scattering vector, *s* (*s* = 4πsinθ/λ where λ is the beam wavelength and θ is the scattering angle). The raw data for RNase R^{723} and RNase R^{WT} are shown as gray circles and rectangles, respectively. Simulated scattering curves that correspond to the SAXS envelope for the RNase R^{723} (shown in panel **C**) and the BUNCH model for RNase R^{WT} (shown in panel **D**) are shown as solid orange and red lines, respectively. The discrepancy between the raw and simulated scattering data is indicated by the value of χ^2. The small χ^2 value observed (1.43 for RNase R^{WT} and 0.68 for RNase R^{723}) demonstrates a robust fit.

2.4.2 Identification of Functionally Important Residues in the K-rich Domain of RNase R

In an effort to uncover the identities of functionally important residues in the K-rich domain, we generated a series of alanine substitution variants of RNase R. We were guided by previous studies of the K-rich domain, which demonstrated that C-terminal truncations from residue 813 to 750 (RNase R^{750}) had no effect on the *trans*-translation related activity of RNase R [36]. These studies also showed that a further truncation of 15 residues in the K-rich domain, to amino acid residue 735 (RNase R^{735}), resulted in a discernible defect in the ability of the enzyme to degrade non-stop mRNA. RNase R truncation variant RNase R^{723}, which lacks the entire K-rich region, exhibited a similar pronounced defect in degradation of non-stop mRNA [36]. Based on these results, we reasoned that some of the critical amino acid residues, responsible for the *trans*-translation activity of RNase R, must lie in the region encompassing residues 735 to 750. To evaluate the validity of this inference, we performed alanine-scanning mutagenesis of conserved amino acid residues in this region and assessed their contribution to the SmpB-tmRNA mediated targeted degradation of non-stop mRNA. To facilitate this assessment, we used plasmid-encoded reporter transcripts that are comprised of the coding sequence for the N-terminal domain of the bacteriophage λ *cI* gene followed by the *trp* operon transcriptional terminator (*trp*At). To ensure evaluation of a non-stop mRNA specific process, we utilized two related versions of this reporter (Figure 2.2A), a non-stop transcript lacking in-frame stop codons (λ-cI-NS), and a "normal" control transcript possessing an in-frame stop codon (λ-cI-S). The λ-cI-NS non-stop transcript has been well characterized and is known to promote ribosome stalling at its 3′ end, whereas the stop codon containing λ-cI-S variant is readily translated and promotes efficient recycling of the translation machinery [57, 60]. The competence of RNase R alanine substitution variants in reporter mRNA decay was analyzed in a strain lacking chromosomal *rnr* and bearing plasmids for controlled expression of both the reporter transcript and one of the RNase R alanine substitution variants. Expression of

RNase R, and its variants, was from a pACYCDuet-based plasmid bearing the *rnr* coding sequence under the control of the arabinose inducible P_{BAD} promoter.

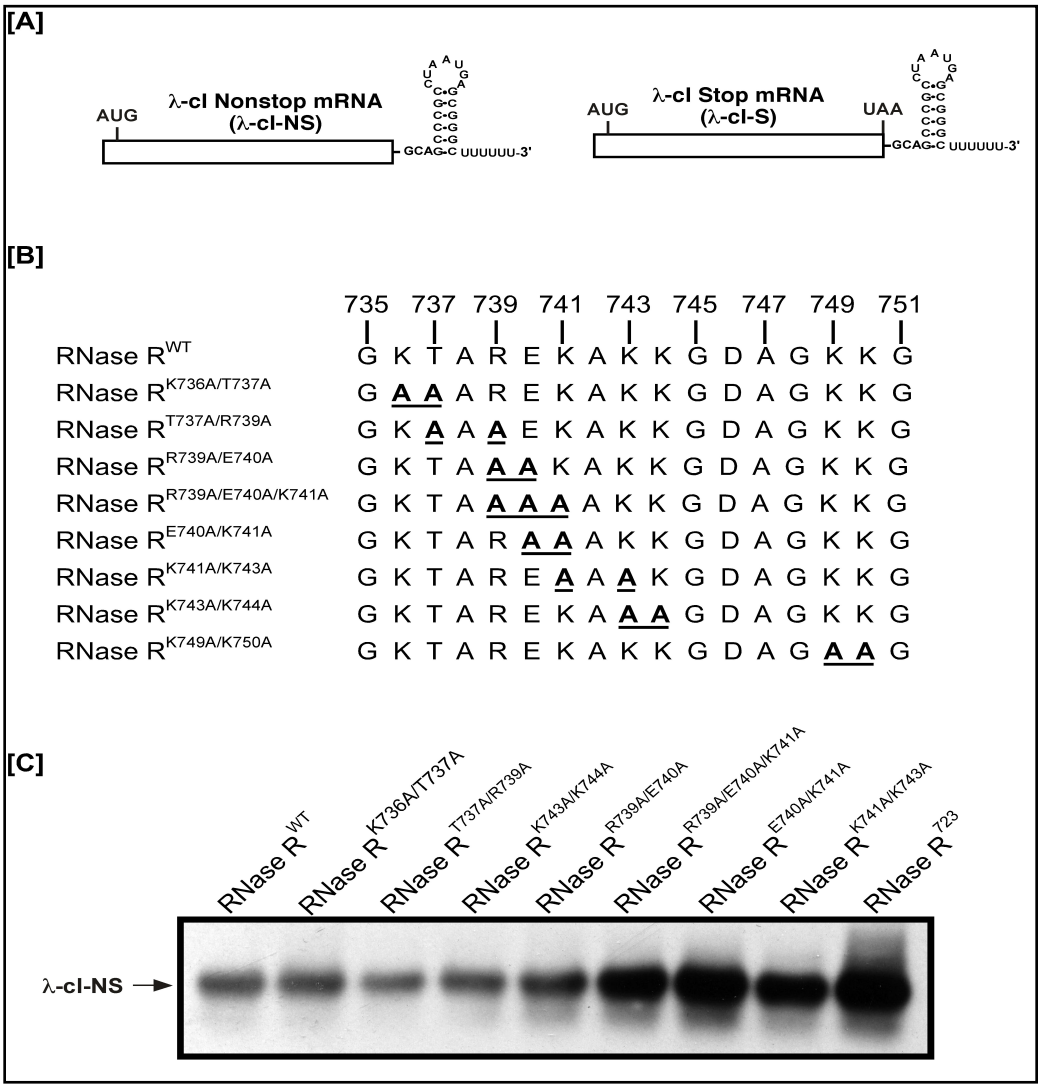

Figure 2.2 Steady state level of nonstop reporter mRNA. (A) A schematic representation of the reporter mRNAs used in this study. The λ-cI non-stop reporter (λ-cI-NS) is composed of the coding region of λ-cI N-terminal domain (depicted as a rectangle) followed by the transcriptional terminator (*trp*At nucleotide sequence at the 3′ end). The corresponding λ-cI stop reporter (λ-cI-S) has an in-frame UAA stop codon before the transcriptional terminator. (**B)** A representation of alanine substitutions in the region between amino acids 735 and 750 of the K-rich domain. (**C)** A representative Northern blot showing the effect of alanine substitutions in the region between residues 735 and 750 on non-stop mRNA accumulation. Cells co-expressing the λ-cI-NS reporter with indicated plasmid-borne RNase R variants were harvested. Total RNA samples isolated from equal number of cells were resolved by electrophoresis on denaturing formaldehyde agarose gels followed by Northern blot analysis with a probe specific for the reporter RNA. Alanine substitutions at residues E740 and K741 exhibit significant defect in non-stop mRNA degradation.

We expressed each RNase R alanine substitution variant alongside the λ-cI-NS reporter mRNA, and measured the relative steady state abundance of the non-stop transcript. For all mRNA stability assessments, we used RNase R^{WT} as a positive control and the previously validated RNase R^{723} truncation variant [36] as a negative control. This analysis showed that various combinations of single and double alanine substitutions at residues K736, T737, and R739 had little or no effect on the steady state level of the reporter mRNA (Figures 2.2B,C). Similarly, single and double alanine substitutions at residues K743 and K744 had no effect on the steady state level of the non-stop reporter mRNA (Figure 2.2C). Alanine substitution at E740 or K741, either individually or in combination with other neighboring residues (RNase $R^{R739A/E740A}$ and RNase $R^{K741A/K742A}$), resulted in measurable increases in the accumulation of non-stop mRNA (Figure 2.2C), indicating a functional role for these adjoining residues in the mRNA decay activity of RNase R. To further investigate their functional contributions, we generated RNase $R^{E740A/K741A}$, a double alanine substitution variant at residues E740 and K741. Assessment of RNase $R^{E740A/K741A}$ revealed profound defects in non-stop mRNA degradation (Figure 2.2C). Alanine substitution of two additional conserved residues (K749 and K750) in the region between 735 and 750 (RNase $R^{K749A/K750A}$) resulted in extensive accumulation of non-stop mRNA, suggesting that these residues also played an important role in the selective non-stop mRNA decay activity of RNase R (Figure 2.3A). Collectively, these data implied that conserved residues E740–K741 and K749–K750 play a crucial role in the *trans*-translation mediated decay of non-stop mRNA.

To obtain a more quantitative measure of the non-stop mRNA degradation defect of the alanine substitution mutants, we selected three double-alanine substitution variants (RNase $R^{T737A/R739A}$, RNase $R^{E740A/K741A}$, and RNase $R^{K749A/K750A}$) for further evaluation. First, we examined the relative differences in the steady state abundance of non-stop mRNA among these variants, using RNase R^{WT} and RNase R^{723} as controls (Figure 2.3A). This analysis showed no significant difference in the ability of RNase R^{WT} and RNase $R^{T737A/R739A}$ in the selective degradation of the λ-cI-NS non-stop mRNA. In contrast, alanine substitution variants RNase $R^{E740A/K741A}$ and RNase $R^{K749A/K750A}$consistently exhibited a 2.5 to 3-fold defect in degradation of the λ-cI-NS

reporter; a defect that was statistically significant and similar to the defect exhibited by RNase R^{723} (Figure 2.3A). To eliminate the possibility that the observed non-stop mRNA stability defects of these RNase R variants were due to differences in their relative abundance, we compared their steady state levels to RNase R^{WT} and RNase R^{723} under identical experimental conditions. This analysis revealed no significant differences in the steady state levels of these RNase R variants (Figure 2.3B), suggesting expression or stability difference could account for the observed non-stop mRNA decay defects exhibited by these RNase R variants.

Next, we measured the *in vivo* decay rate and half-life ($t_{1/2}$) of the λ-cI-NS non-stop mRNA in the presence of RNase R^{WT}, RNase $R^{E740A/K741A}$, and RNase $R^{K749A/K750A}$ (Figure 2.4). Consistent with previous studies, RNase R^{WT} degraded the λ-cI-NS report transcript very efficiently, with a $t_{1/2}$ of 0.8 ± 0.3 min (Figure 2.4A). RNase $R^{E740A/K741A}$ had a strong defect in the non-stop mRNA degradation, increasing $t_{1/2}$ by roughly 4-fold to 3.2 ± 0.4 min (Figures 2.4A,B). We found this deficiency in non-stop mRNA decay reminiscent of the defect observed with the RNase R^{723} truncation variant. Similarly, in the presence of RNase $R^{K749A/K750A}$, we detected a substantial increase in the stability of the non-stop reporter mRNA with a $t_{1/2}$ of 2.0 ± 0.1 min (Figure 2.4C). Based on these findings, we conclude that residues E740–K741 and K749–K750 in the K-rich domain of RNase R play important but distinct roles in the selective degradation of non-stop mRNA.

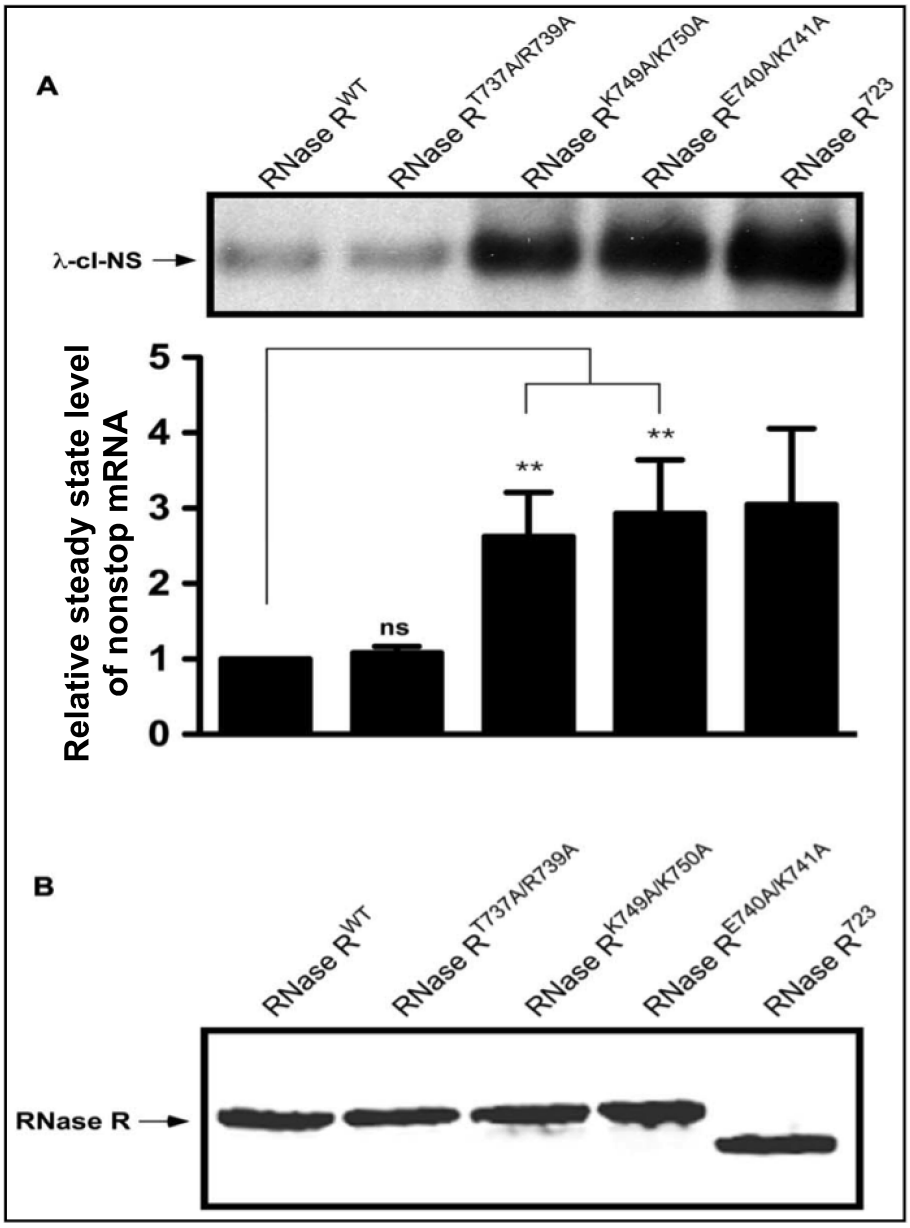

Figure 2.3 Non-stop reporter mRNA accumulates in the presence of RNase $R^{K749A/K750A}$, and RNase $R^{E740A/K741A}$. (A) A representative Northern blot showing the steady state level of nonstop mRNA in the presence of RNase $R^{T737A/R739A}$, RNase $R^{K749A/K750A}$, and RNase $R^{E740A/K741A}$. The latter two variants are defective in non-stop mRNA degradation. *P*-values were calculated by performing student's *t*-test analysis with RNase R^{WT} and RNase $R^{K749A/K750A}$ ($^{**}P$ <0.005) or RNase R^{WT} and RNase $R^{E740A/K741A}$ ($^{**}P$ <0.003). The graph represents the fold change in the steady state level of λ-cI-NS mRNA in the presence of indicated RNase R variants with respect to RNase R^{WT}. The data are combined from three independent experiments (MEAN ± SEM, standard error of the mean). ns = not statistically significant. **(B)** Steady state levels of RNase R variants are similar. A representative Western blot examining the relative steady state levels of RNase R and its alanine-substitution variants is shown. MG1655 *rnr* strain harboring each p*rnr* variant plasmid was grown in LB with 0.01% arabinose and 30 µg/ml of chloramphenicol. Equal numbers of cells were harvested in mid-log phase and processed for Western blot analysis, using RNase R specific antibodies.

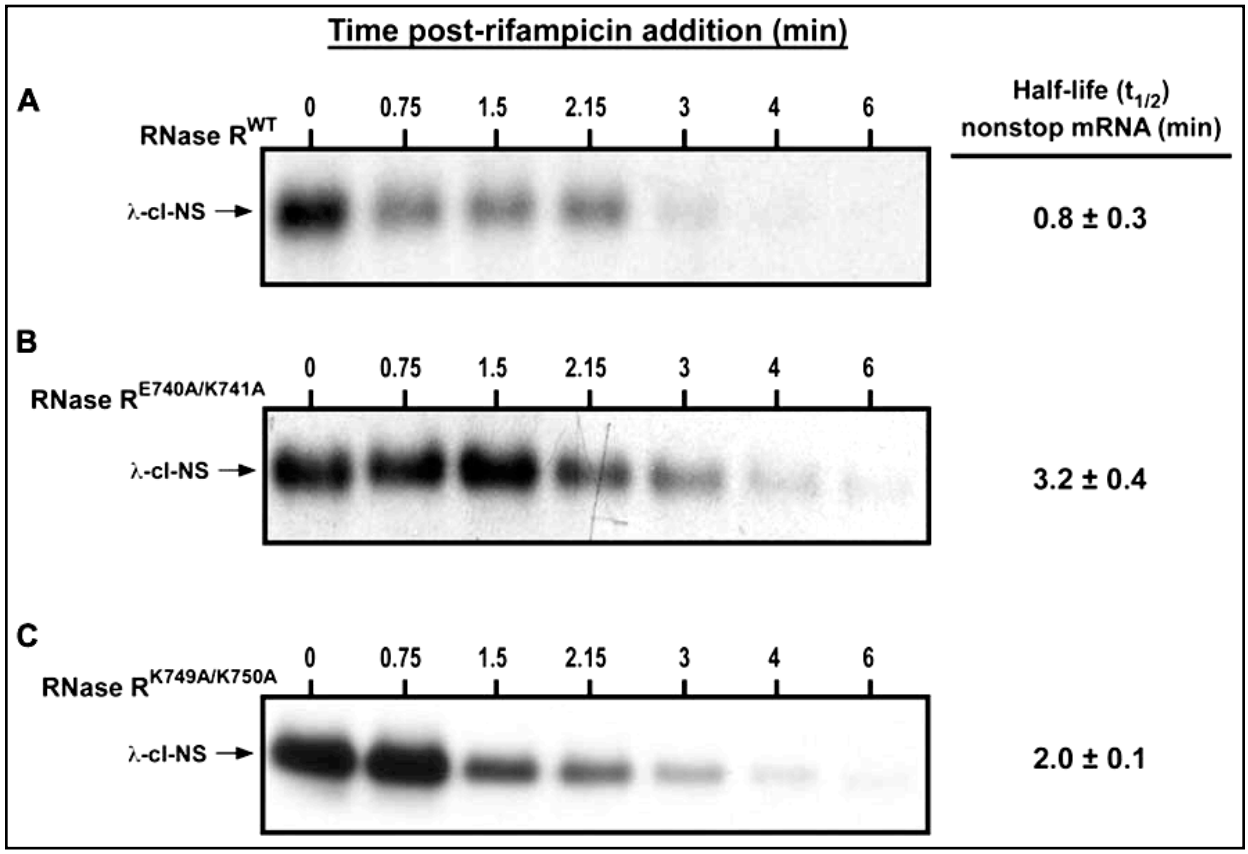

Figure 2.4 Non-stop mRNA half-life increase in the presence of RNase $R^{E740A/K741A}$ and RNase $R^{K749A/K750A}$. Cells co-expressing λ-cI-NS with the indicated plasmid-borne RNase R variants were harvested at the indicated time points after the addition of rifampicin. Total RNA samples isolated from equal number of cells were subjected to Northern analysis. Intensities of the bands corresponding to the λ-cI-NS reporter were quantified using ImageJ. Non-stop mRNA half-life was calculated by linear regression analysis using the Prism software. The data are combined from three independent experiments (MEAN ± SEM). **(A)** Non-stop mRNA is degraded rapidly ($t_{1/2}$ = 0.8 ± 0.3 min) in the presence of RNase R^{WT}. **(B)** RNase $R^{E740A/K741A}$ is considerably defective in non-stop mRNA degradation ($t_{1/2}$ = 3.2 ± 0.4 min). **(C)** RNase $R^{K749A/K750A}$ exhibited moderate defect in the degradation of non-stop mRNA ($t_{1/2}$ = 2.0 ± 0.1 min).

2.4.3 Mutations in the K-rich Domain of RNase R do not Affect its Catalytic Activity *in vitro*

One possible mechanistic explanation for the observed non-stop mRNA decay defect of RNase $R^{E740A/K741A}$ and RNase $R^{K749A/K750A}$ could be that these residues (K740–K741 and K749–K750) interact directly with the catalytic core of RNase R to modulate its ribonuclease activity. To assess this possibility, we examined the exoribonuclease activity of each alanine substitution variant in an *in vitro* RNA degradation assay. To this end, we overexpressed RNase R^{WT}, RNase $R^{E740A/K741A}$, and RNase $R^{K749A/K750A}$, in an *rnr*$^{-}$ *rnb*$^{-}$ strain, and purified each protein to near homogeneity (Figure 2.5A). The ribonuclease activity of each purified enzyme was assessed by its ability to degrade the *trp*At-A_{10} substrate, a 32-nucleotide long structured RNA containing the *trpA*-terminator stem-loop followed by a stretch of 10 adenines at its 3′ end. Degradation reactions were initiated by the addition of the respective RNase R variant and terminated at the indicated time points by the addition of denaturing sample buffer. The reaction products were resolved by electrophoresis on denaturing polyacrylamide gels (Figure 2.5B), with the activity of each RNase R variant indicated by the disappearance of the full-length substrates and appearance of lower-molecular-weight 2–5 nucleotide products. Using this assay, we observed that RNase $R^{E740A/K741A}$ and RNase $R^{K749A/K750A}$ were as proficient in degradation of this structured RNA substrate as RNase R^{WT} (Figures 2.5B,C). This result indicated that alanine substitutions at amino acid pairs E740–K741 and K749–K750 did not compromise the ability of RNase R to unwind and degrade this RNA substrate, implying that these defined alterations did not impact intramolecular interactions of the K-rich domain with the catalytic core but rather had a specific effect on the *trans*-translation dependent activity of RNase R.

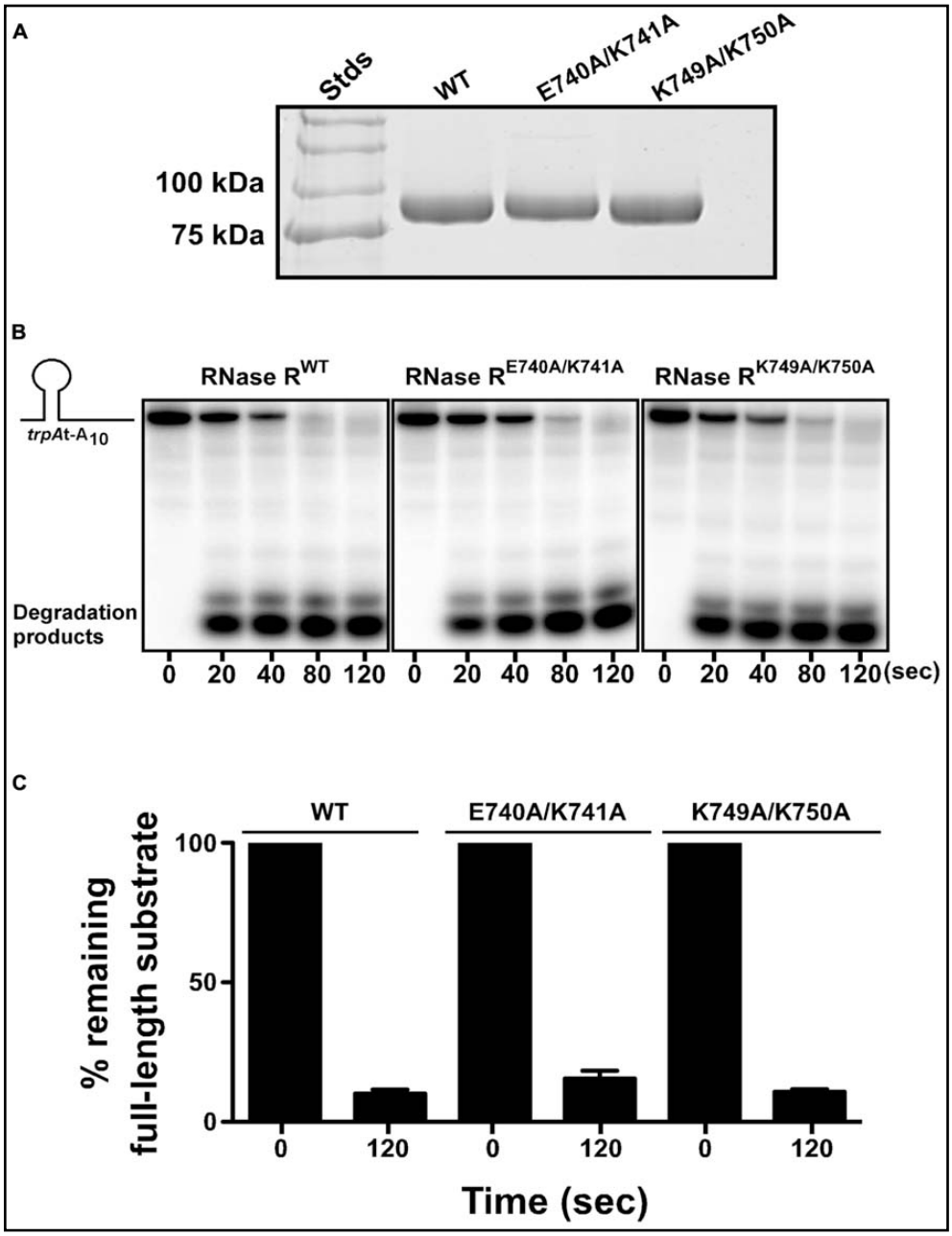

Figure 2.5 RNase R variants degrade RNA substrates *in vitro*. (A) Coomassie stained protein gel showing purified RNase R variants. RNase R and its variants (RNase $R^{E740A/K741A}$ and RNase $R^{K749A/K750A}$) were purified from an *rnr*$^{-}$ rnb^{-} strain, resolved by electrophoresis on a 10% SDS-polyacrylamide gel, and stained with Coomassie Brilliant blue. **(B)** Representative autoradiographs showing the degradation of *trp*At-A_{10} RNA substrate by indicated RNase R variants. The ^{32}P-labeled RNA substrate was used to test the degradation capability of RNase $R^{E740A/K741A}$ and RNase $R^{K749A/K750A}$. Purified RNase R variants were incubated with the RNA substrate at 37°C. The reactions were stopped at indicated times, using denaturing RNA loading dye, and resolved by electrophoresis on denaturing polyacrylamide gel. **(C)** The autoradiographs obtained were used to quantify the amount of full-length RNA substrate present at the start (0 s) and the end (120 s) of the reaction. The data are combined from three independent experiments (MEAN ± SEM).

2.4.4 Residues E740–K741 and K749–K750 are Essential for RNase R Enrichment on Stalled Ribosomes

The SmpB-tmRNA system rescues ribosomes stalled at the 3′ end of non-stop mRNAs and recruits RNase R to initiate non-stop mRNA decay [36, 37, 57]. Our previous studies revealed that the inability of C-terminal truncation variant RNase R^{723} to degrade non-stop mRNA was due to a defect in ribosome enrichment [36]. This result suggested that the K-rich domain was essential for association of RNase R with rescued ribosomes. We hypothesized that the stabilization of non-stop mRNA in the presence of RNase $R^{K749A/K750A}$and RNase $R^{E740A/K741A}$ could similarly be due to their inability to productively engage tmRNA-rescued ribosomes. To examine this inference, we used the ribosome enrichment assay [57] to analyze the effect of the K-rich domain alanine substitution variants on the association of RNase R with tmRNA-rescued ribosomes. To ensure the RNase R recruitment process was specific to the λ-cI-NS non-stop transcript, and to verify that we were examining tmRNA-rescued ribosomes, we used the stop codon containing λ-cI-S reporter as a negative control, and routinely examined the captured ribosome fractions for the presence and enrichment of SmpB protein. As expected, analysis of the λ-cI-NS reporter in *rnr*$^-$ cells expressing the plasmid borne full-length enzyme showed enrichment of RNase R on ribosomes expressing the non-stop reporter (Figure 2.6A). Quantification of ribosome enrichment data, from several independent experiments, showed greater than 3-fold RNase R^{WT} enrichment on ribosome translating the λ-cI-NS non-stop reporter as compared to the λ-cI-S control transcript (Figure 2.6B). In contrast, ribosome enrichment analysis of the RNase $R^{E740A/K741A}$ variant in *rnr*$^-$ cells revealed only background level of ribosome association in cells expressing either the λ-cI-NS or λ-cI-S reporter transcript (Figure 2.6). Although we consistently detected a small but reproducible increase in enrichment of the RNase $R^{K749A/K750A}$variant on stalled ribosomes (Figures 2.6A,B), this level of enrichment did not fully reflect the observed increase in non-stop mRNA half-life. We attribute this difference to the fact that the ribosome enrichment assay, which involves several *in vitro* processing steps, is not sensitive enough to detect intermediate level enrichment of RNase R variants, whereas the rifampicin-chase assay is more

sensitive in detecting subtle differences in non-stop mRNA degradation rates. Based on these findings, we conclude that the non-stop mRNA decay defect of RNase $R^{E740A/K741A}$ and RNase $R^{K749A/K750A}$ is due to the failure of these variants to productively engage tmRNA-rescued ribosomes.

Alanine substitution at residues E740 and K741 appears to have a profound effect on the *trans*-translation related activity of RNase R. Given the nature of these amino acids, it was conceivable that they interacted with each other, perhaps by forming a salt bridge required for maintaining intramolecular contacts. The presence of these contacts might be important for the non-stop mRNA degradation activity of RNase R. We reasoned that swapping the positions of these residues could preserve these interactions, and hence the *trans*-translation activity of RNase R on stalled ribosomes. To assess this possibility, we constructed the RNase $R^{E740K/K741E}$ switch variant and performed ribosome enrichment assays. This analysis showed that the E–K switch variant (RNase $R^{E740K/K741E}$) had a strong defect in association with tmRNA-rescued ribosomes (Figure 2.7). This finding indicated that the position and orientation of residues E740 and K741 are important for productive engagement of RNase R with the *trans*-translation machinery.

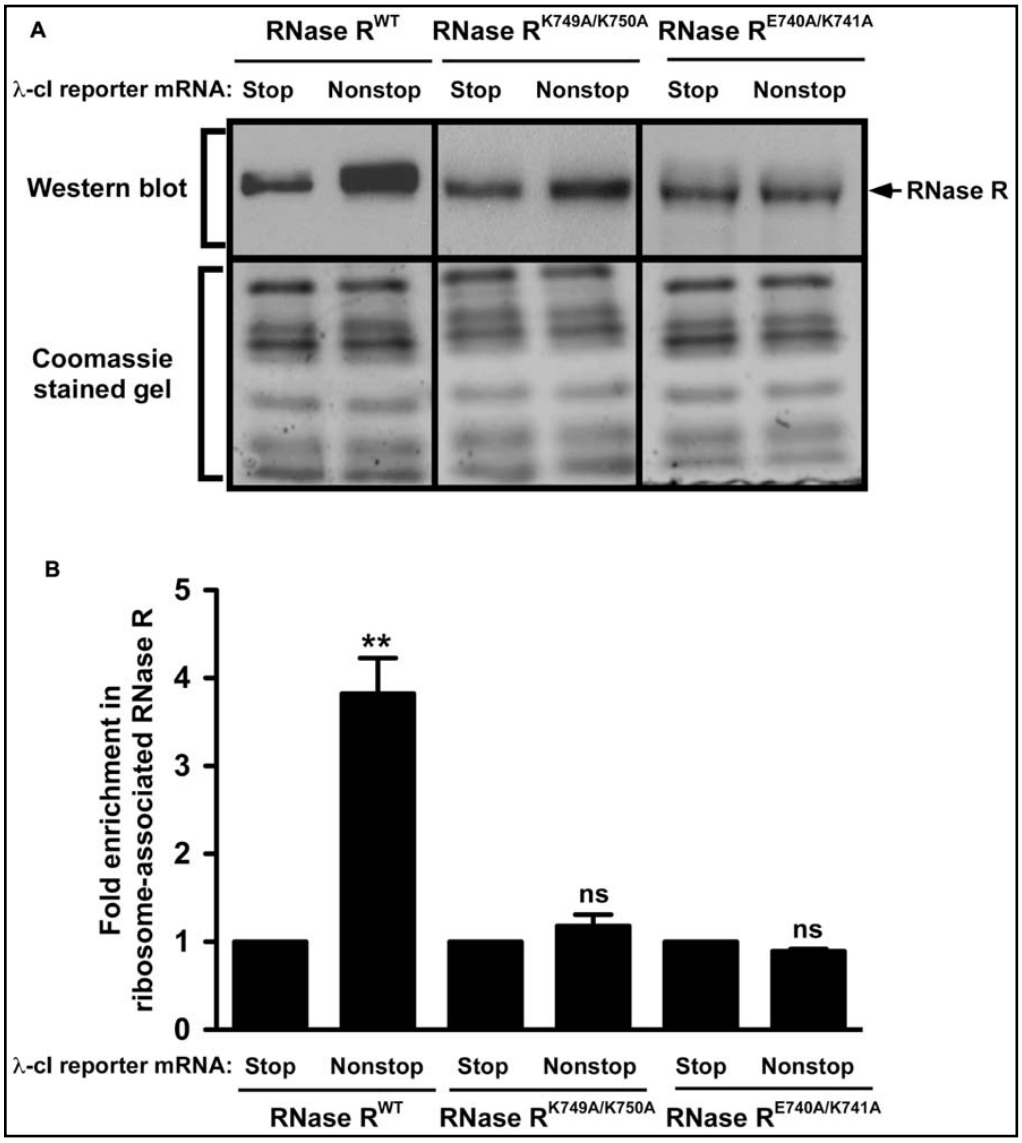

Figure 2.6 RNase R variants exhibit defects in enrichment on ribosomes translating non-stop mRNA. (A) Total ribosomes were obtained from cells co-expressing indicated RNase R variants with the λ-cI-S or λ-cI-NS reporter mRNAs. Ribosomes translating the reporter RNAs were isolated from the total ribosomes pool using Ni^{2+}-NTA affinity chromatography. Equal numbers of ribosomes were resolved by electrophoresis on 10% SDS-polyacrylamide gels. Western blot analysis was performed to detect the presence of RNase R. The intensity of the band corresponding to RNase R was quantified using ImageJ. The top panel shows a representative Western blot, using an RNase R specific antibody, and the bottom panel shows a section of the corresponding Coomassie stained gel displaying equal protein loading. **(B)** The graph represents fold RNase R enrichment on ribosomes translating the λ-cI-NS reporter compared to ribosomes translating the control λ-cI-S reporter. The data are combined from three independent experiments (MEAN ± SEM). *P*-values were calculated by performing student's *t*-test analysis on the association level of RNase R^{WT} and RNase $R^{K749A/K750A}$ (**P <0.003) or RNase R^{WT} and RNase $R^{E740A/K741A}$ (**P <0.002) on stalled ribosomes translating λ-cI-NS reporter. ns = not statistically significant.

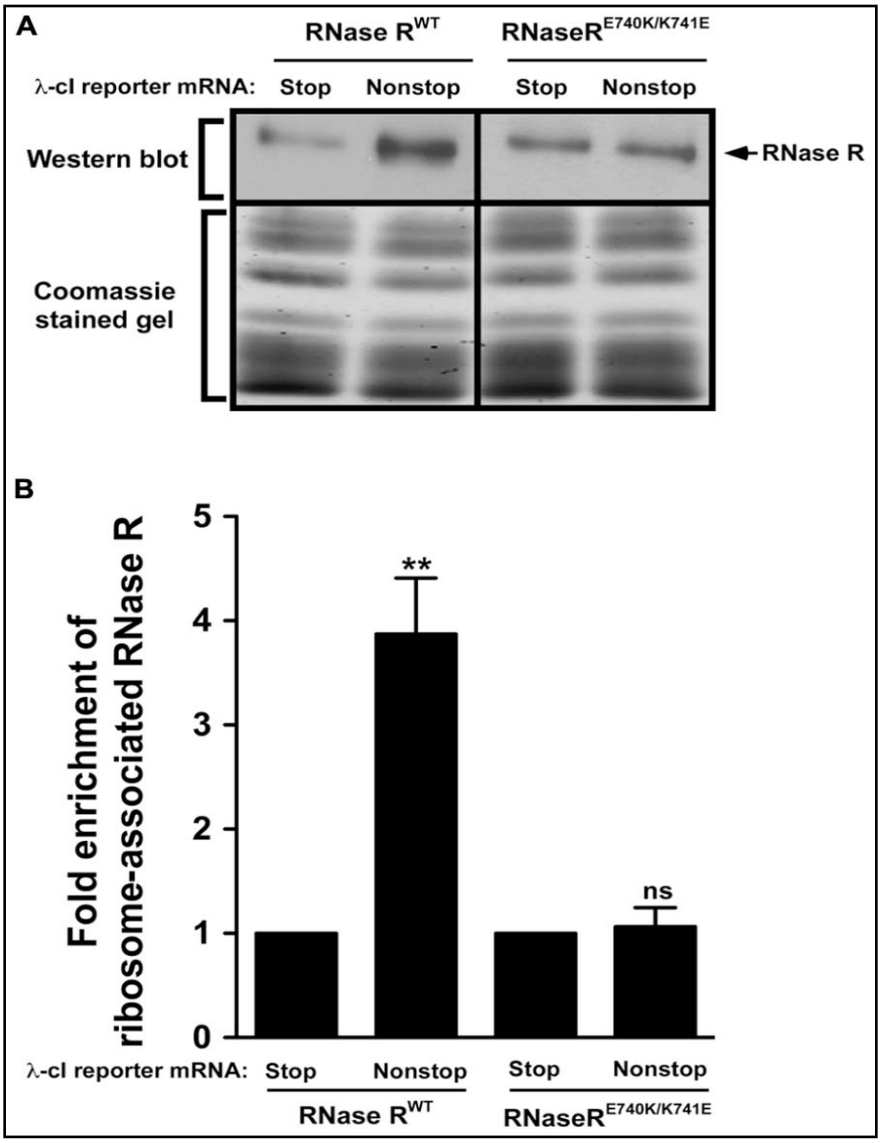

Figure 2.7 Swapping of residues E740 and K741 renders RNase R defective in enrichment on stalled ribosomes. (A) Enriched ribosomes were obtained from cells co-expressing RNase R^{WT} or the RNase $R^{E740K/K741E}$ switch variant with either the λ-cI-S or λ-cI-NS reporter mRNA. Western blot analyses were performed as described in Figure 2.6. Intensities of the bands were quantified using ImageJ. The top panel shows a representative Western blot, using an RNase R specific antibody, and the bottom panel shows a section of the corresponding Coomassie stained gel displaying equal protein loading. **(B)** The graph represents fold enrichment of RNase R on stalled ribosomes compared to its corresponding background level with the control λ-cI-S reporter. The data are combined from three independent experiments (MEAN ± SEM). *P*-values were calculated by performing student's *t*-test analysis on the association level of RNase R^{WT} and RNase $R^{E740K/K741E}$ (**P <0.008) on stalled ribosomes translating λ-cI-NS reporter. ns = not statistically significant.

2.5 Discussion

RNase R is a versatile 3′–5′ exoribonuclease with the distinctive ability to unwind and degrade structured RNA substrates without ATP consumption [61, 62]. RNase R does not exhibit sequence specificity and is thus involved in the processing and turnover of a diverse array of cellular RNAs, including mRNA, rRNA, and tRNAs [63, 64]. Given the broad range of RNase R functions, it is of high interest to understand its overall architecture and the spatial arrangement of its distinct N- and C-terminal domains. Similarly, given its lack of substrate specificity it is of particular interest to understand how this general exoribonuclease is recruited to stalled ribosomes to carry out selective degradation of non-stop mRNAs. Our explorations into the global architecture of the *E. coli* RNase R have yielded the first glimpses of its overall shape and domain arrangement, indicating a tri-lobed structure with a core catalytic domain that is highly similar to the known crystal structure of RNase II. Our data show that the unique N- and C-terminal domains of RNase R flank the catalytic core of the protein. Consistent with bioinformatics analysis [59], our SAXS and homology modeling data suggest that in the absence of any bound partners or substrates the K-rich domain has significant structural flexibility. Our findings are thus consistent with the notion that the K-rich domain is disordered in solution but might adopt a more ordered structure upon binding to interacting partners, such as RNA or ribosomal components.

Recent studies suggest that the K-rich domain confers a variety of properties on RNase R, including enhancing its affinity for RNA, modulating its ability to degrade structured substrates [59] and regulating its *in vivo* stability. Our data suggest potential contacts between the catalytic core and the K-rich domain of RNase R. This indication is consistent with the notion that the K-rich region interacts with the core of the enzyme and plays a regulatory role. Characterization of one such contact suggested that acetylation of Lys544 plays a key regulatory role in interactions of the K-rich domain and the catalytic core of the enzyme, with implications for both function and stability of the protein [45]. It was proposed that the un-acetylated form of K544 prevents binding of the

SmpB-tmRNA complex and as a consequence prevents degradation of RNase R by cellular proteases [45]. Although the key components of the *trans*-translation system play a role in destabilization of RNase R, it has not been determined whether this is a direct consequence of the *trans*-translation process. Furthermore, the precise amino acid residues necessary for this intramolecular interaction have not been identified.

Previous work from our lab established that the unique K-rich domain of RNase R is required for the *trans*-translation mediated decay of non-stop mRNAs. These studies also suggested that some of the key functional amino acids reside in the region between residues 735 and 750 of the K-rich domain. Here, we presented a detailed analysis of the contributions of this functionally important region of the K-rich domain to the *trans*-translation process. We have identified key amino acid residues (E740, K741, K749, and K750) in the K-rich domain that are involved in the selective and SmpB-tmRNA dependent elimination of non-stop mRNA. Alanine substitution of residues E740 and K741 significantly weaken the recruitment of RNase R to tmRNA-rescued ribosomes and as a consequence diminish its ability to selectively degrade the associated non-stop mRNA. In addition, simultaneous mutation of residues K749 and K750 renders RNase R markedly defective in non-stop mRNA decay. It is interesting to note that the effect of these alanine substitutions is specific to the *trans*-translation related activity of RNase R, as they do not compromise its catalytic activity. These four conserved residues, particularly E740 and K741, might exert their influence on the activity of RNase R by participating in decisive intra- or intermolecular interactions. Our data suggest that these amino acids most likely participate in intermolecular interactions with components of the rescued ribosome. We proposed that ribosomal RNA or ribosomal proteins might interact directly with these residues, thereby enabling RNase R to productively engage stalled ribosomes. Taken together, these investigations have shed new light on the global architecture and the relative spatial arrangement of the N- and C-terminal domains of RNase R and highlight the functional significance of key conserved residues in the *trans*-translation related activities of this versatile enzyme.

Chapter 3: Distinct tmRNA and SmpB Sequence Elements Facilitate RNase R Dependent Nonstop mRNA Decay

3.1 Abstract

trans-Translation, orchestrated by SmpB and tmRNA, is the principal eubacterial pathway for resolving stalled translation complexes. RNase R, the leading nonstop mRNA surveillance factor, is recruited to stalled ribosomes in a *trans*-translation dependent process. To elucidate the contributions of SmpB and tmRNA to RNase R recruitment, we evaluated chimeric *E. coli* – *Francisella tularensis* variants of tmRNA and SmpB. This analysis showed that while the hybrid tmRNA supported nascent polypeptide tagging and ribosome rescue, it suffered defects in facilitating RNase R recruitment to stalled ribosomes and nonstop mRNA decay. To gain further insights, we used established tmRNA and SmpB variants that impact distinct stages of the *trans*-translation process. Analysis of select tmRNA variants revealed that the ultimate and penultimate codons of the tmRNA ORF play a crucial role in facilitating RNase R recruitment to rescued ribosomes. Analogously, examination of defined SmpB C-terminal tail variants (Gly132Glu, and Ile153Asp/Met154Glu) highlighted the importance of establishing the correct tmRNA reading frame, and provided clues into the timing of RNase R recruitment to rescued ribosomes. Taken together, these studies demonstrate that productive engagement of RNase R on tmRNA-rescued ribosomes requires active *trans*-translation, and suggest that RNase R captures the emerging nonstop mRNA post establishment of the tmRNA ORF as the surrogate mRNA template.

3.2 Introduction

Ribosomes perform the essential task of protein synthesis in all cells. The translation machinery use genetic information encoded within messenger RNAs (mRNAs) to synthesize new polypeptides. However, defective mRNAs that lack some of the required information content arise routinely and cause a myriad of problems for the cell. For instance, generation of nonstop mRNAs, mRNAs that lack an in-frame stop codon, trigger ribosome stalling and sequestration of the components of the translation machinery [15, 22, 38-40, 65]. Such unproductive sequestration of ribosomes could lead to severe reduction in the protein-synthesis capacity of the cell, diminishing its ability to respond to environmental changes and compete for resources with its neighbors.

Nature has evolved a variety of quality control mechanisms to counteract futile ribosome-stalling events, and ensure the efficiency and accuracy of protein synthesis. Among the three pathways discovered in bacteria, *trans*-translation is the major mode of translational quality control. The importance of this system is exemplified by the fact that it is essential for survival and/or virulence of several pathogenic bacterial species [7, 17-19, 66]. The two key components of this highly conserved system are transfer-messenger RNA (tmRNA) encoded by the *ssrA* gene [16] and its essential protein partner Small protein B (SmpB) [42]. The 3′ and 5′ ends of tmRNA fold to form a tRNA-like domain that is recognized and aminoacylated by alanyl-tRNA synthetase. tmRNA also contains an mRNA-like domain with a short open reading frame (ORF) in lieu of the anticodon loop. SmpB is a small globular protein that binds to the tRNA-like domain of tmRNA and delivers it to stalled ribosomes [42]. Previous studies have shown that the C-terminal tail of SmpB plays an important role in proper accommodation and accurate decoding of the tmRNA ORF [11, 13]. Together with elongation factor Tu (EF-Tu) and GTP, alanine-charged tmRNA and SmpB form a quaternary complex that recognizes stalled ribosomes with an empty A-site, devoid of coding information. Once Ala-tmRNA is accommodated in the A-site, the nascent polypeptide chain is transferred to the

alanine residue on the tRNA-like domain of tmRNA. By a mechanism that is facilitated in part by amino acid residues in the C-terminal tail of SmpB, the lead ribosome switches from the defective mRNA template, and starts decoding the tmRNA ORF as a surrogate template [11]. The tmRNA ORF also encodes for an in-frame stop codon that ensures proper termination of protein synthesis, ribosome rescue, and recycling of components of the translation machinery. As a consequence, the nascent polypeptide is co-translationally appended with a short peptide sequence (the ssrA tag or degron) encoded by the tmRNA ORF. The ssrA degron marks the nascent polypeptide for degradation by various cellular proteases [16, 67-70].

Persistence of aberrant nonstop transcripts in the cell could lead to futile cycles of translation. Targeted elimination of such defective mRNA transcripts is a distinct outcome of the *trans*-translation process. In order to capture and degrade aberrant mRNAs, a 3'-5' exoribonuclease, RNase R, is recruited to SmpB-tmRNA rescued ribosomes. Recent studies have demonstrated that the unique C-terminal lysine-rich domain of RNase R is essential for the *trans*-translation related activity of RNase R [37, 71]. Investigations into the importance of the tmRNA ORF in nonstop mRNA decay revealed that mutating the last two codons in the tmRNA ORF increase the half-life of nonstop mRNAs in the cell [72]. Although it is known that SmpB and tmRNA are essential for selective degradation of defective mRNAs, their precise role in enabling RNase R to perform this targeted task is not clearly understood.

The SmpB-tmRNA ribosome rescue complex recognizes and binds stalled ribosome with an empty decoding center. A recent structural model of the ribosome-bound SmpB-tmRNA complex revealed finer details of the initial A-site binding stage of the *trans*-translation process [73]. Consistent with biochemical studies, upon binding to the stalled ribosome, the C-terminal tail of SmpB occupies the empty mRNA channel, presumably making critical contacts with components of the channel and the A-site decoding center [11, 13, 74]. These putative contacts must subsequently be disrupted in order for the tmRNA ORF to be established as the surrogate mRNA template. Biochemical analyses of SmpB protein show that mutations in the hinge region, especially the highly conserved Gly132 and residues Ile153 and Met154 in the C-

terminal tail, abolish proper establishment of tmRNA ORF and the subsequent peptide tagging activity [11, 13]. The functions of SmpB and tmRNA in directed-proteolysis of nascent polypeptide have been studied in great detail. However, the mechanistic detail of when and how the SmpB-tmRNA system facilitates proper engagement of RNase R has remained unexplored.

In studies described herein, we present biochemical evidence that provide insights into the effect of SmpB and tmRNA on the productive engagement of RNase R on rescued ribosomes. In an effort to decipher the contributions of specific SmpB and tmRNA sequence elements to nonstop mRNA decay, we designed hybrid versions of SmpB and tmRNA, from genetically distant bacterial species, in which the mRNA-like domain of tmRNA or the C-terminal tail of SmpB from *E. coli* was substituted with the equivalent sequences from *Francisella tularensis*. From the study of hybrid constructs, we observed that while the tmRNA ORF hybrid was functionally active in rescuing stalled ribosomes and tagging the defective polypeptides, it exhibited significant defects in recruitment of RNase R to stalled ribosomes. Furthermore, these defects were not mitigated when the cognate SmpB C-terminal tail hybrid was co-expressed. We also used well-characterized SmpB and tmRNA variants that affect defined stages of the *trans*-translation process to ascertain the requirements for RNase R engagement on rescued ribosomes and commencement of nonstop mRNA decay. This analysis revealed that sequence elements within the distal part of the tmRNA ORF and the C-terminal tail of SmpB play decisive roles in the facilitating RNase R enrichment on stalled ribosomes and initiating nonstop mRNA decay. Taken together, our investigations demonstrate that productive engagement of RNase R with the rescued ribosome requires the presence of specific tmRNA sequence elements, and occurs after establishment of the tmRNA ORF as the surrogate template.

3.3 Materials and methods

3.3.1 Strains and plasmid

E. coli strain W3110 *rnr::kan*^{r} Δ*smpBssrA* was obtained by P1 transduction using Keio deletion strains as donors [48]. The coding region of N-terminal domain of λ-cI protein was used as the reporter gene (pλ-cI-nonstop or pλ-cI-NS). A corresponding stop reporter plasmid (pλ-cI-stop or pλ-cI-S) was synthesized by introducing two tandem stop codons (TAA) before the transcriptional terminator sequence by PCR based site-directed mutagenesis. It has six histidine (His6) codons at the 5' end of the coding region. pACYCDuet-1 plasmid harboring *E. coli* SmpB-SsrA under native promoter in MCS-1 and *E. coli*- or *F. tularensis*-derived RNase R under P_{BAD} promoter in MCS-2 was used as a template to synthesize single and double hybrids of SmpB and tmRNA (pBA-R). *E. coli* – *F. tularensis* hybrid of SmpB (SmpB^{FT}) was synthesized by swapping the region coding for residues 128 – 160 of *E. coli* SmpB with the region coding for residues 128 – 157 of *F. tularensis* SmpB. tmRNA ORF hybrid (tmRNA^{FT}) was synthesized by swapping tmRNA ORF and helix 5 of *E. coli* (bases 90 – 150) with that of *F. tularensis* (bases 110 – 200). SmpB I154D/M155E and SmpB G132E variants in pBA-R plasmid were obtained by PCR based site-directed mutagenesis. The last two alanine codons of *E. coli* tmRNA ORF in pBA-R plasmid were mutagenized to two aspartic acid codons (pBA^{DD}-R) by PCR based site-directed mutagenesis. To generate pBA^{ED}-R plasmid, encoding the tmRNA^{ED} variant, codons for aspartic acid and glutamic acid at positions three and four of the tmRNA ORF were swapped by PCR based site-directed mutagenesis. Various plasmid constructs used in this study are listed in the Table 1.

Plasmid	MCS1	MCS2
pBA-R	SmpB-tmRNA from *E. coli*	RNase R from *E. coli*
$pB^{FT}A$-R	SmpB C-terminal tail swapped with that of *F. tularensis* (residues 129 – 157)	RNase R from *E. coli*
pBA^{FT}-R	tmRNA ORF swapped with that of *F. tularensis*	RNase R from *E. coli*
pBA-R^{FT}	SmpB-tmRNA from *E. coli*	RNase R from *F. tularensis*
$pB^{FT}A$-R^{FT}	SmpB C-terminal tail swapped with that of *F. tularensis*	RNase R from *F. tularensis*
pBA^{FT}-R^{FT}	tmRNA ORF swapped with that of *F. tularensis*	RNase R from *F. tularensis*
$pB^{DE}A$-R	SmpB variant I154D and M155E	RNase R from *E. coli*
$pB^{G132E}A$-R	SmpB variant G132E	RNase R from *E. coli*
pBA^{DD}-R	$tmRNA^{DD}$ (A9D and A10D)	RNase R from *E. coli*
pBA^{ED}-R	$tmRNA^{ED}$ (D3E and E4D)	RNase R from *E. coli*

Table 1. List of plasmids used in this study and their nomenclature

3.3.2 Northern blot analysis

E. coli W3110 *rnr::kan*^{r} Δ*smpBssrA* harboring pBA-R or pBA-R^{FT} or pBA-R based SmpB-tmRNA variants was co-transformed with pλ-cI-NS or pλ-cI-S. Overnight cultures of the strains were diluted 1:100 times in Luria-Bertani Broth containing 0.01% arabinose, 100 µg/ml of Ampicillin, and 30 µg/ml of Chloramphenicol. The cells were grown at 37˚C shaking at 180 rpm. Upon reaching mid-log OD_{600}, the reporter gene expression was induced by the addition of 1mM final concentration of isopropyl β-D-thiogalactoside (IPTG). Normalized amounts of cells were harvested and total RNA was isolated using TRI Reagent as per manufacturer's instruction (MRC Inc.) Equal amounts of total RNA from all the samples were resolved in 1.5% formaldehyde-agarose gel. The RNA was capillary transferred to Hybond N+ membrane (GE Healthcare Life Sciences) overnight. Biotin-labeled DNA oligonucleotide probe 5′ - TTCATAAATTGCTTTAAGGCGACGTGCGTCCTCAAGCTGCTCTTGTGTTA - 3′ was hybridized to the membrane for 16 h at 42˚C. The membrane was developed using

BrightStar® BioDetect™ Nonisotopic Detection Kit (Applied Biosystems) and exposed to HyBlot CL® autoradiography films. The bands were scanned and quantified using Image-J (http://rsbweb.nih.gov/ij/).

3.3.3 Western blot analysis

Pelleted cells were resuspended in 1X Laemmli sample buffer, and boiled at 100°C for 30 min. For the purpose of analyzing the levels of RNase R, the samples were resolved in 10% SDS-polyacrylamide gel. Resolved proteins were electrophoretically transferred to PVDF membrane. Western blot analysis was done using primary polyclonal anti-RNase R antibody and secondary donkey anti-rabbit antibody conjugated to HRP. The bands were quantified using Image-J. To analyze lambda reporter gene expression, the samples were resolved in 15% Tris-Tricine polyacrylamide gel. Resolved proteins were electro-transferred to PVDF membrane. Western blot analysis was done using primary monoclonal anti-His6 antibody and secondary goat anti-mouse antibody conjugated to a fluorescent dye. The bands were detected using Odyssey Infrared Imaging System.

3.3.4 Ribosome enrichment assay

This assay was performed as per previously published protocol [57, 71]. *E. coli* W3110 *rnr::kan*^{r} Δ*smpB* Δ*ssrA* harboring pBA-R or pBA-R^{FT} or pBA-R based SmpB-tmRNA variants was co-transformed with pλ-cI-NS or pλ-cI-S. Cells were grown in Luria-Bertani (Miller) broth containing ampicillin, chloramphenicol and 0.02% arabinose until OD_{600} ~ 0.8. Reporter gene expression was induced using 1mM final concentration of IPTG. Harvested cells were resuspended in enrichment buffer (50 mM Tris-HCl pH 7.5, 300 mM NH_4Cl, 20 mM $MgCl_2$, 2 mM β-ME and 10 mM Imidazole) and lysed by French press. Clarified cell lysate was layered onto 32% sucrose solution in enrichment buffer and the ribosomes were pelleted by ultracentrifugation at 100,000 X *g* for 16-18

h. Ribosomes translating the reporter mRNA was separated from the tight-coupled ribosomes by Ni^{2+}-NTA chromatography. The ribosomes were then eluted using 250 mM imidazole in the lysis buffer. RNase R associated with the ribosomes was detected by Western blot analysis.

3.4 Results

3.4.1 Nonstop mRNA accumulates in the presence of tmRNA^{FT} hybrid

SmpB and tmRNA perform the intricate task of *trans*-translation. A unique consequence of *trans*-translation is the selective elimination of aberrant mRNAs that cause ribosome stalling. Given the central role played by the C-terminal tail of SmpB and the mRNA-like domain of tmRNA, we sought to ascertain whether specific sequence determinants within these regions contributed to nonstop mRNA decay. To identify key SmpB and tmRNA sequence elements that facilitate nonstop mRNA decay, we engineered an SmpB hybrid composed of the RNA-binding core of the *E. coli* SmpB protein and the C-terminal tail of the *F. tularensis* SmpB, generating SmpB^{FT}, and a tmRNA hybrid where the ssrA-peptide coding sequence of *E. coli* tmRNA (tmRNA) was replaced with the corresponding sequence of *F. tularensis* tmRNA, generating tmRNA^{FT}. Using various combinations of single and double hybrid constructs in an *smpBssrA* deficient strain, we determined the steady state abundance of the λ-cI-NS nonstop mRNA – which lacks an in-frame stop codon and promotes ribosome stalling – as a reporter of SmpB-tmRNA mediated ribosome rescue and nonstop mRNA decay (Figure 3.2A). As a negative control throughout these studies, we used the related stop codon containing λ-cI-S mRNA, which does not elicit ribosome stalling or require SmpB-tmRNA activity. Consistent with previous studies, analysis of these reporter mRNAs showed that the λ-cI-NS mRNA does not accumulate in the presence of wild type (WT) *E. coli* surveillance factors (SmpB, tmRNA, and RNase R). By contrast, there is ~ 4-fold increase in the accumulation of λ-cI-NS mRNA in the presence of the tmRNA^{FT} hybrid, suggesting that specific tmRNA determinants are required for proper engagement of

RNase R on stalled ribosomes. Our lab has recently shown that while the tmRNA^{FT} hybrid could productively engage stalled ribosomes, it is unable to accurately establish the correct tmRNA reading frame [11]. However, cognate hybrid SmpB (SmpB^{FT}), carrying the *F. tularensis* C-terminal tail, is required to restore accurate tagging activity. Since the *F. tularensis* tmRNA ORF sequence is highly divergent from that of *E. coli* tmRNA (Figure 3.1), it was possible that *E. coli* SmpB was unable to make functionally relevant contacts with tmRNA^{FT} to promote nonstop mRNA degradation. We reasoned that the observed nonstop mRNA decay defect of tmRNA^{FT} might be due to the absence of cognate SmpB^{FT}. Remarkably, co-expression of the SmpB^{FT} and tmRNA^{FT} hybrids did not mitigate the observed nonstop mRNA degradation defect associated with tmRNA^{FT} (Figure 3.2A). In contrast, expression of SmpB^{FT} alongside *E. coli* tmRNA (SmpB^{FT}-tmRNA) resulted in clearance of the nonstop mRNA to levels indistinguishable from cells expressing WT *E. coli* SmpB and tmRNA (Figure 3.2A). This result suggested that SmpB^{FT} makes the required contacts with *E. coli* tmRNA, and likely the translation machinery, to facilitate RNase R enrichment and nonstop mRNA decay. To rule out the possibility that there was a general increase in the reporter mRNA abundance in the presence of the tmRNA^{FT} hybrid, we analyzed the steady state level of the corresponding stop-codon containing control reporter mRNA (λ-cI-S) by Northern blot analysis. This evaluation showed that the levels of λ-cI-S mRNA in the presence of single and double hybrids were indistinguishable from cells expressing WT SmpB and tmRNA (Figure 3.2B), indicating that the observed mRNA decay defect was specific to the *trans*-translation related deficiencies of the tmRNA^{FT} hybrid. Taken together, these data suggested that swapping the *E. coli* tmRNA ORF with the corresponding *F. tularensis* sequence selectively impacted nonstop mRNA decay.

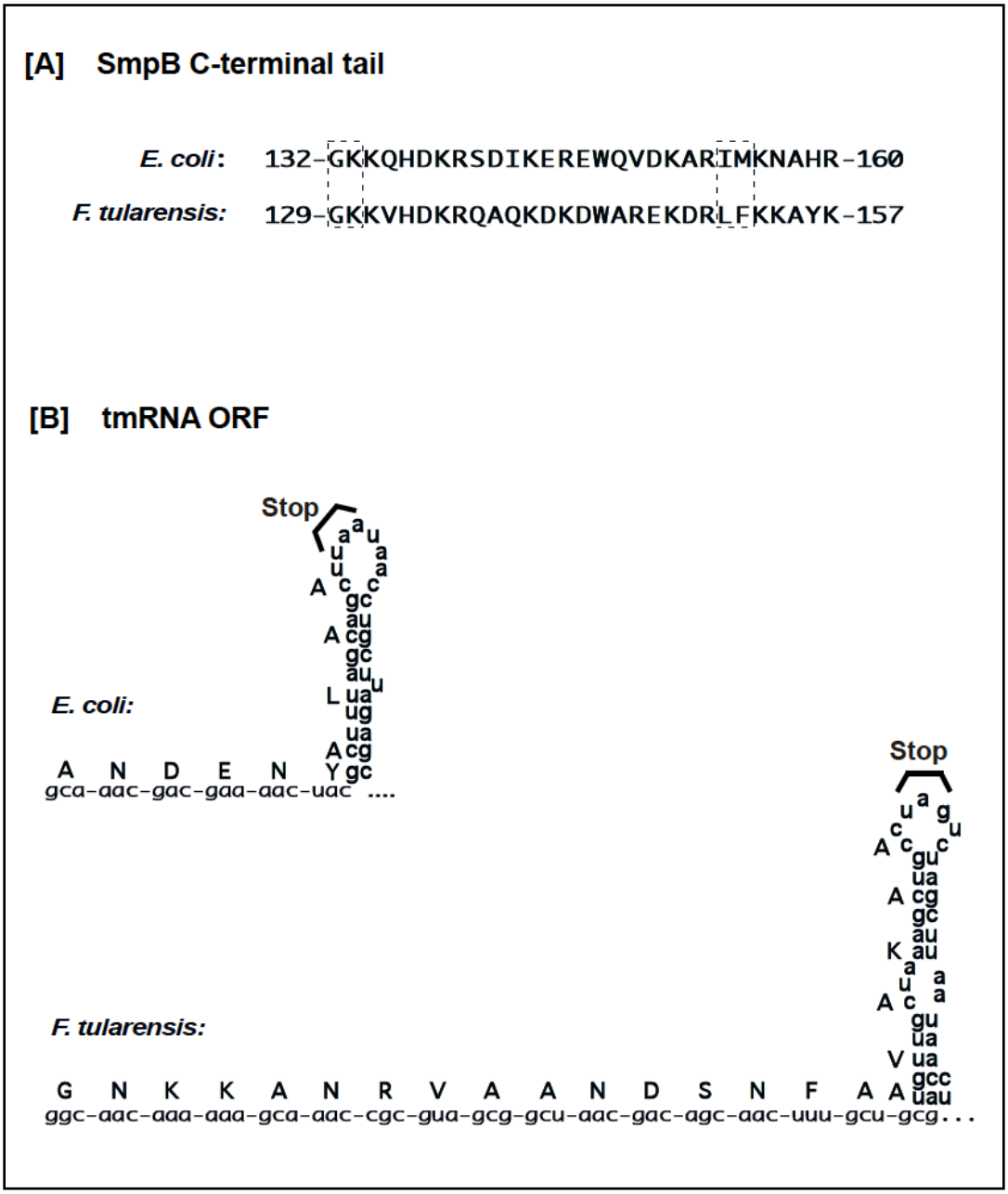

Figure 3.1 Sequences of SmpB C-terminal tail and tmRNA ORF of *E. coli* and *F. tularensis*. (A) Amino acid sequence of the SmpB C-terminal tail from *E. coli* and *F. tularensis*. The dotted box represents the residues that are important for supporting tmRNA tagging activity in *E. coli* (G132 and I153/M154), and the corresponding residues in *F. tularensis* SmpB C-terminal tail. **(B)** Nucleotide sequence of tmRNA ORF and the corresponding amino acids from *E. coli* and *F. tularensis*. *E. coli* tmRNA ORF codes for 10 amino acids whereas *F. tularensis* tmRNA ORF codes for 22 amino acids.

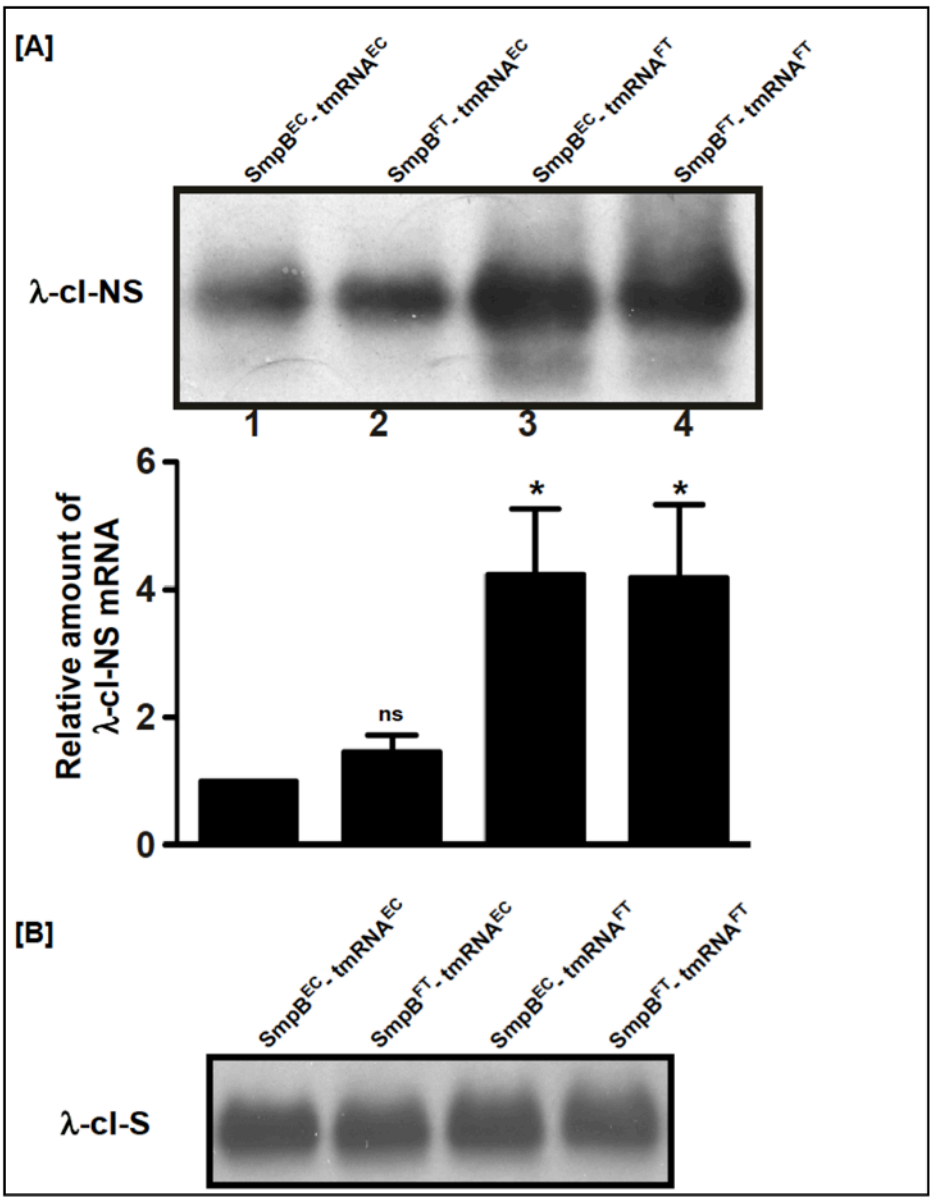

Figure 3.2 tmRNA ORF alterations lead to accumulation of nonstop mRNA. **(A)** The top panel depicts a representative Northern blot showing the steady state abundance of the λ-cI-NS nonstop mRNA in the presence of the hybrid variants of SmpB and tmRNA. The accumulation of nonstop mRNA in the presence of single and double tmRNA ORF hybrids (lanes 3 and 4) is approximately 4-fold higher than that of *E. coli* derived SmpB-tmRNA. *P*-values were calculated by performing Student's *t*-test analysis with SmpB-tmRNA and $SmpB^{FT}$-tmRNA (*ns,* not statistically significant), SmpB-tmRNA and SmpB-$tmRNA^{FT}$ (**P* = 0.035), or SmpB-tmRNA and $SmpB^{FT}$-$tmRNA^{FT}$ (**P* = 0.049). The accompanying graph represents the fold change in the steady state level of λ-cI-NS mRNA in the presence of indicated SmpB and tmRNA variants with respect to SmpB-tmRNA. The data are combined from three independent experiments (mean ± SEM, standard error of means). **(B)** A representative Northern blot showing similar steady state levels of the control λ-cI-S stop mRNA in the presence of indicated SmpB and tmRNA hybrids.

3.4.2 SmpB^{FT} and tmRNA^{FT} hybrids are active in tagging and ribosome rescue

Previous studies have shown that tmRNA nucleotides 86-122, in the region encompassing the mRNA-like domain, play a crucial role in the peptide tagging activity of tmRNA [11, 72]. Therefore, it was possible that the tmRNA^{FT} hybrid was compromised in its ability to participate in *trans*-translation. To assess this possibility, we examined the capacity of the SmpB-tmRNA^{FT} single and SmpB^{FT}-tmRNA^{FT} double hybrid to co-translationally tag the λ-cI protein, the product of the nonstop reporter mRNA. This analysis showed that both hybrid constructs were equally proficient in co-translationally appending the ssrA degron to the reporter polypeptide, indicating that stalled ribosomes were successfully recognized and rescued by the SmpB^{FT}-tmRNA^{FT} double hybrid (Figure 3.3A).

SmpB and tmRNA regulate the intracellular stability of RNase R [75]. Therefore, we examined whether the absence of either cognate *E. coli* SmpB or *E. coli* tmRNA altered the *in vivo* stability of RNase R, thus resulting in the observed differences in the abundance of nonstop mRNA. To assess this possibility, we compared the steady state levels of RNase R in cells expressing SmpB-tmRNA with cells expressing various combinations of the SmpB^{FT} and tmRNA^{FT} hybrids. This analysis showed that the SmpB^{FT} and tmRNA^{FT} hybrids had no measurable impact on the steady state level of RNase R (Figure 3.3B).

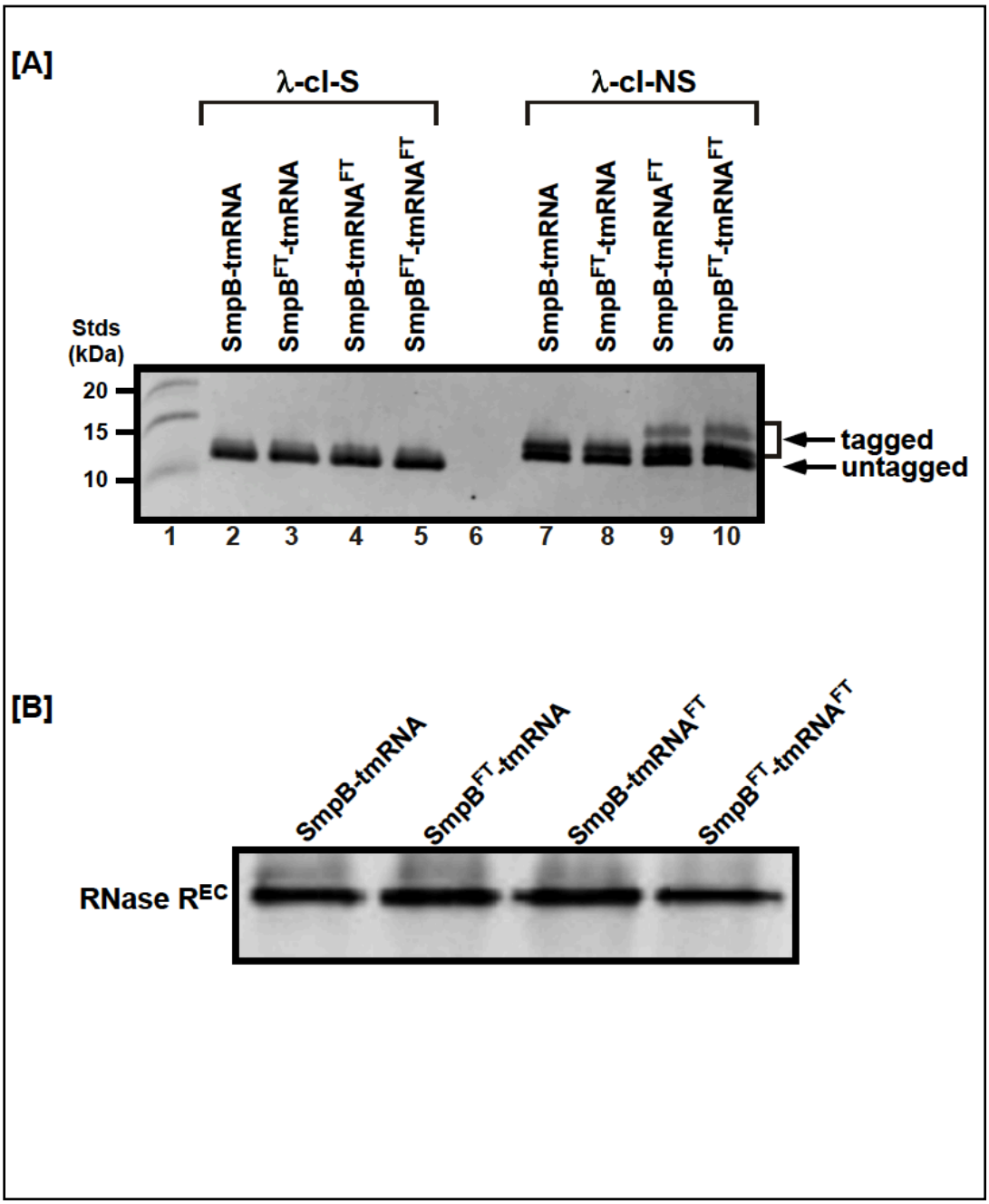

Figure 3.3 tmRNA ORF alterations do not affect the tagging activity or the steady state levels of RNase R. **(A)** A representative Western blot showing the expression levels of the λ-cI stop (lanes 2-5) and nonstop (lanes 7-10) reporter protein in the presence of indicated SmpB and tmRNA hybrids. The λ-cI reporter protein is tagged in the presence of SmpB-tmRNA hybrids whereas the corresponding stop reporter is untagged. **(B)** A representative Western blot showing similar steady state levels of *E. coli* RNase R (RNase R^{EC}) in the presence of indicated SmpB-tmRNA hybrids.

3.4.3 The tmRNA^{FT} hybrid affects RNase R enrichment on stalled ribosomes

We reasoned that the observed accumulation of the nonstop mRNA in cells expressing tmRNA^{FT} could be due to a defect in the recruitment of RNase R to stalled ribosomes. This possibility was compelling as it suggested that the SmpB-tmRNA mediated peptide tagging and ribosome rescue were insufficient for productive engagement of RNase R on rescued ribosomes. Moreover, it suggested that tmRNA sequence elements must make additional discrete contacts with the translation machinery to promote effective RNase R engagement –contacts that could not be made by the divergent mRNA-like domain of tmRNA^{FT}. Furthermore, these contacts must be unique to the tmRNA ORF and independent of SmpB, since co-expressing SmpB^{FT} did not alleviate the nonstop mRNA defect of tmRNA^{FT}. The inability to establish such crucial contacts could lead to accumulation of nonstop mRNA in the cell. In order to ascertain whether RNase R could productively engage on tmRNA^{FT}-rescued ribosomes, we performed ribosome enrichment assays [57, 60, 71]. Ribosomes decoding either the λ-cI-NS or the control λ-cI-S reporter mRNAs, both of which carry an N-terminal His6 epitope tag, were captured by Ni^{2+}-NTA affinity chromatography from individual pools of tight-coupled ribosomes [57]. The captured ribosomes were subjected to Western blot analysis to assess the recruitment of RNase R to rescued ribosomes in the presence of the various combinations of single and double SmpB-tmRNA hybrids (Figure 3.4). Using this analysis, we observed a 3-fold enrichment of RNase R on ribosomes in the presence of the SmpB^{FT}-tmRNA hybrid, suggesting that RNase R was able to productively engage tmRNA rescued ribosome and capture the nonstop mRNA. In contrast, RNase R failed to productively engage on ribosomes rescued by the SmpB-tmRNA^{FT} and SmpB^{FT}-tmRNA^{FT} hybrids. These results suggested that the tmRNA^{FT} hybrid, despite being capable of peptide tagging and ribosome rescue, is unable to establish the necessary contacts required for facilitating RNase R recruitment to rescued ribosomes. We routinely observe a low background level association of RNase R with ribosomes translating the control λ-cI-S reporter mRNA. Curiously, ribosomes rescued from the λ-cI-NS nonstop mRNA by the tmRNA^{FT} hybrid consistently yielded

RNase R enrichment levels that were below the control λ-cI-S reporter. Taken together, these data suggest that the tmRNA ORF contains additional elements that make discrete functional contacts with the translation machinery to facilitate effective engagement of RNase R on rescued ribosomes. We infer from these findings that peptide tagging, and productive engagement of RNase R on stalled ribosomes are two independent attributes of the SmpB-tmRNA mediated *trans*-translation process.

3.4.4 RNase R^{FT} does not mitigate the nonstop mRNA decay defect of $tmRNA^{FT}$

It was conceivable that the observed nonstop mRNA decay defect of the $tmRNA^{FT}$ hybrid was due to incompatibility of the *E. coli* RNase R (RNase R^{EC}) with sequence elements within the mRNA-like domain of $tmRNA^{FT}$. Alternatively, it was also possible that changes in the coding region of $tmRNA^{FT}$ had an indirect effect on RNase R recruitment, owing to alterations in interactions of the mRNA-like domain of $tmRNA^{FT}$ with the translation machinery. To distinguish between these possibility, we expressed *F. tularensis* RNase R (RNase R^{FT}) along with various combinations of SmpB and tmRNA hybrids, and analyzed the steady state level of the λ-cI-NS reporter mRNA. Expression of RNase R^{FT} and *E. coli* SmpB-tmRNA resulted in a basal level accumulation of the λ-cI-NS reporter that was indistinguishable from that of RNase R^{EC} (Figure 3.5A). Additionally, co-expression of RNase R^{FT} with the $SmpB^{FT}$ hybrid ($SmpB^{FT}$-tmRNA) resulted in low basal level accumulation of the λ-cI-NS reporter, indicating that RNase R^{FT} was functional in the context of the *E. coli trans*-translation. Surprisingly, however, when RNase R^{FT} was co-expressed with $tmRNA^{FT}$ (SmpB-$tmRNA^{FT}$), ~ 5-fold higher levels of the nonstop mRNA accumulated in these cells (Figure 3.5B). Furthermore, the nonstop mRNA accumulation defect elicited by $tmRNA^{FT}$ was not alleviated in the presence of $SmpB^{FT}$, wherein the functional pair was operating in concert to rescue stalled ribosome (Figure 3.5B). These data suggested

that distinct sequence elements within the mRNA-like domain of tmRNA make specific contacts with the translation apparatus to facilitate RNase R recruitment.

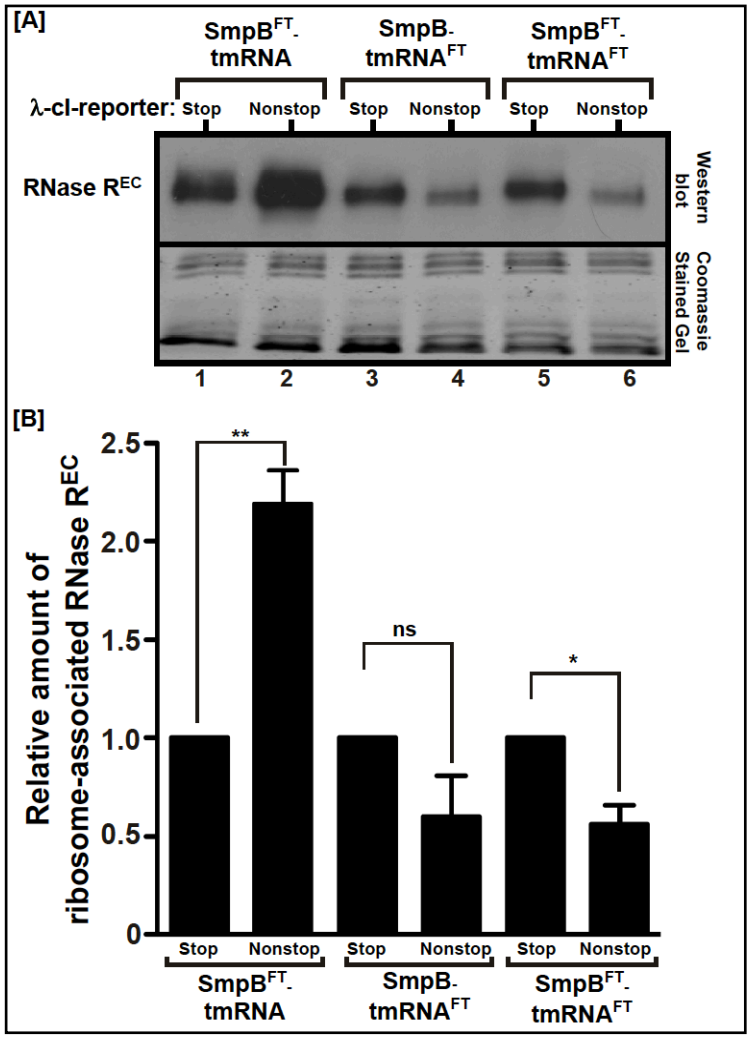

Figure 3.4 Ribosomes rescued by hybrid tmRNA exhibit defects in RNase R recruitment. **(A)** Total ribosomes were obtained from cells co-expressing the indicated SmpB and tmRNA hybrid variants with the λ-cI-S or λ-cI-NS reporter mRNAs. Ribosomes translating the reporter mRNAs were isolated from the total ribosomes pool using Ni^{2+}-NTA affinity chromatography. Equal numbers of captured ribosomes were resolved by electrophoresis on 10% SDS-polyacrylamide gels. Western blot analysis was performed to detect the presence of *E. coli* RNase R (RNase R^{EC}). The intensity of the band corresponding to RNase R^{EC} was quantified using ImageJ. The top panel shows a representative Western blot, using an RNase R^{EC} specific antibody, and the bottom panel shows a section of the corresponding Coomassie stained gel displaying equal protein loading. **(B)** The graph represents fold RNase R^{EC} enrichment on ribosomes translating the λ-cI-NS reporter compared to ribosomes translating the control λ-cI-S reporter (mean ± SEM). *P*-values were calculated by performing Student's *t*-test analysis on the association level of RNase R^{EC} with ribosomes translating λ-cI-S and λ-cI-NS in the presence of SmpB^{FT}-tmRNA (**P = 0.0022, n=5), SmpB-tmRNA^{FT} (ns, n=4), or SmpB^{FT}-tmRNA^{FT} (*P = 0.01, n=5).

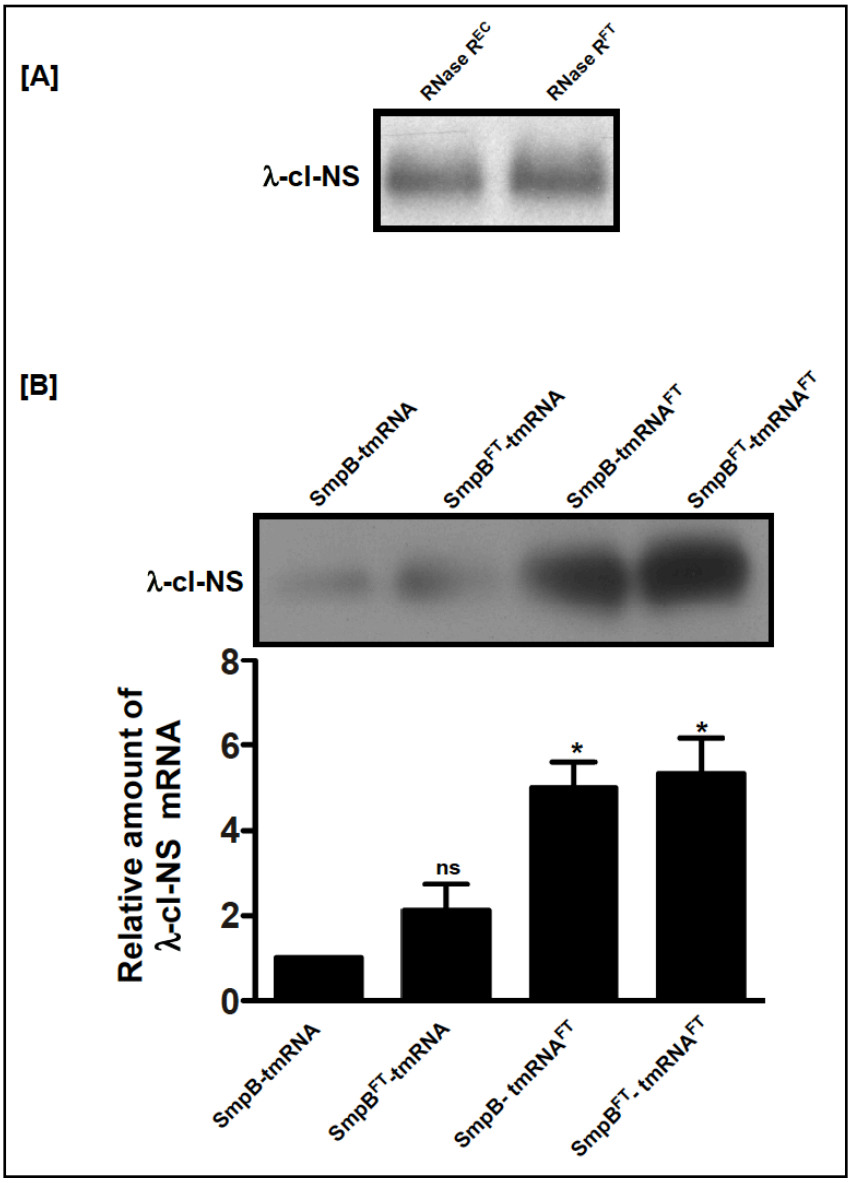

Figure 3.5 tmRNA ORF alterations lead to nonstop mRNA accumulation in the presence of *F. tularensis* RNase R. (A) A representative Northern blot showing similar steady state abundance of λ-cI-NS nonstop mRNA in the presence of *E. coli*- and *F. tularensis*-derived RNase R (RNase R^{EC} and RNase R^{FT}), respectively. **(B)** The top panel depicts a representative Northern blot showing the steady state level of λ-cI-NS nonstop mRNA in the presence of the indicated SmpB and tmRNA hybrid variants and RNase R^{FT}. The level of nonstop mRNA accumulation in the presence of single and double tmRNA ORF hybrids (lanes 3 and 4) is approximately 5-fold higher than that of *E. coli* derived SmpB-tmRNA. *P*-values were calculated by performing Student's *t*-test analysis with SmpB-tmRNA and $SmpB^{FT}$-tmRNA (*P* = ns), SmpB-tmRNA and SmpB-$tmRNA^{FT}$ (**P* = 0.007), or SmpB-tmRNA and $SmpB^{FT}$-$tmRNA^{FT}$ (**P* = 0.0135). The accompanying graph representing the fold change in the steady state level of λ-cI-NS mRNA in the presence of indicated SmpB and tmRNA variants with respect to WT *E. coli* SmpB-tmRNA. The data are combined from four independent experiments (mean ± SEM).

3.4.5 tmRNA ORF elements are essential for RNase R recruitment to stalled ribosomes

We inferred from these observations that the key elements involved in facilitating productive engagement of RNase R with stalled ribosomes reside within the tmRNA ORF. Mutational studies have revealed that alterations in the ultimate and penultimate codons of the tmRNA ORF result in accumulation of nonstop mRNA [72]. We reasoned that these sequence elements might play an important role in facilitating RNase R recruitment to stalled ribosomes. To test this hypothesis, we used a tmRNA variant where the two terminal alanine codons are changed to aspartic acid codons (tmRNA$^{A9D/A10D}$, henceforth tmRNA^{DD}). The tmRNA^{DD} variant is known to be proficient in peptide tagging and ribosome rescue [16, 17, 67]. To examine the effect of these defined tmRNA sequence changes on selective nonstop mRNA decay, we performed ribosome enrichment and nonstop mRNA stability assays in *smpBssrA rnr::kan* cells expressing *E. coli* RNase R, SmpB, and tmRNA^{DD}. We evaluated the association of RNase R with ribosomes stalled on the λ-cI-NS reporter. We observed that introduction of these modest tmRNA ORF changes were sufficient for disrupting the productive recruitment of RNase R to tmRNA-rescued ribosomes. Furthermore, the disruptive effect the tmRNA^{DD} variant was specific to this segment of the tmRNA ORF, as equivalent alterations elsewhere, for instance the third and fourth codons (tmRNA$^{D3E/E4D}$, henceforth tmRNA^{ED}), did not hamper RNase R association with stalled ribosomes (Figure 3.6). We also examined the stability of the λ-cI-NS reporter mRNA in the presence of the tmRNA^{DD} variant and observed stabilization of the reporter RNA, suggesting that specific tmRNA sequence elements are important for facilitating RNase R ribosome enrichment and the ensuing nonstop mRNA decay (Figure 3.7).

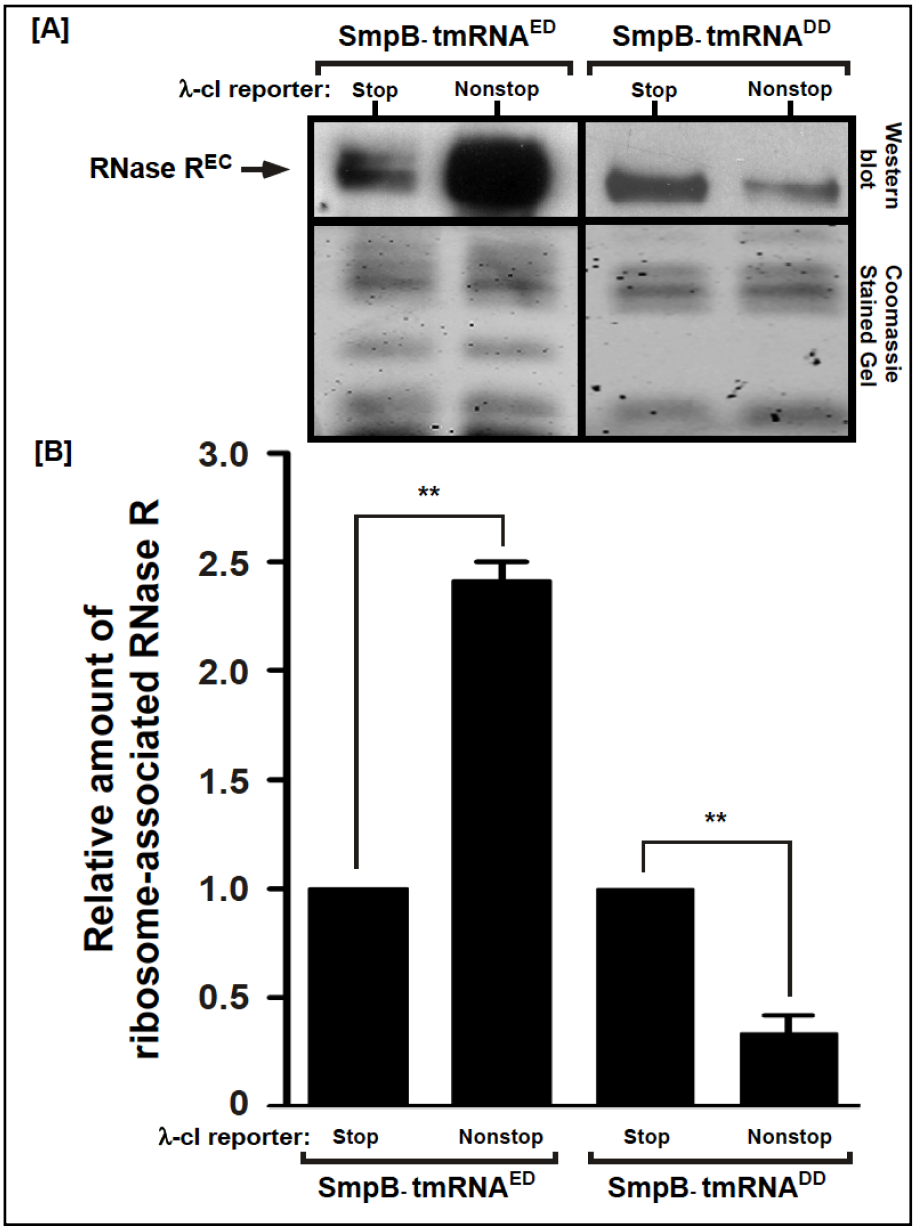

Figure 3.6 *E. coli* RNase R exhibits defects in enrichment on ribosomes rescued by tmRNA^{DD}. (A) Total ribosomes were obtained from cells expressing the tmRNA^{ED} or the tmRNA^{DD} variants with the λ-cI-S or λ-cI-NS reporter mRNAs. Ribosomes translating the reporter mRNAs were isolated from the total ribosomes pool using Ni^{2+}-NTA affinity chromatography. Equal numbers of ribosomes were resolved by electrophoresis on 10% SDS-polyacrylamide gels. Western blot analysis was performed to detect the presence of wild type *E. coli* RNase R. The intensity of the band corresponding to RNase R was quantified using ImageJ. The top panel shows a representative Western blot, using an RNase R specific antibody, and the bottom panel shows a section of the Coomassie stained gel displaying equal protein loading. **(B)** The graph represents fold RNase R enrichment on ribosomes translating the λ-cI-NS reporter compared to ribosomes translating the control λ-cI-S reporter (mean ± SEM). *P*-values were calculated by performing Student's *t*-test analysis on the association level of RNase R with ribosomes translating λ-cI-S and λ-cI-NS mRNAs in the presence of tmRNA^{ED} (**P = 0.004, n=3) or tmRNA^{DD} (**P = 0.0042, n=4).

3.4.6 RNase R captures defective mRNA after establishment of the tmRNA ORF

Previous studies have demonstrated that enrichment of RNase R on stalled ribosomes is dependent on the activity of SmpB and tmRNA. Yet, the precise step at which RNase R performs its function has not been elucidated. In an effort to ascertain the mechanistic time frame during which RNase R initiates defective mRNA degradation, we utilized SmpB mutants that impair specific stages of the *trans*-translation process. Our lab has shown that key residues in the C-terminal tail of SmpB play a critical role in engaging the ribosome and establishing the tmRNA ORF [11, 13]. For instance, glycine 132 (Gly132) acts as a hinge that confers flexibility on the C-terminal tail of SmpB, thus enabling proper positioning and establishment of the correct reading frame on the tmRNA ORF [11]. Substitution of Gly132 with Glutamate ($SmpB^{G132E}$) prevents accommodation of tmRNA in the ribosomal A-site. Isoleucine 154 and Methionine 155 are crucial for tmRNA tagging activity. Substitution of these SmpB residues with negatively charged aspartic acid and glutamic acid ($SmpB^{DE}$) results in substantial defects in its *trans*-translation function with retention of very low level of tagging activity [13]. Interestingly, both SmpB C-terminal tail variants are fully capable of binding tmRNA and delivering it to stalled ribosomes.

We sought to examine the effect of these SmpB variants on selective nonstop mRNA decay. To this end, we evaluated the steady state abundance of the λ-cI-NS reporter mRNA in the presence of WT *E. coli* RNase R and either the $SmpB^{DE}$ or $SmpB^{G132E}$ variant and observed that RNase R-mediated nonstop mRNA degradation was markedly hindered (Figure 3.7A). The level of nonstop mRNA accumulation in the presence of the $SmpB^{DE}$ and $SmpB^{G132E}$ variants was ~ 2.5 fold higher than that of $tmRNA^{DD}$ variant. This difference in nonstop reporter accumulation cannot be attributed to the variation in the steady state expression level of RNase R in presence of SmpB and tmRNA variants (Figure 3.7B), and was thus likely due to a defect in the specific capture of the nonstop mRNA. To scrutinize this inference, we performed ribosome enrichment assay in the presence of the $SmpB^{DE}$ and $SmpB^{G132E}$ variants and assessed RNase R recruitment to ribosomes translating the λ-cI-NS reporter mRNA. This analysis

revealed that both SmpB variants were incapable of facilitating RNase R enrichment on stalled ribosomes (Figure 3.8). Although there was a substantial defect in RNase R enrichment with the SmpB C-terminal tail and tmRNA ORF variants (Figure 3.8), we consistently observed a significant defect in nonstop mRNA degradation in the presence of $SmpB^{DE}$ and $SmpB^{G132E}$, as compared to $tmRNA^{DD}$, (Figure 3.7A). We reasoned that since the peptide tagging activity and ORF establishment activities of the $tmRNA^{DD}$ variant are not compromised, stalled ribosomes undergo proper termination, and the ribosomal subunits are efficiently recycled. As a result, the aberrant mRNA is exposed to other cellular ribonucleases for degradation, resulting in the observed relatively lower abundance of nonstop mRNA with the $tmRNA^{DD}$ variant as compared to the $SmpB^{DE}$ and $SmpB^{G132E}$ variants.

We infer from the sum of these results that the productive recruitment of RNase R to stalled ribosomes requires accurate establishment of tmRNA ORF. We postulate that specific sequence elements in the distal portion of the mRNA-like domain of tmRNA makes distinct contacts with the translation apparatus to facilitate optimal engagement of RNase R on stalled ribosomes, thus enabling the specific capture and targeted decay of nonstop mRNAs.

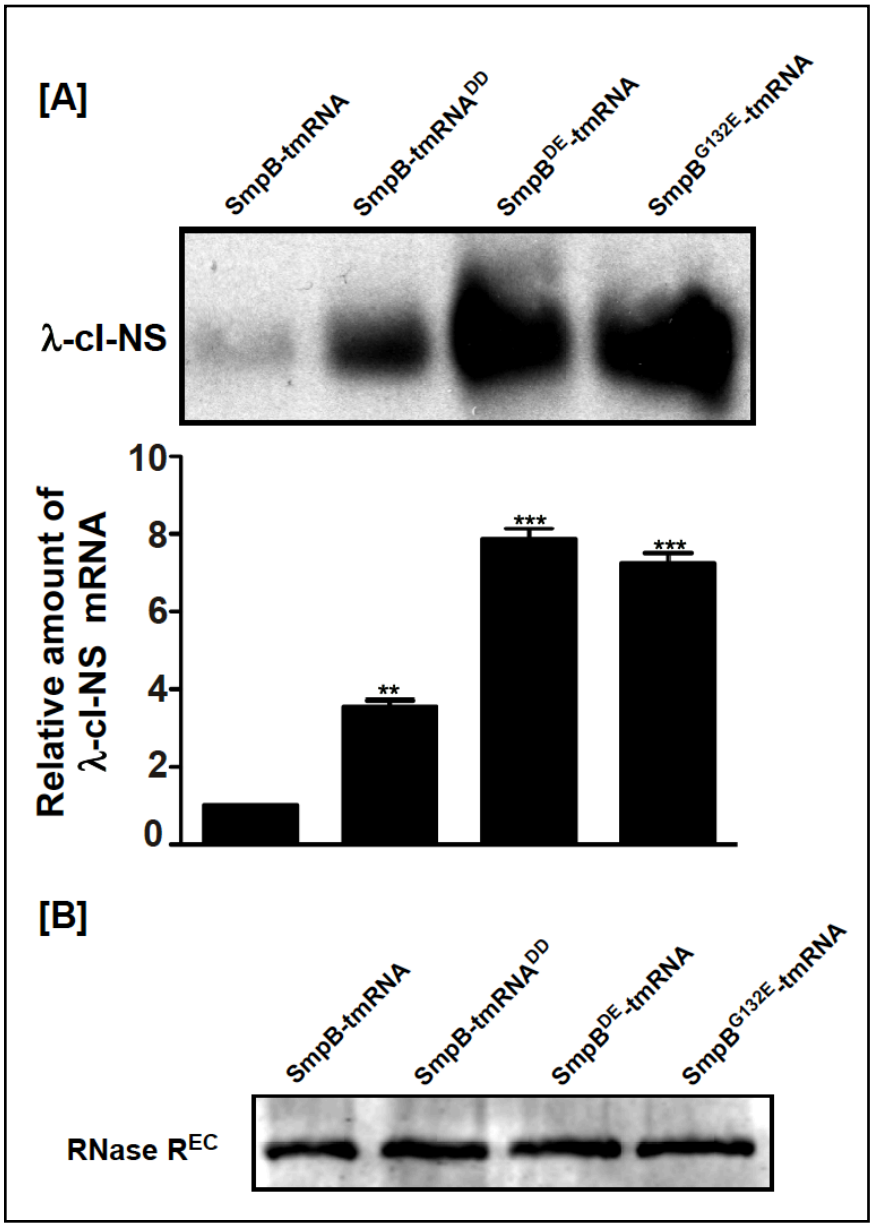

Figure 3.7 RNase R initiates nonstop mRNA decay after establishment of the tmRNA reading frame. (A) A representative Northern blot showing the steady state abundance of λ-cI-NS nonstop mRNA in the presence of SmpB-tmRNA, SmpB-tmRNA^{DD}, SmpB^{DE}-tmRNA, and SmpB^{G132E}-tmRNA. The accompanying graph shows the relative steady state abundance of the λ-cI-NS nonstop mRNA in the presence of indicated variants with reference to SmpB-tmRNA. RNase R exhibits severe defect in degrading nonstop mRNA when ribosomes are rescued by SmpB^{DE}-tmRNA or SmpB^{G132E}-tmRNA. RNase R exhibits a moderate defect in degrading nonstop mRNA in the presence of SmpB-tmRNA^{DD}, wherein the reading frame is accurately established. *P*-values were calculated by performing Student's *t*-test analysis on the relative steady state abundance of the λ-cI-NS nonstop mRNA in the presence of SmpB-tmRNA and SmpB-tmRNA^{DD} (***P* = 0.0039), SmpB-tmRNA and SmpB^{DE}-tmRNA (***P* = 0.0017), or SmpB-tmRNA and SmpB^{G132E}-tmRNA (***P* = 0.002). The data are combined from three independent experiments (mean ± SEM). **(B)** A representative Western blot showing similar expression levels of RNase R in the presence of indicated SmpB and tmRNA variants.

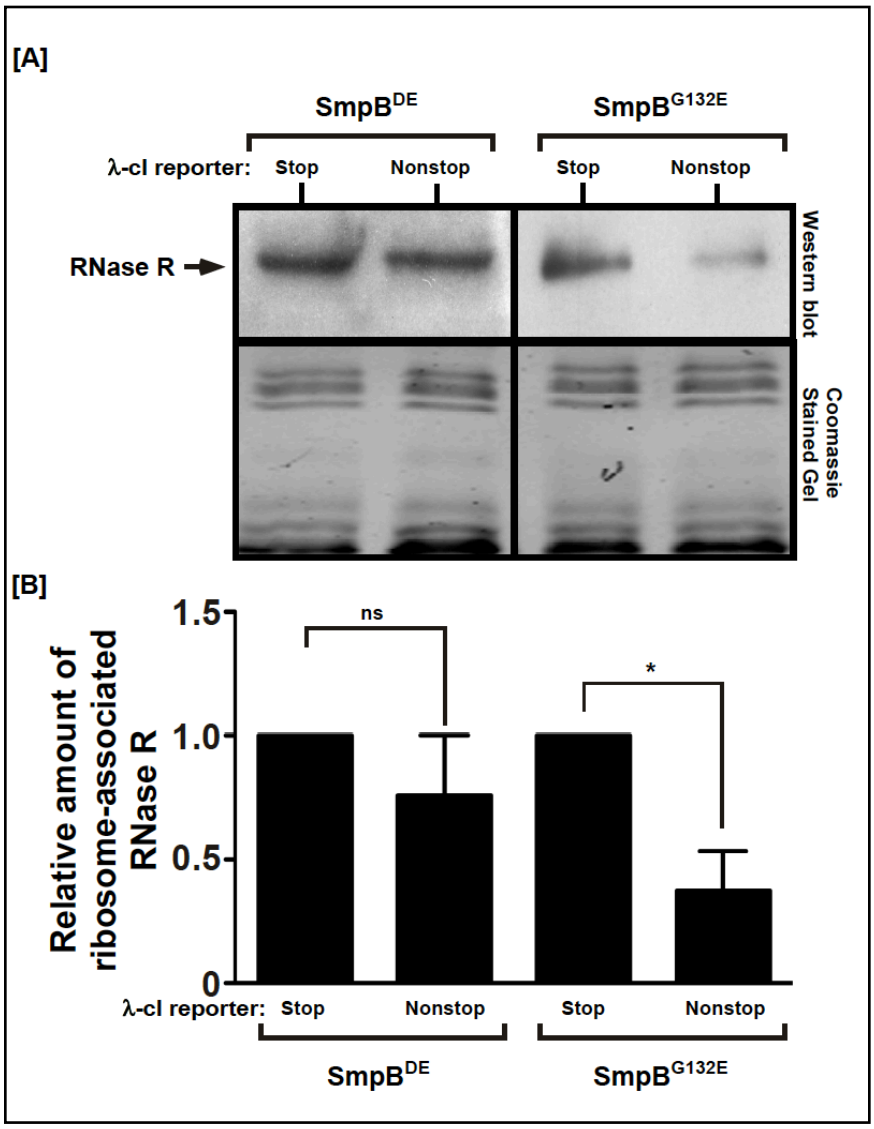

Figure 3.8 *E. coli* RNase R exhibits defects in enrichment on ribosomes rescued by SmpB C-terminal tail variants. (A) Total ribosomes were obtained from cells co-expressing $SmpB^{DE}$ or $SmpB^{G132E}$ variants with the λ-cI-S or λ-cI-NS reporter mRNAs. Ribosomes translating the reporter mRNAs were isolated from the total ribosomes pool using Ni^{2+}-NTA affinity chromatography. Equal numbers of ribosomes were resolved by electrophoresis on 10% SDS-polyacrylamide gels. Western blot analysis was performed to detect the presence of RNase R. The intensity of the band corresponding to RNase R was quantified using ImageJ. The top panel shows a representative Western blot, using an RNase R specific antibody, and the bottom panel shows a section of the corresponding Coomassie stained gel displaying equal protein loading. **(B)** The graph represents fold RNase R enrichment on ribosomes translating the λ-cI-NS reporter compared to ribosomes translating the control λ-cI-S reporter. The data are combined from three independent experiments (mean ± SEM) (mean ± SEM). *P*-values were calculated by performing Student's *t*-test analysis on the association level of RNase R with ribosomes translating λ-cI-S and λ-cI-NS in the presence of $SmpB^{DE}$ (*P* = ns), and $SmpB^{G132E}$ (**P* = 0.022).

3.5 Discussion

The SmpB-tmRNA complex orchestrates the elaborate process of *trans*-translation, marshaling stalled ribosome to resume translation and proceed to normal termination and recycling. A hallmark of the *trans*-translation process is the RNase R-mediated targeted decay of nonstop mRNAs. Given that recruitment of RNase R to stalled ribosomes is reliant on SmpB and tmRNA, it has been of particular interest to delineate SmpB and tmRNA sequence elements that influence this targeted RNase R function. Our investigations reveal that the mere recognition of stalled ribosomes by the SmpB-tmRNA complex is insufficient for productive recruitment of RNase R to rescued ribosomes. Analyses of defined SmpB C-terminal tail variants, with distinct defects in establishment of the tmRNA ORF, demonstrate that RNase R mediated nonstop mRNA decay requires proper establishment of the tmRNA ORF. SmpB C-terminal tail variants that are competent in tmRNA binding and ribosome recognition but fail to support establishment of the tmRNA ORF as the surrogate template also fail to productively recruit RNase R to rescued ribosomes. We interpret these data to signify that RNase R is recruited to rescued-ribosomes soon after establishment of the tmRNA ORF as a surrogate template. Analysis of well-known tmRNA ORF variants, that are fully competent in peptide tagging and ribosome rescue, uncovered a novel role for distal elements of the tmRNA ORF that are required for making crucial contacts with the translation machinery and recruitment of RNase R. Studies of the $SmpB^{FT}$ and $tmRNA^{FT}$ hybrids suggest that these unique sequence elements of tmRNA interact directly with components of the ribosomal 30S subunit rather than RNase R. The observation that the $SmpB^{FT}$ hybrid could not restore $tmRNA^{FT}$ associated nonstop mRNA decay defect and that the divergent RNase R^{FT} was fully proficient in nonstop mRNA decay in the presence of *E. coli* SmpB-tmRNA complex supports this conclusion. The mRNA-like region and helix 5 of $tmRNA^{FT}$ differs significantly from *E. coli* tmRNA both in length and nucleotide composition (Fig. S1). The $tmRNA^{FT}$ ORF is greater than twice the length, encoding for a 22 amino acid tag, whereas the $tmRNA^{EC}$ ORF encodes for a 10 amino acid tag. Although the last two codons of both the *E. coli* and *F. tularensis* tmRNA ORF

code for alanine, the sequence of the two synonymous alanine codons is dissimilar –the tmRNA^{FT} ORF uses 5'-GCU-GCC-3' whereas the *E. coli* tmRNA ORF uses 5'-GCA-GCU-3' as alanine codons. We reason that these differences in length and sequence composition result in a less than ideal positioning of the ultimate and penultimate codons and helix 5A with respect to the components of the mRNA entry channel, thus rendering tmRNA^{FT} deficient in RNase R recruitment and nonstop mRNA decay. We infer from these observations that the putative contacts made by tmRNA ORF with the translation apparatus are not essential for the peptide tagging and ribosome rescue activities. Rather, they are a prerequisite for facilitating productive engagement of RNase R with rescued ribosomes. We propose that the tmRNA ORF, more specifically the ultimate and penultimate codons, make necessary contacts with the translation apparatus to set the stage for RNase R recruitment and selective nonstop mRNA decay. We postulate that interactions of the tmRNA ORF with 30S ribosomal RNA or protein(s) play a significant role in coordinating this process.

Ribosomes are dynamic molecular machines capable of exploring a range of functional conformational states. The structural dynamics of ribosomal 30S and 50S subunits play pivotal roles at various stages of the decoding process. Recent biochemical and structural studies confirm the capacity of the ribosome to explore a number of previously undetected conformations in response to distinct translation factor or RNA sequence signals [73, 76-80]. For instance, a hyper-rotated state is observed for ribosomes translating frame-shift inducing structured mRNAs, with the structured sequences poised at the mRNA entry channel [77]. The inference drawn from these and related studies could be that interactions of structured mRNAs with components of the mRNA entry channel stimulate a conformational state that influences frame-shifting efficiency. Similarly, a recent cryo-EM study sheds new light on the dynamic structural changes that occur in the 30S subunit during accommodation of the mRNA-like domain of tmRNA [73]. Of particular interest is the large movement of 30S latch (wide-open latch state) –resulting in a gap of ~20Å between helix 34 and the G530 region of the 30S subunit– that permits the loading of mRNA-like domain of tmRNA into the ribosomal mRNA entry channel. Intriguingly, the distal part of the tmRNA ORF appears to interact directly with components of the mRNA entry channel during this stage of *trans*-

translation. Specific interactions of this segment of the mRNA-like domain with elements of the 30S subunit could explain the species-specific nature of the impact of the tmRNA ORF on nonstop mRNA decay. We propose that crucial interactions of the ultimate and penultimate codons of the tmRNA ORF with the 30S subunit educe unique conformational states of the 30S subunit that are essential for RNase R to gain access to the 3′ end of the defective mRNA.

In light of these findings, there are two possible mechanisms for RNase R to engage the rescued ribosomes and gain access to the 3′ end of the nonstop mRNA. One pathway could be analogous to eukaryotic nonstop mRNA decay, where Ski7p, the SKI protein complex and the exosome gain access to ribosomal A-site, capture nonstop mRNA, and promote ribosomal subunit disassembly [4, 81]. The alternative pathway could involve selective recruitment of RNase R to the vicinity of the mRNA exit channel, where the ribonuclease is strategically positioned to capture the emerging nonstop mRNA. Since establishment of the tmRNA reading frame and commencement of the *trans*-translation process are prerequisites for recruitment of RNase R, it is unlikely that the nonstop mRNA would be captured via an exosome-like pathway. We reason that the bacterial nonstop mRNA surveillance system is fundamentally distinct from the known eukaryotic surveillance pathways, as it requires continuation of translation for marking of the aberrant nascent polypeptide for proteolysis and relies on normal translation termination, on a stop codon provided by the tmRNA ORF, for ribosome recycling. While further experiments are necessary to decipher the intricate details of this process, it is tempting to speculate that select contacts of the distal part of the tmRNA ORF with the components of the mRNA entry channel educe a unique conformational state of the 30S subunit that provides a spatio-temporally controlled window of opportunity for RNase R to bind in the vicinity of the mRNA exit channel and capture the emerging nonstop mRNA.

Chapter 4: A Novel Function of Ribosomal Protein S6 and its Post-translational Modification in *trans*-Translational Dependent Nonstop mRNA Decay

4.1 Abstract

Ribosomal proteins and RNAs undergo a variety of posttranslational modifications that seem to be influenced by a range of factors including the growth phase of the cell, environmental conditions and the stage of ribosomal subunit maturation and assembly. One such unique modification of ribosomal proteins is the RimK-catalyzed posttranslational addition of up to four glutamate residues to the C-terminus of ribosomal protein S6. However, there is very little understanding of the biological significance of these modifications. *trans*-Translation is the leading rescue system evolved to relieve ribosomes stalled on defective messenger transcripts. A distinct outcome of this unique pathway is the targeted elimination of aberrant mRNAs. To this end, the SmpB-tmRNA complex specifically recruits RNase R to the stalled ribosome. In order to identify the binding partners necessary for RNase R engagement on stalled ribosomes, we performed RNA CLIP followed by high throughput sequencing using RNase R, crosslinked to the ribosomes, as the bait. Our preliminary search indicated that RNase R docks near the mRNA exit site close to the binding site of S6:S18 complex. We analyzed the contributions of ribosomal protein S6 and its unique posttranslational modification to RNase R-mediated nonstop mRNA decay. Our data demonstrated that RNase R requires the unique S6 C-terminal tail modification to preferentially enrich on tmRNA-rescued ribosomes to degrade nonstop mRNA. In the absence of the RimK-mediated posttranslational modification of S6, RNase R association with tmRNA-rescued ribosomes is severely hampered resulting in the stabilization of nonstop mRNA. However, chromosomally hardcoding glutamate residues in the C-terminus of S6 restored RNase R association in the absence of RimK to wild type levels. The biochemical evidence presented in this study is the first of its kind that reveals the biological function of ribosomal protein S6 and its modification.

4.2 Introduction

Ribosome is a macromolecular ribonucleoprotein assembly that performs the essential task of protein synthesis in all living cells. Ribosomal proteins and RNAs have long been known to undergo numerous posttranslational and posttranscriptional modifications respectively. An unsolved conundrum in understanding ribosome biology deals with unraveling the functional significance of a myriad of ribosomal protein modifications. In late 1970s and 1980s, the Isono group identified and characterized several genes encoding for ribosomal modification (*rim*) enzymes [82-87]. Although some of the ribosomal proteins that get modified are essential, the corresponding *rim* genes are non-essential in *E. coli*. Strains with *rim* genes deleted do not exhibit severe growth defects under standard conditions. This suggests that the lack of modifications on the ribosomal proteins do not have a drastic effect on the translation machinery and the protein production capacity of the cell. For instance, ribosomal protein S5 is positioned in the mRNA entry channel of the 30S subunit, and ribosomal protein S18 is located close to the anti-Shine-Dalgarno sequence on the 30S subunit. The genes encoding these highly conserved ribosomal proteins *rpsE* (S5) and *rpsR* (S18) are essential in *E. coli*. They undergo N-terminal acetylation at alanine residue by non-essential enzymes RimJ and RimI respectively [82, 85]. It is conceivable that the ribosomal proteins modifications might be temporally controlled, or occur according to the cellular needs. These modifications can also lead to the formation of specialized ribosomes that are equipped to perform certain intricate tasks, which are distinct from the canonical ribosomes. However, the exact purpose of such ribosomal protein modifications has remained relatively unexplored till date.

A recent study characterized the function of *rimO*, which encodes for a SAM-dependent methylthiotransferase that catalyzes the methylthiolation of a universally conserved Asp88 residue of ribosomal protein S12 [88]. While Asp88 is essential, its corresponding modification is not critical for cell survival. Another report has indicated that β-methylthioaspartic acid of S12 is required for binding of RNase R to the ribosomes, although direct pull-down assays were not conducted. Furthermore, the effect of the S12 modification on the translation of *rnr* mRNA was not analyzed. The

study concluded that the binding of RNase R to the modified form of S12 on the ribosome is required to increase the intracellular half-life of RNase R [89].

Another unique ribosomal modification is the posttranslational addition of glutamate residues to the C-terminus of ribosomal protein S6 [83]. S6 is a slightly acidic protein (pI = 5.23) composed of 131 amino acids with an unstructured C-terminal tail rich in negatively charged amino acids. In complex with S18, S6 binds to the ribosome near the mRNA exit channel in the 30S subunit [90]. *In E. coli*, S6 and S18 are encoded by a highly conserved operon (rpsF-priB-rpsR-rplI). Unlike *rpsR*, deletion of *rpsF* (S6) is not lethal. However, *rpsF* mutant cells exhibit severe growth defects, and a cold-sensitive phenotype [91]. RimK, an ATP dependent L-glutamyl ligase, has been shown to catalyze the S6 modification. It is estimated to post-translationally extend the S6 C-terminus by up to four glutamate residues *in vivo*. *In vitro,* RimK has the capacity to synthesize 46-mer of poly-α-glutamic acid (maximum) depending on the reaction conditions. RimK exhibits high specificity for glutamate residues. Mutation of the penultimate C-terminal glutamate residue (E130) of S6 prohibits RimK from catalyzing the glutamate ligation reaction [83, 92, 93]. However, the precise biological role of this modification of S6 by RimK has not been defined.

Translation of aberrant mRNAs leads to futile arresting of ribosomes. *trans*-Translation is a unique translational quality control pathway evolved in bacteria to relieve such stalled ribosomes and avert its deleterious consequences. This mechanism is primarily coordinated by a hybrid transfer-messenger RNA (tmRNA) and its essential protein partner small protein B (SmpB). Previous studies have shown that RNase R is recruited to stalled ribosomes to selectively degrade defective mRNAs in an SmpB-tmRNA dependent manner [36-38, 42]. The distinct lysine-rich domain of RNase R is required for this process. The initiation of defective mRNA decay occurs after the establishment of accurate tmRNA open reading frame. Co-purification of RNase R with the stalled ribosomal complex under stringent conditions suggests that RNase R interaction with the ribosomal components is relatively stable [36]. However, the ribosomal partners required for RNase R to bind and carry out its function are not known. Given that RNase R is a 3'-5' exoribonuclease, it is conceivable that RNase R

will be favorably positioned near the mRNA entry channel or the exit channel to capture the emerging defective mRNA. Identification of the location of RNase R docking in the ribosomal landscape will provide a glimpse into its mechanism of action.

In the studies described herein, we present biochemical evidence that provide insights into the requirements for productive engagement of RNase R on stalled ribosomes. From *in vivo* RNA-protein crosslinking and immunoprecipitation experiments, we show that RNase R crosslinks to nucleotides 657-682 on the 16S rRNA in a region close to the binding site of the S6:S18 complex. Analyses of *E. coli* strains with either S6 C-terminal truncation variant ($S6^{102}$) or *rimK* deletion show that RNase R association with the stalled ribosomes is severely hampered in these backgrounds. As a result, nonstop mRNA is stabilized despite the presence of active *trans*-translation. Furthermore, hardcoding of four- glutamate residues in the C-terminus of S6 in a *rimK* deletion background restored RNase R enrichment on stalled ribosomes to wild type levels. This confirmed that no other function of RimK but the S6 modification is essential for RNase R engagement on tmRNA-rescued ribosomes. In contrast, deletion of *rimO* had no effect on RNase R association with the stalled ribosomes, and the consequent decay of nonstop mRNA. Deletion of *rimI*, which acetylates S18, the binding partner of S6, also did not affect RNase R association with the stalled ribosomes. From mass spectrometric analyses, we found that the RimK-catalyzed modification of S6 is not dependent on *trans*-translation, suggesting that this step precedes or is independent of rescue of stalled ribosomes by the SmpB-tmRNA complex. Taken together, these data demonstrate that RNase R binds near the mRNA exit channel, and the unique S6 C-terminal tail modification by RimK is essential for the tightly coordinated process of RNase R-mediated nonstop mRNA decay.

4.3 Materials and Methods

4.3.1 Strains and plasmids

Escherichica coli strain MG1655 *rnr::kan, rimK::kan*, *rimO::kan* were obtained by P1 transduction using respective Keio disruption strains as donors [48]. Chromosomal variants of S6 were made in *E. coli* strain MG1655 using previously published protocol [94]. Mutations made in the chromosome were verified by DNA sequencing. A plasmid expressing the coding region of N-terminal domain of cI protein (pλ-cI-NS), which encodes for an N-terminal His6 epitope but lacks in-frame stop codons, served as the source of the non-stop reporter mRNA. A control reporter plasmid (pλ-cI-S), which encodes for an N-terminal His6 epitope and has two tandem in-frame stop codons, served as the source of the "normal" or stop codon containing reporter mRNA. A pACYCDuet-1 plasmid (p*rnr*) harboring the *E. coli rnr* gene under the control of the arabinose inducible P_{BAD} promoter was used as a template to synthesize RNase R variants by site directed mutagenesis. A plasmid encoding N-terminal HA-tagged RNase R (prnr^{HA}) was constructed by inserting four tandem HA tag coding sequences at the 5′ end of *rnr* gene in p*rnr* by PCR-based site directed mutagenesis.

4.3.2 RNA CLIP and sequencing analysis

E. coli MG1655 *rnr::kan* cells harboring prnr^{HA} with pλ-cI-NS or pλ-cI-S were grown at 37ºC in Luria-Bertani broth containing 0.01% arabinose, 100 µg/ml of Ampicillin, and 30 µg/ml of Chloramphenicol. Upon reaching mid-log OD_{600}, the reporter gene expression was induced by the addition of 1mM final concentration of isopropyl β-D-thiogalactoside (IPTG). After 1 hour of induction, the cells were pelleted and resuspended in 2 ml of 1X PBS. After the cells were UV-crosslinked in UV Stratalinker® 1800 (Stratagene) with 800 mJ of energy, 10 ml of enrichment buffer (50 mM Tris-HCl

pH 7.5, 300 mM NH4Cl, 20 mM MgCl2, 2 mM β-ME and 10 mM Imidazole) was added to each sample. The resuspended cells were lysed using French press. Total and enriched ribosomes were isolated as per previously published protocol.

HA-tagged RNase R crosslinked to total or enriched ribosomes were pulled out using anti-HA magnetic beads (MBL INTERNATIONAL CORPORATION). RNase R-crosslinked RNA fragments were cloned using a modified HITS-CLIP protocol [95, 96]. The resulting DNA library was sequenced using GAII machine from Illumina Inc. Sequencing reads were filtered for quality, adapter sequences were clipped off (FASTX-toolkit) and the resulting reads were mapped using Bowtie program with up to 2 mismatches against *E. coli* K12 genome or specific RNA molecules: 16S rRNA, 23S rRNA, 5S rRNA, tmRNA and the reporter sequence [97]. Samtools and bedtools were used to generate bedgraphs, which were visualized using IGV [98-100].

Reporter mRNA stability and Ribosome Enrichment Analysis were performed as listed in Section 2.3.3.

4.3.3 Mass spectrometric analysis

Total or enriched ribosomes from various *E. coli* strains were isolated as per previously published protocol. 15 picomoles of ribosomes were resuspended in 1X Laemmli sample buffer, and boiled at 100ºC for 5 min. The samples were resolved in 15% SDS-polyacrylamide gel. To visualize the bands, the gel was subjected to silver staining as per manufacturer's instructions (SilverQuest™ Silver Staining Kit, Invitrogen). Bands corresponding to the molecular weight of S6 (~15.2 kDa) were cut and subjected to in-gel digestion using trypsin. Sample preparation and injection into the mass spectrometer was done as per previously published protocol [101]. Tryptic peptides corresponding to the C-terminus of S6 (trypsin cleavage site in S6, C-terminal

to R112) were searched for in +2 charge state. The *m/z* values of the peptides analyzed are listed in Table 2.

Peptide sequence	~ *m/z* at +2 charge state
RDDFANETADDAEAGDSEE	1029
RDDFANETADDAEAGDSEE**E**	1094
RDDFANETADDAEAGDSEE**EE**	1159
RDDFANETADDAEAGDSEE**EEE**	1222
RDDFANETADDAEAGDSEE**EEEE**	1287

Table 2. Modified forms of S6 C-terminus and their corresponding *m/z* values. Trypsin prefers to cleave after Arg112 residue in the C-terminus of S6. The theoretical *m/z* values of various modified forms of S6 C-terminus are listed here. Based on these values, mass spectra were searched for to ascertain the presence of the peptides in the samples.

4.4 Results

4.4.1. RNase R binds near the mRNA exit channel on the 30S subunit

As evident from several studies, RNase R stably associates with ribosomes prepared under stringent purification conditions (includes 32% sucrose cushion with 300 mM NH_4Cl). Additionally, we have shown that RNase R initiates nonstop mRNA decay on stalled 70S ribosomal complexes [36]. This emphasizes the notion that RNase R has preferred ribosomal protein and/or RNA binding partners that are required for the docking on the ribosome to perform its task. To ascertain the exact binding site of

RNase R on 70S ribosomes, we performed *in vivo* UV crosslinking and enriched for ribosomes bound to HA-tagged RNase R. We performed RNA crosslinking, immunoprecipitation, and sequencing (RNA CLIP-Seq) of RNA fragments crosslinked to RNase R obtained from total or enriched ribosomes translating the nonstop reporter mRNAs. Surprisingly, the RNA hits from all these samples mapped to distinct locations on the ribosomal RNAs as described in detail below.

First, we analyzed the RNA CLIP-Seq results for the occurrence of nonspecific signals. The starting material used for this assay was tight-coupled ribosomes passed through 32% sucrose cushion. Further, to isolate RNase R-crosslinked ribosomes, we immunoprecipitated RNase R from total or stalled ribosomes samples. Therefore, the majority of the cellular RNAs should be removed during the preparation. As a result, we expected to see little to no mapping of sequencing reads to protein coding regions in the *E.coli* genome. The specificity of RNase R crosslinking was confirmed by mapping the sequencing libraries to the *E. coli* genome. Figure 4.1A shows the distribution of counts for the uniquely mapping reads to ribosomal RNAs and *E. coli* genome. This histogram depicts the occurrence (frequency) of unique sequencing reads vs the peak counts of signals (unique sequencing reads) mapping to either ribosomal RNAs or the *E. coli* genome. To begin, we mapped reads other than the rRNA sequences to the *E. coli* genome to analyze the proportion of nonspecific hits. From the *E. coli* genome histogram, we saw that the distribution was highly skewed towards low counts indicating that there was no site in the genome with more than 20 counts. This implies that none of the mRNAs (including the highly transcribed genes) have high count binding site that constitute the nonspecific signal. The number of binding sites in chromosomal transcripts was low which constitutes the background noise. This can be the result of either the artefactual mapping of short reads or transient interactions of RNase R with abundant transcripts.

Based on our previous biochemical results, we predicted that RNase R most likely binds near the mRNA exit site. 5S ribosomal RNA is not located in the vicinity of mRNA exit site. To control for the sequencing reads mapping to ribosomal RNAs nonspecifically, we analyzed the number of reads that mapped to 5S rRNA. The reads

mapping to the 5S rRNA showed skewed distribution towards low count similar to that of *E. coli* genome indicating that RNase R did not crosslink to all ribosomal RNAs nonspecifically (Figure 4.1A). This gave us more confidence on the specificity of RNase R crosslinking and immunoprecipitation.

In contrast, the 16S and 23S rRNAs reads were distinct in having an additional long tail towards the high-count crosslinked sites in the distribution plots (Figure 4.1A). Figure 4.1 B and C show the profile of sequencing reads for 16S and 23S rRNA respectively. Both 16S and 23S rRNAs show a single major site reproducibly found in all of the samples, with additional minor binding sites often present in only few samples. The major binding sites are not only the ones which have the most reads, they are also outliers on the distribution plots, with no continuity in distribution histogram between them and the rest of the site population. Additionally, they show these features in all of the replicates, strongly suggesting they are the primary binding sites of RNase R. The sequence reads mapping to the antisense sequence of the rRNA was taken as a negative control for the artefactual mapping, since no such sequences should be generated from our ribosomal samples. However, in both 16S minus and 23S minus strands where such sites were detected, there were just six such sites with the typical corresponding read count being 1-2, with 10 being the absolute maximum. If a count of 20 is taken as a safe conservative cutoff value, the emerging image of RNase R interactions comes very clear with two major binding sites candidates, and a few additional minor binding site candidates (Table 3).

Based on the analysis of the distribution plot, we identified the following sites as the potential RNase R binding site candidates. The 16S rRNA site spans a stretch of 26 nucleotides, from position number 657 to 682, while the 23S rRNA site is 25 nucleotides long, from position number 178 to 202, albeit the signal intensity of region 178-202 in the 23S rRNA is lower than that of 16S rRNA.

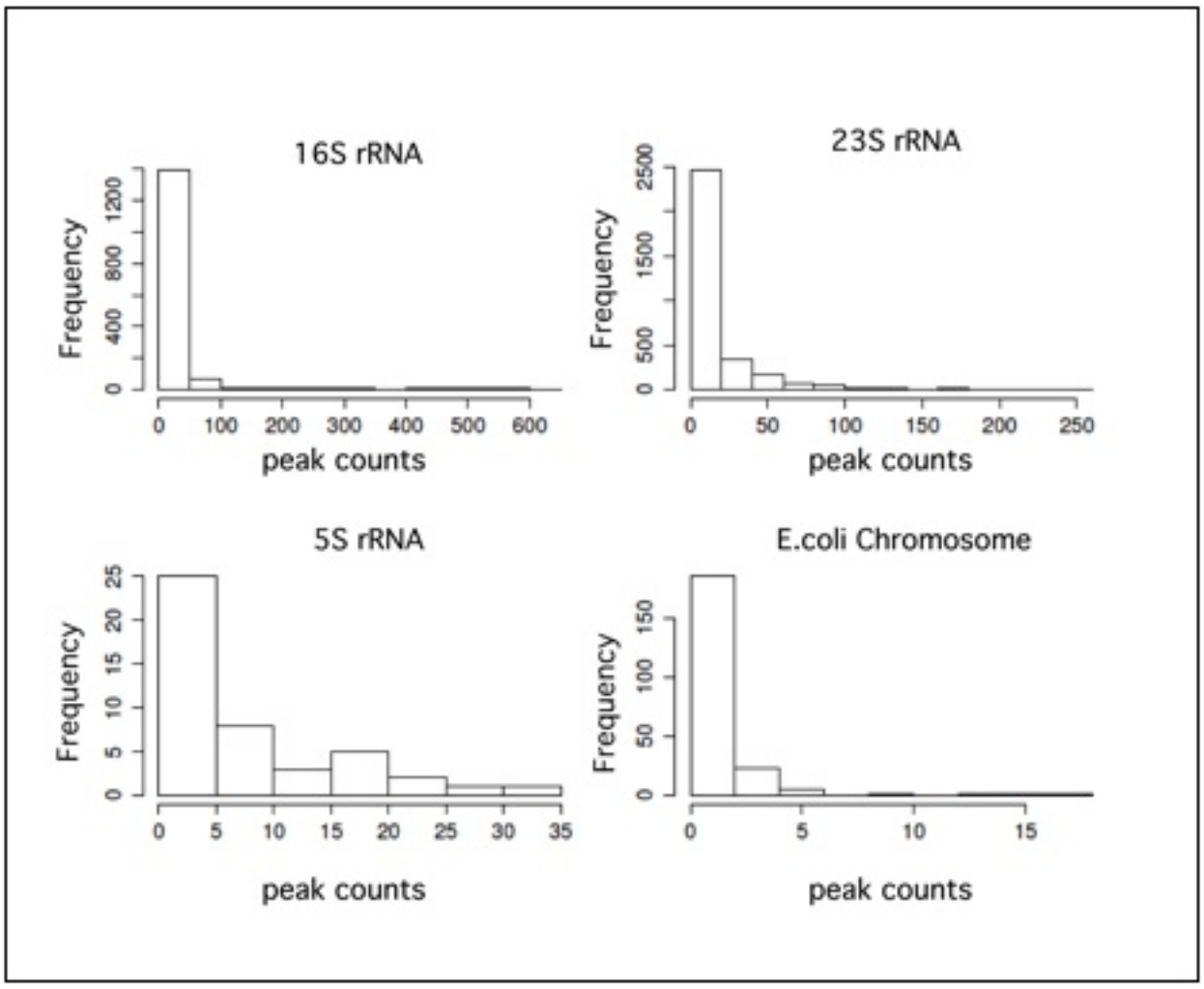

Figure 4.1A. Distribution plots of peak counts vs. frequency of RNA sequencing reads. Sites that are potentially crosslinked to RNase R are expected to have high counts. To have higher confidence on the signals, the frequency of occurrence of such sites should be low. In these distribution plots, the majority (frequency) of unique sequencing reads that map to ribosomal RNAs or the *E. coli* chromosome are towards the lower side of the peak counts (signals). Highest signal (with over 400 peak counts) in case of 16S rRNA was not found in greater frequency. This indicated the presence of few potential unique crosslinked sites with strong signal. Similarly, in the case of 23S rRNA, the presence of few potential unique crosslinked sites with over 100 peak counts. Peak counts corresponding to 5S rRNA and *E. coli* chromosome fall in the background level indicating that RNase R crosslinked site candidates lay in 16S rRNA and 23S rRNA.

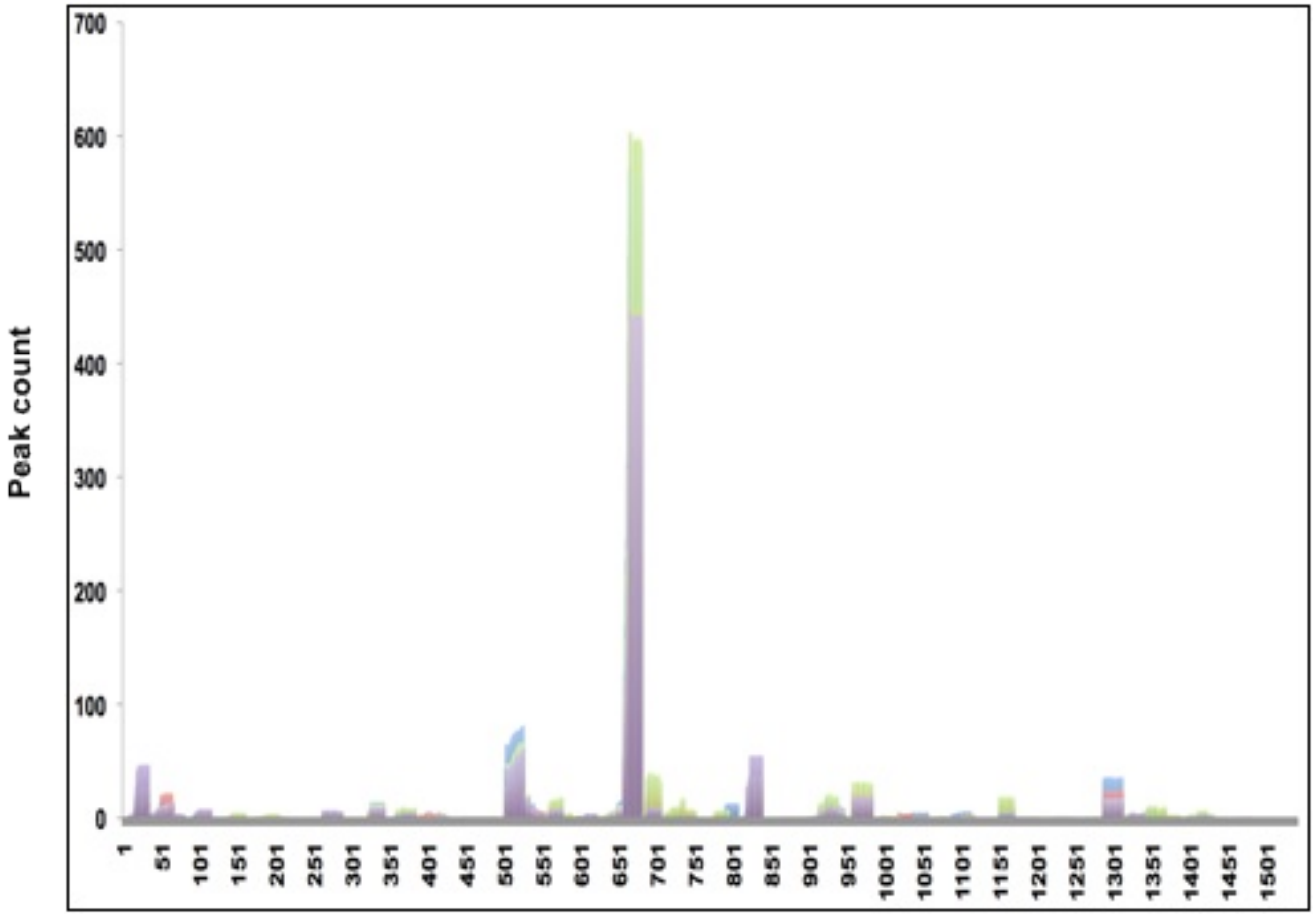

Figure 4.1B RNA sequencing reads mapped on 16S rRNA. RNA sequencing reads obtained from replicates of total ribosomes (blue and red) or enriched ribosomes translating nonstop reporter (green and purple) were clustered and plotted in this graph. The X-axis denotes the nucleotide position on the 16S rRNA and Y-axis denotes the corresponding peak counts. Region 657-682 showed the maximum signal in all the samples sequenced.

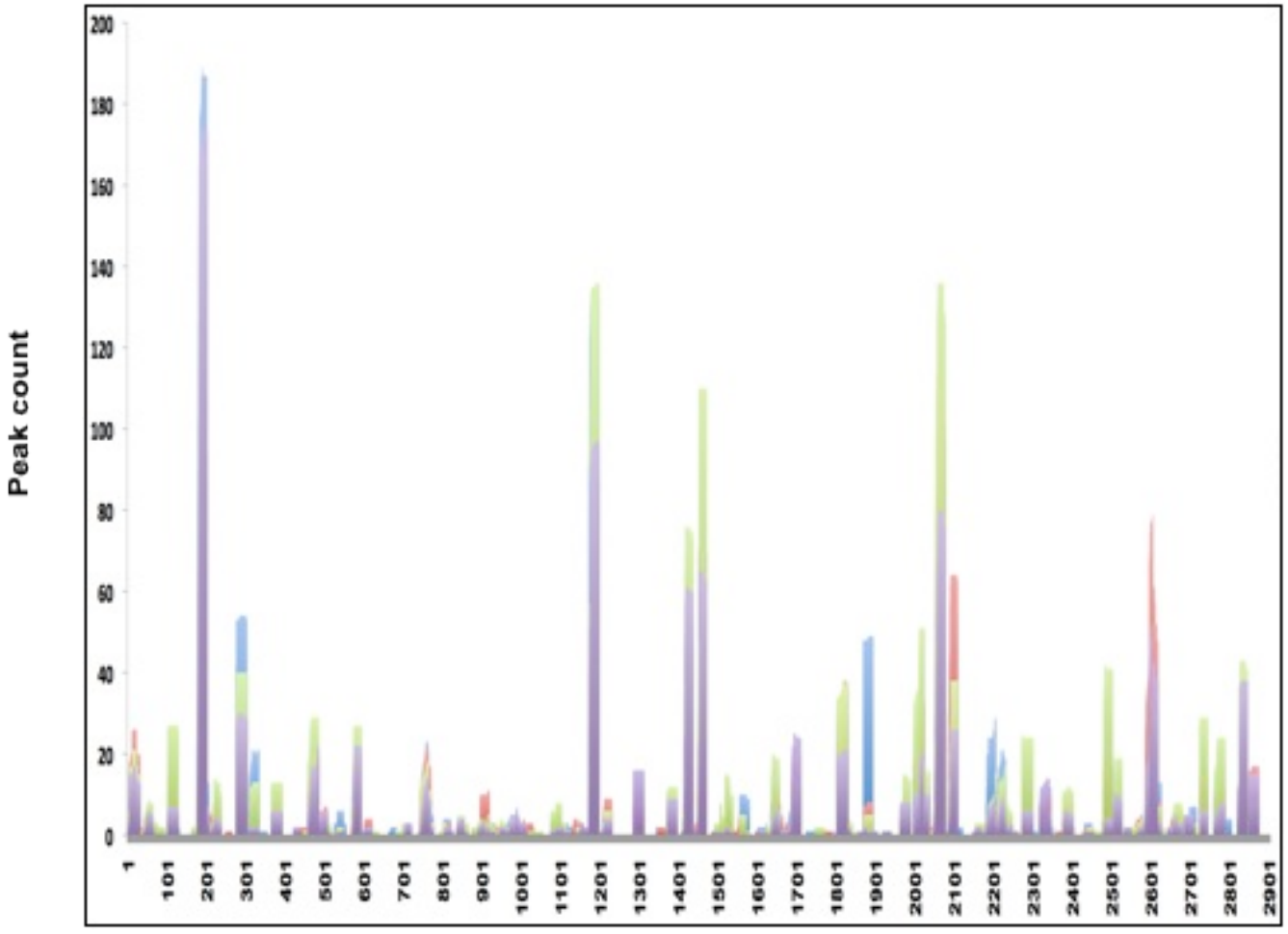

Figure 4.1C RNA sequencing reads mapped on 23S rRNA. RNA sequencing reads obtained from replicates of total ribosomes (dark blue and red) or enriched ribosomes translating nonstop reporter (green and purple) were clustered and plotted in this graph. The X-axis denotes the nucleotide position on the 23S rRNA and Y-axis denotes corresponding peak counts. Region 178-202 showed the maximum signal in all the samples sequenced although the intensity of this peak is lower than that of 16S rRNA.

16S rRNA binding location	23S rRNA binding location
501-522	178 - 202
657-682	1178 - 1198
	2011 - 2038
	2057 - 2078
	2092 - 2116
	2595 - 2619

Table 3. **Potential binding sites of RNase R on 30S and 50S subunits**. The sites (numbers) denote the position of nucleotides on the 16S and 23S rRNA. These sites were obtained from RNA crosslinking-immunoprecipitation and high throughput sequencing on Genome Analyzer IIx platform.

We sought to investigate the contributions of the ribosomal proteins in the vicinity of the region found from RNA CLIP-Seq results. Upon mapping the 657 to 682 region in the 16S rRNA onto the *E. coli* ribosomal structure (PDB: 2WWL; 2WWQ), we found that this region lies in the vicinity of the S6:S18 complex (Figure 4.2A). However, the 178-202 region and other minor peaks with the exception of region 2092-2116 on the 23S rRNA mapped to the interior of the large subunit (Figure 4.2B). Therefore, these locations were ruled out as possible on pathway RNase R binding sites. Presence of these hits on the large subunit might be due to extensive rRNA crosslinking and incomplete digestion with RNases during the preparation of sequencing library. Region 2092-2116 on the 23S rRNA is present in the vicinity of region 657-682 in the 16S rRNA. On the other hand, the minor peak in the 16S rRNA corresponding to the 501-

522 region mapped near the mRNA entry channel and the decoding center close to ribosomal protein S12 (Figure 4.2C). However, the intensity of this signal was considerably lower (~8 fold) than signal corresponding to the 657-682 region. In light of this analysis, we proceeded to evaluate the effect of ribosomal proteins S6, S18 and S12 on nonstop mRNA decay.

4.4.2 The C-terminus of S6 is important for RNase R-mediated nonstop mRNA decay

Upon examining the C-terminus of S6 (amino acid positions 102-131), we hypothesized that this region of S6, due to the presence of negatively charged amino acid residues (~40%), might potentially interact with the K-rich domain of RNase R (Figure 4.3A). Besides, the posttranslational addition of up to four glutamate residues by RimK might be essential to further augment the engagement of RNase R on stalled ribosomes, and facilitate nonstop mRNA decay. To test this possibility, we engineered *E. coli* MG1655 strain that expresses $S6^{102}$, a chromosomal S6 C-terminal truncation variant. This S6 variant is not a substrate for RimK. Since S6 is a ribosomal protein, and is a part of a highly conserved operon along with S18, any changes made to S6 coding region might affect general translation processes in the cell. Hence, we compared the expression and tagging of the λ-cI-NS reporter protein in wild type (WT), $S6^{102}$, and a *rimK*$^{-}$ strain. We observed no detectable difference in the expression pattern and tagging of λ-cI nonstop reporter protein, indicating that the *trans*-translation process was not compromised in these mutant strains (Figure 4.3B).

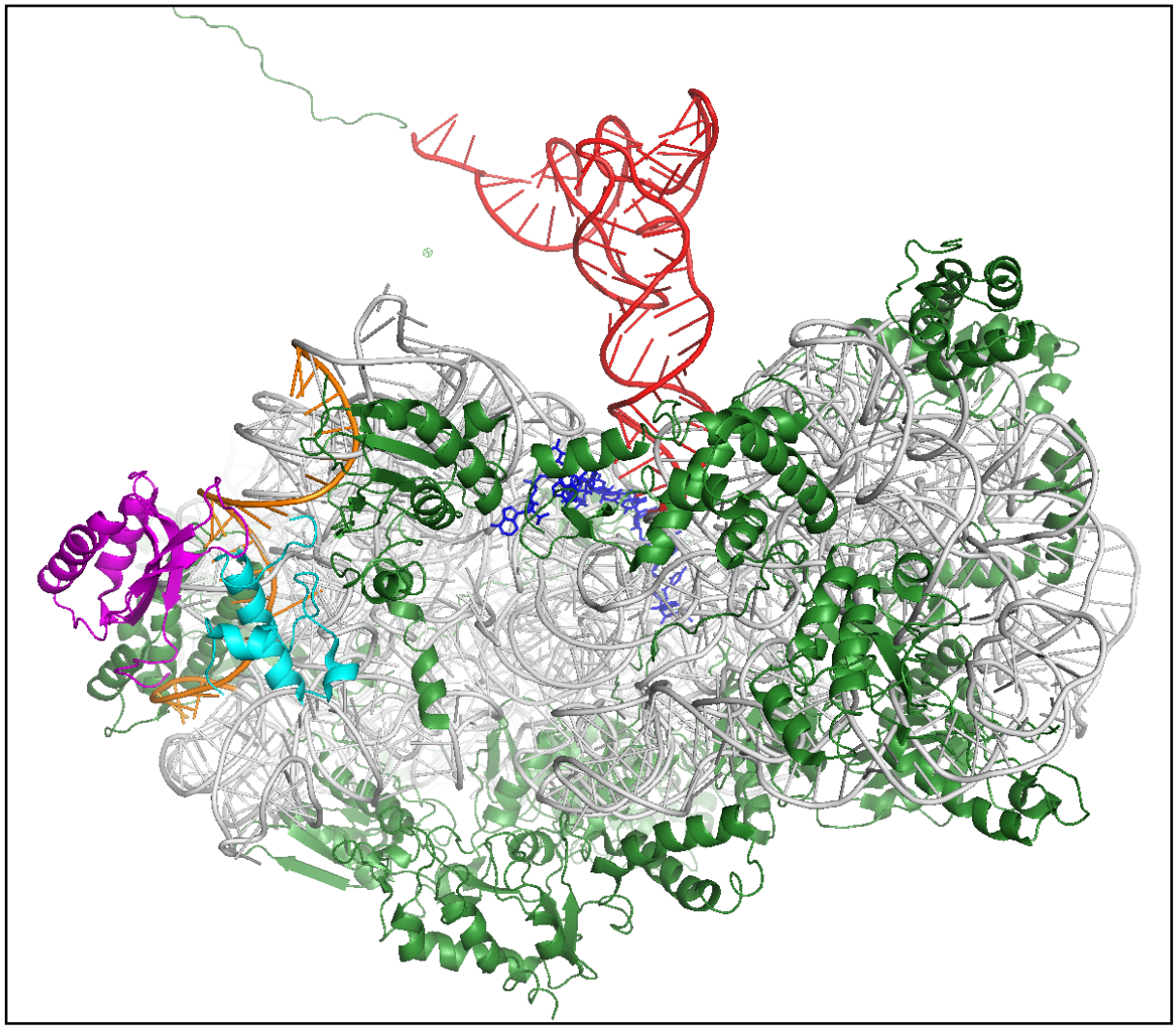

Figure 4.2A Crystal structure of *E. coli* 30S subunit with RNA CLIP-Seq read mapping. The region between nucleotides 657-682 (orange) on the 16S rRNA maps near the mRNA exit channel. Ribosomal proteins S6 (magenta) and S18 (cyan) are in the vicinity of this location. Messenger RNA is shown in dark blue, peptidyl tRNA in red, other ribosomal proteins in green, and rest of 16S rRNA in gray. PDB structure 2WWL was used to obtain this picture.

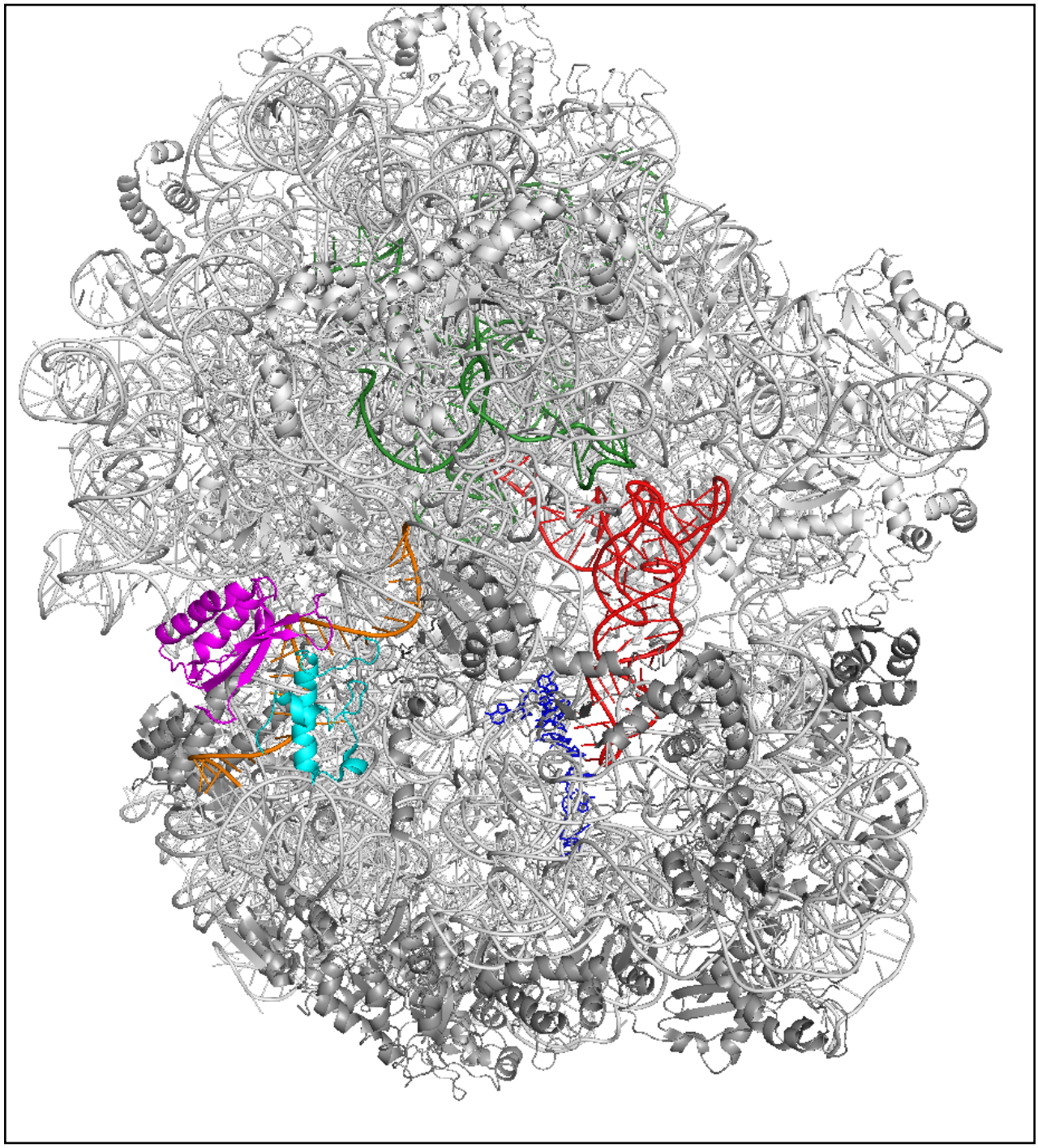

Figure 4.2B Crystal structure of *E. coli* 70S subunit with RNA CLIP-Seq read mapping. The region between nucleotides 657-682 (orange) on the 16S rRNA maps near the mRNA exit channel. RNAs CLIPSeq hits corresponding to 23S rRNA predominantly mapped to the interior locations of the 50S subunit except for the 2092-2116 region. Highlighted are: Ribosomal proteins S6 (magenta) and S18 (cyan), Messenger RNA (dark blue), peptidyl tRNA (red), other ribosomal proteins and rest of the rRNAs in gray. PDB structure 2WWL and 2WWQ were used to obtain this picture.

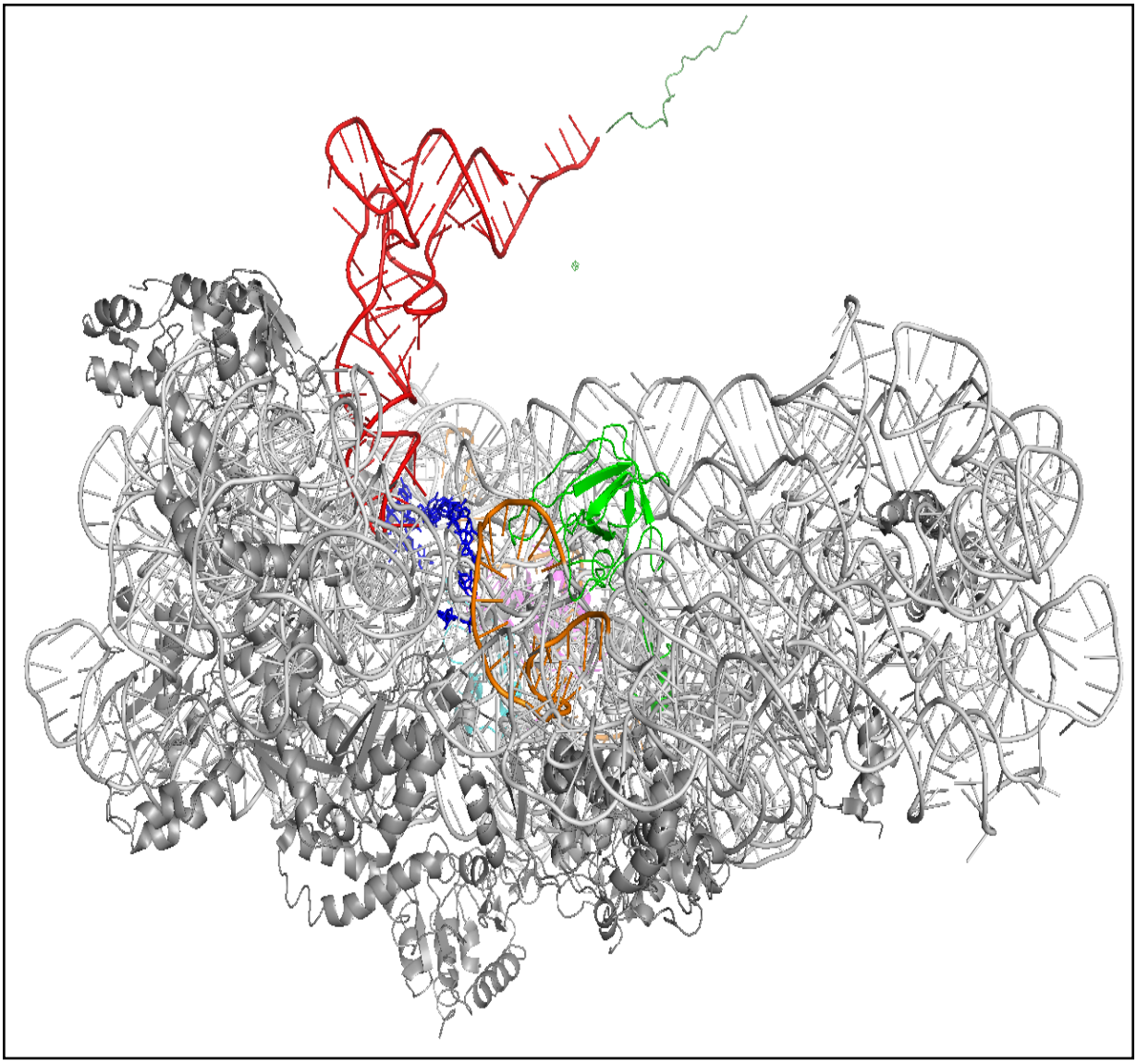

Figure 4.2C Crystal structure of *E. coli* 30S subunit with RNA CLIP-Seq read mapping. Minor peak corresponding to the region between 501-522 (orange) mapped near the mRNA entry channel close to the decoding center G530 on the 16S rRNA. This region is in the vicinity of ribosomal protein S12 (light green). Highlighted are: Ribosomal proteins S6 (pale pink in the background) and S18 (pale cyan in the background), messenger RNA (dark blue), peptidyl tRNA (red), other ribosomal proteins and rest of the rRNAs in gray. PDB structure 2WWL was used to obtain this picture.

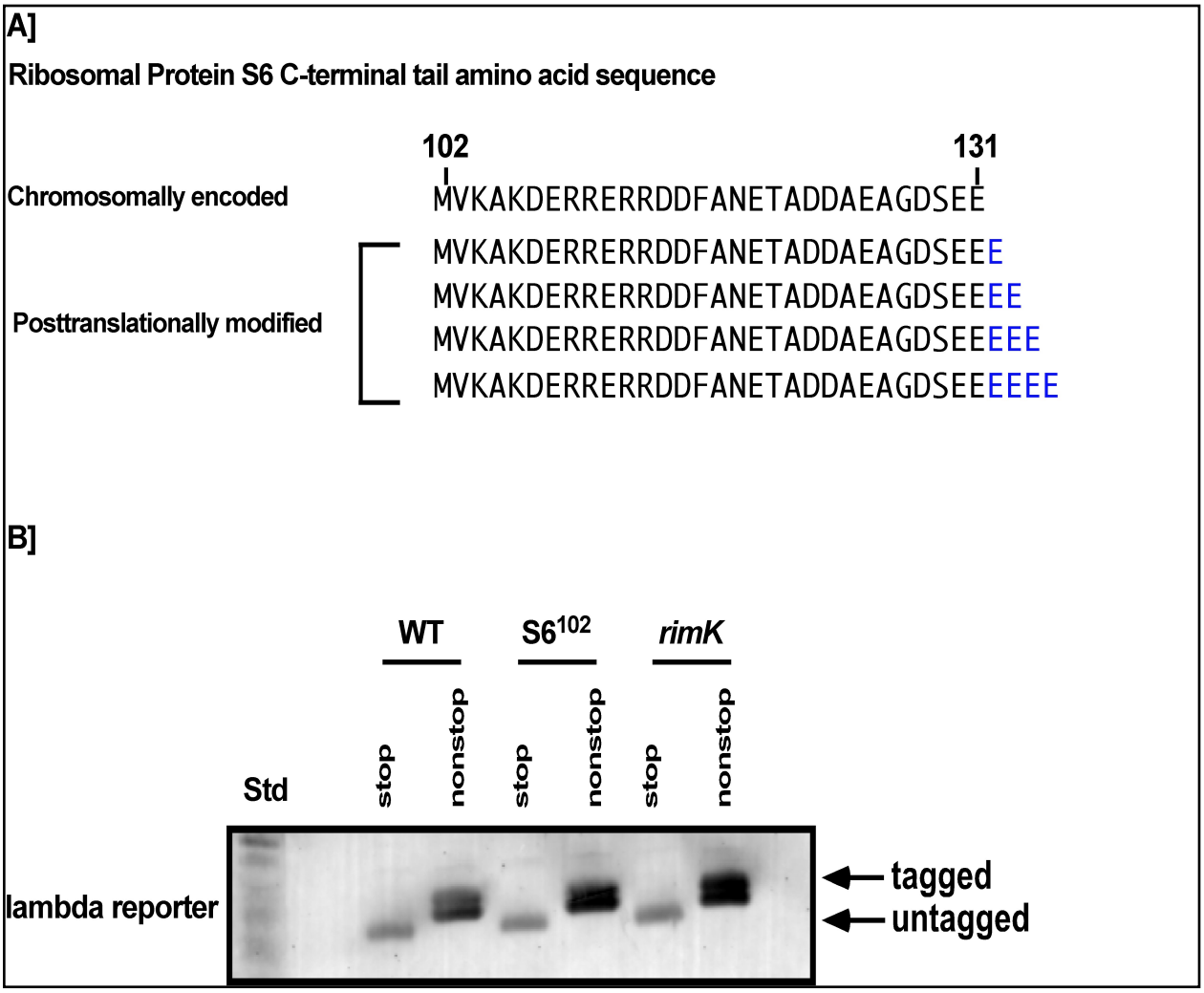

Figure 4.3 Amino acid sequence of S6 C-terminal tail and expression of λ-cI stop and nonstop reporter in various strain backgrounds. **(A)** The C-terminus of S6 is rich in negatively charged amino acids. Posttranslational modification adds up to four glutamate residues (highlighted in blue) to the C-terminus. **(B)** Western blot analysis of λ-cI stop and nonstop reporter protein expression levels in WT, a strain encoding $S6^{102}$, and a *rimK* deletion strain. The reporter protein was probed with anti-his monoclonal antibody. There was no defect detected in the reporter protein expression.

We evaluated the effect of S6 C-terminus on RNase R mediated nonstop mRNA decay by performing steady state λ-cI-NS reporter mRNA abundance analysis. Consistent with the hypothesis that the S6 C-terminal modification is important for RNase R recruitment, we observed stabilization of nonstop mRNA in the presence of the $S6^{102}$ variant (~2-fold) in comparison to the parental wild type (WT) strain (Figure 4.4A). This suggested that the C-terminal tail of S6 plays a role in nonstop mRNA

decay. Interestingly, the mere deletion of *rimK* in the presence of full length S6 was sufficient to affect nonstop mRNA decay, to a similar level as that seen with $S6^{102}$. We also confirmed that this difference in the nonstop mRNA accumulation was not due to variations in the steady state expression levels of RNase R in different strain backgrounds (Figure 4.4B). Taken together, these data suggest that the C-terminal tail, specifically the posttranslational modification of ribosomal protein S6 affects nonstop mRNA decay.

We next examined the enrichment of RNase R on stalled ribosomes in a strain expressing $S6^{102}$, and a *rimK*$^-$ strain, both of which lack the ability to modify the S6 C-terminal tail. In contrast to the wild type background, there was a severe defect in RNase R enrichment on stalled ribosomes in the presence of $S6^{102}$ or unmodified S6 in the *rimK*$^-$ strain. These results are consistent with the observed stabilization of the nonstop mRNA reporter in the $S6^{102}$ and *rimK*$^-$ backgrounds (Figure 4.4C). Overall, these results demonstrate that the recruitment of RNase R to the stalled ribosomes requires the presence of modified ribosomal protein S6 along with active *trans*-translation process.

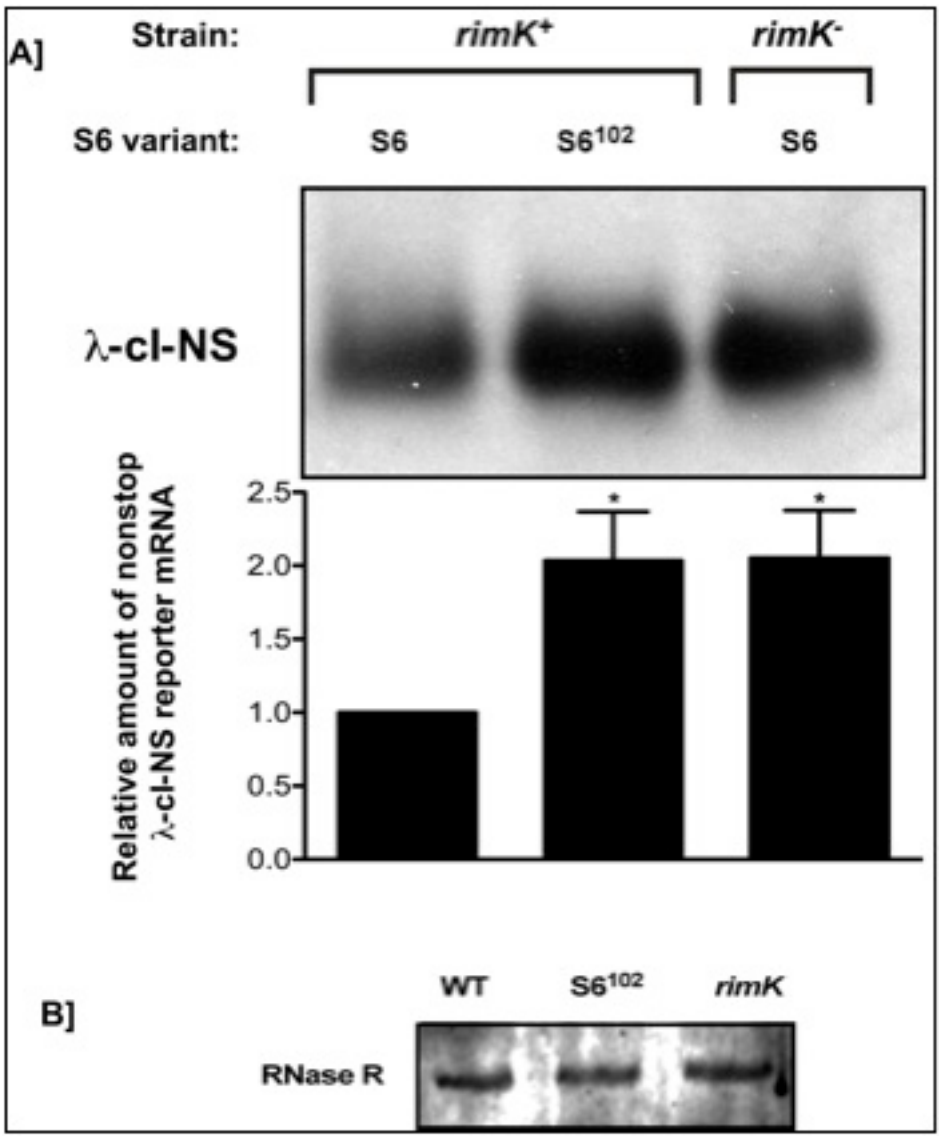

Figure 4.4 A-B Effect of S6 C-terminal tail variants on nonstop mRNA decay. **(A)** A representative Northern blot showing the effect of $S6^{102}$ and *rimK* deletion on non-stop mRNA accumulation. Cells co-expressing the λ-cI-NS reporter with plasmid-borne RNase R were harvested. Total RNA samples isolated from equal number of cells were resolved by electrophoresis on denaturing formaldehyde agarose gels followed by Northern blot analysis with a probe specific for the reporter RNA. Deletion of S6 C-terminus, particularly the lack of S6 modification by RimK, hampers nonstop mRNA degradation. *P*-values were calculated by performing Student's *t*-test analysis with wild type (WT) and $S6^{102}$ (**P* = 0.0425) or WT and *rimK*$^{-}$ (**P* = 0.0177). The data are combined from three independent experiments (MEAN±SEM) **(B)** Steady state levels of RNase R in wild type (WT) and the indicated mutant strains are similar. A representative Western blot examining the relative steady state levels of RNase R is shown. MG1655 WT, $S6^{102}$, and *rimK* deletion strain harboring p*rnr* plasmid was grown in LB with 0.01% arabinose and 30 μg/ml of chloramphenicol. Equal numbers of cells were harvested in mid-log phase and processed for Western blot analysis, using RNase R specific antibodies.

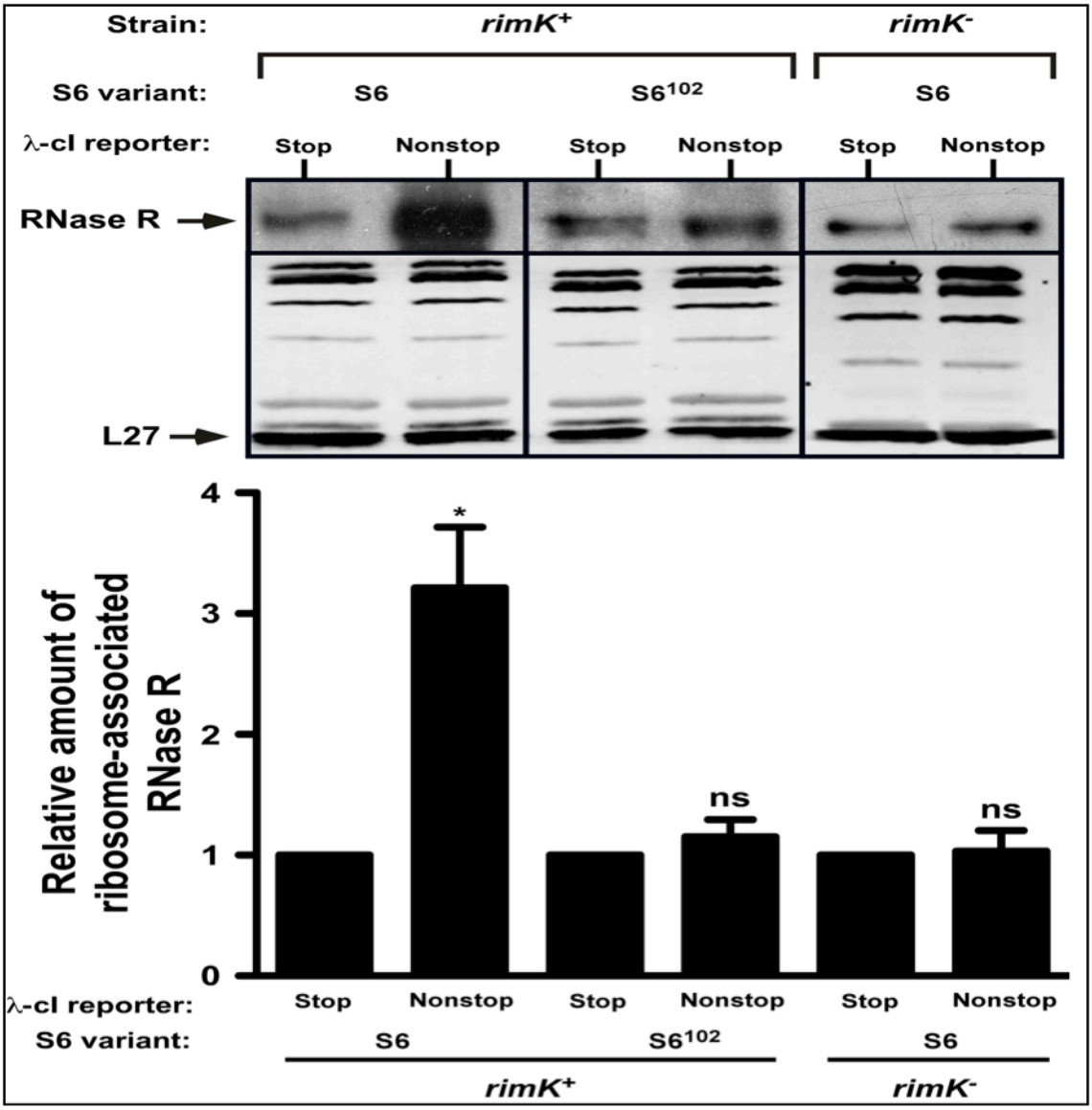

Figure 4.4C RNase R exhibits defects in enrichment on ribosomes translating nonstop mRNA in the absence of S6 C-terminal tail. Total ribosomes were obtained from cells of indicated strains co-expressing RNase R with the λ-cI-S or λ-cI-NS reporter mRNAs. Ribosomes translating the reporter RNAs were isolated from the total ribosomes pool using Ni^{2+}-NTA affinity chromatography. Equal numbers of ribosomes were resolved by electrophoresis on 10% SDS-polyacrylamide gels. Western blot analysis was performed to detect the presence of RNase R and ribosomal protein L27. The intensity of the band corresponding to RNase R was quantified using ImageJ. The top panel shows a representative Western blot, using an RNase R specific antibody, and the bottom panel shows a representative Western blot, using an anti-L27 serum displaying equal protein loading. The graph represents fold RNase R enrichment on ribosomes translating the λ-cI-NS reporter compared to ribosomes translating the control λ-cI-S reporter. The data are combined from three independent experiments (MEAN ± SEM). *P*-values were calculated by performing student's *t*-test analysis on the association level of RNase R with ribosomes translating stop and nonstop reporter in wild type background (**P* = 0.041) or mutant background (*P* = ns). ns = not statistically significant.

4.4.3 RNase R–mediated nonstop mRNA decay is independent of RimO modification on ribosomal protein S12

Previous reports indicated that the association of RNase R with ribosome requires β-methylthiolation of Asp88 residue in S12 [88]. It was also proposed that the loop region of S12, which harbors the modified D88 residue, is involved in direct binding with RNase R. This interaction of RNase R with the ribosome is thought to protect it from cellular proteases [89]. Consequently, deletion of *rimO* led to a faster rate of degradation of RNase R in the cell. This prompted us to investigate the effect of RimO on RNase R enrichment on stalled ribosomes, and subsequent nonstop mRNA decay. Analysis of the steady state expression levels of RNase R in wild type, *rimO*$^{-}$, and *rimK*$^{-}$ background revealed no discernible difference in the RNase R level. Intriguingly, deletion of *rimO* did not affect RNase R association and enrichment on stalled ribosomes, or the ensuing nonstop mRNA degradation (Figure 4.5A-B). From this result, we infer that the modification state of ribosomal protein S12 does not impact RNase R association with tmRNA-rescued ribosomes.

4.4.4 Modified S6 C-terminus in *rimK* deletion strain is sufficient for RNase R enrichment on rescued ribosomes

Ribosomal protein S6 is the only known *in vivo* substrate of RimK. It was possible that RimK-mediated modification of another unidentified substrate might enhance RNase R association with stalled ribosomes. To test whether the modification of the C-terminus of S6 directly impacts RNase R enrichment levels, we engineered S6 variants that chromosomally code for the additional C-terminal glutamate residues in an MG1655 *rimK*$^{-}$ background. We tested for RNase R association with stalled ribosomes in *rimK*$^{-}$ strains with S6 variants that code for three ($S6^{EEE}$) or four ($S6^{EEEE}$) extra glutamate residues. Our analysis revealed that the defect in RNase R enrichment observed in

rimK^{-} background was restored to wild type levels in the presence S6^{EEEE} (Figure 4.6A). Similar preliminary results were obtained in the presence of either S6^{EEE} (Figure 4.6B). Taken together, these data strongly suggest that the unique C-terminal glutamate modification of S6 is sufficient to enable productive engagement of RNase R on tmRNA-rescued ribosomes.

4.4.5 RimK-catalyzed modification of S6 C-terminus does not require the presence of *trans*-translation system.

We next determined whether RimK requires the presence of active *trans*-translation process to catalyze the addition of glutamate residues to C-terminus of S6. To this end, we assessed the S6 modification pattern in wild type and *smpBssrA* deletion backgrounds using mass spectrometric analysis. We isolated total ribosomes and ribosomes translating either λ-cI-S or λ-cI-NS reporter mRNAs. Tryptic peptides obtained from the respective samples were injected into the mass spectrometer, and the resulting spectra were analyzed for the presence of modified versions of S6 peptide P1 (amino acids 113-131: RDDFANTEDDAEAGDSEE) and its modified forms (Table 2, Figure 4.3A). In both wild type and *smpBssrA* deletion strains, we found unmodified and modified forms of peptide P1 (Figure 4.7). Remarkably, in the total and enriched ribosomes samples in both backgrounds, the predominantly modified form ofS6 contained addition of one glutamate residue. Peptide species with three or four glutamate residues addition at the C-terminus were not detected, suggesting that this population might be present in lower levels in the cell. These results indicate that presence of pivotal components of *trans*-translation process is not a prerequisite for RimK-mediated S6 C-terminal tail modification. The modification of S6 even in ribosomes translating λ-cI-S reporter mRNA might explain the background level association of RNase R on ‘normal’ ribosomes. It is still not clear what factors trigger S6 modification by RimK.

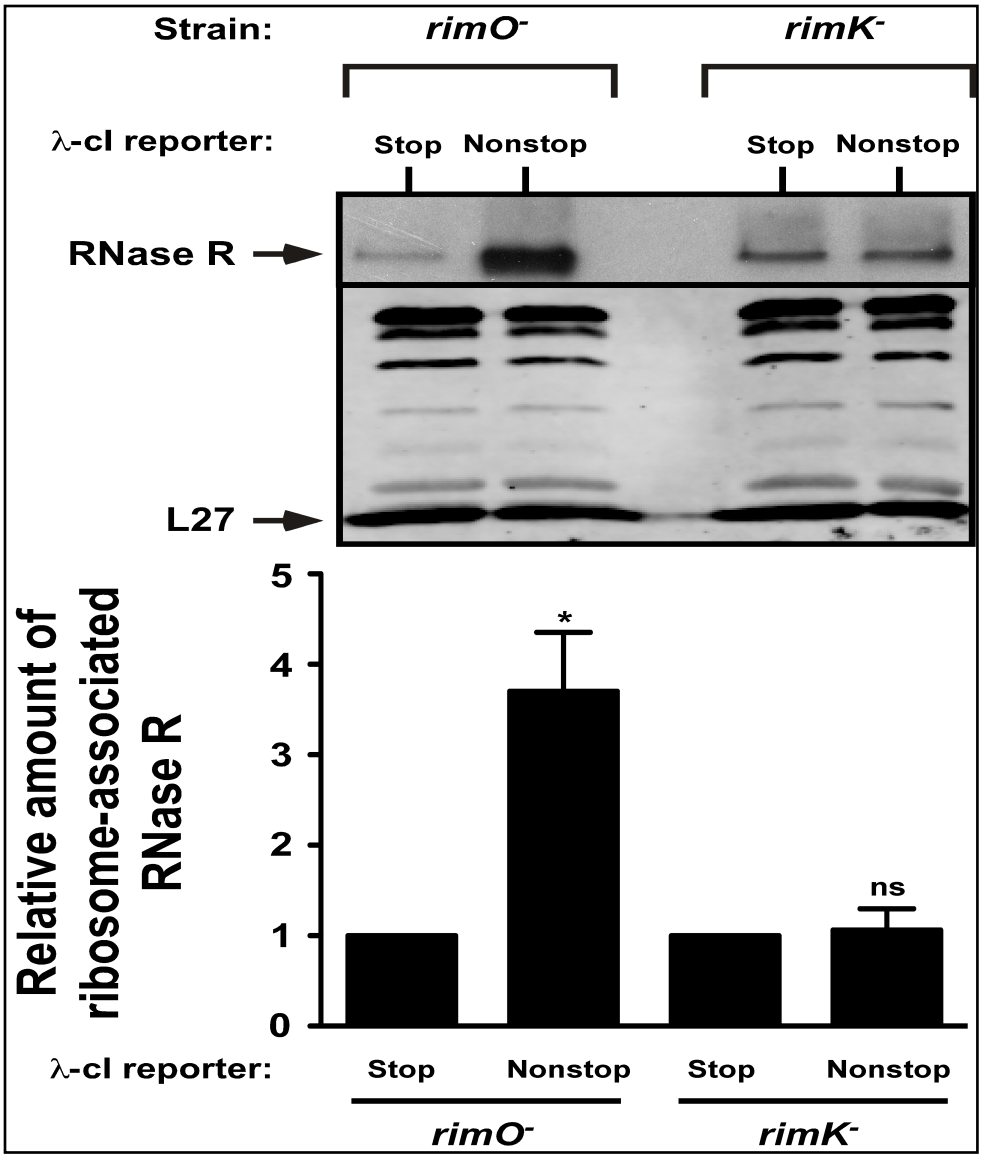

FIGURE 4.5A The absence of RimO modification on S12 does not affect RNase R enrichment on ribosomes translating nonstop mRNA. Total ribosomes were obtained from cells of indicated strains co-expressing RNase R with the λ-cI-S or λ-cI-NS reporter mRNAs. Ribosomes translating the reporter RNAs were isolated from the total ribosomal pool using Ni^{2+}-NTA affinity chromatography. Equal numbers of ribosomes were resolved by electrophoresis on 10% SDS-polyacrylamide gels. Western blot analysis was performed to detect the presence of RNase R and ribosomal protein L27. The intensity of the band corresponding to RNase R was quantified using ImageJ. The top panel shows a representative Western blot, using an RNase R specific antibody, and the bottom panel shows a representative Western blot, using an anti-L27 serum displaying equal protein loading. The graph represents fold RNase R enrichment on ribosomes translating the λ-cI-NS reporter compared to ribosomes translating the control λ-cI-S reporter. The data are combined from three independent experiments (MEAN ± SEM). *P*-values were calculated by performing student's *t*-test analysis on the association level of RNase R with ribosomes translating stop and nonstop reporter in wild type background (**P* = 0.0056) or mutant cells (*P* = ns). ns = not statistically significant.

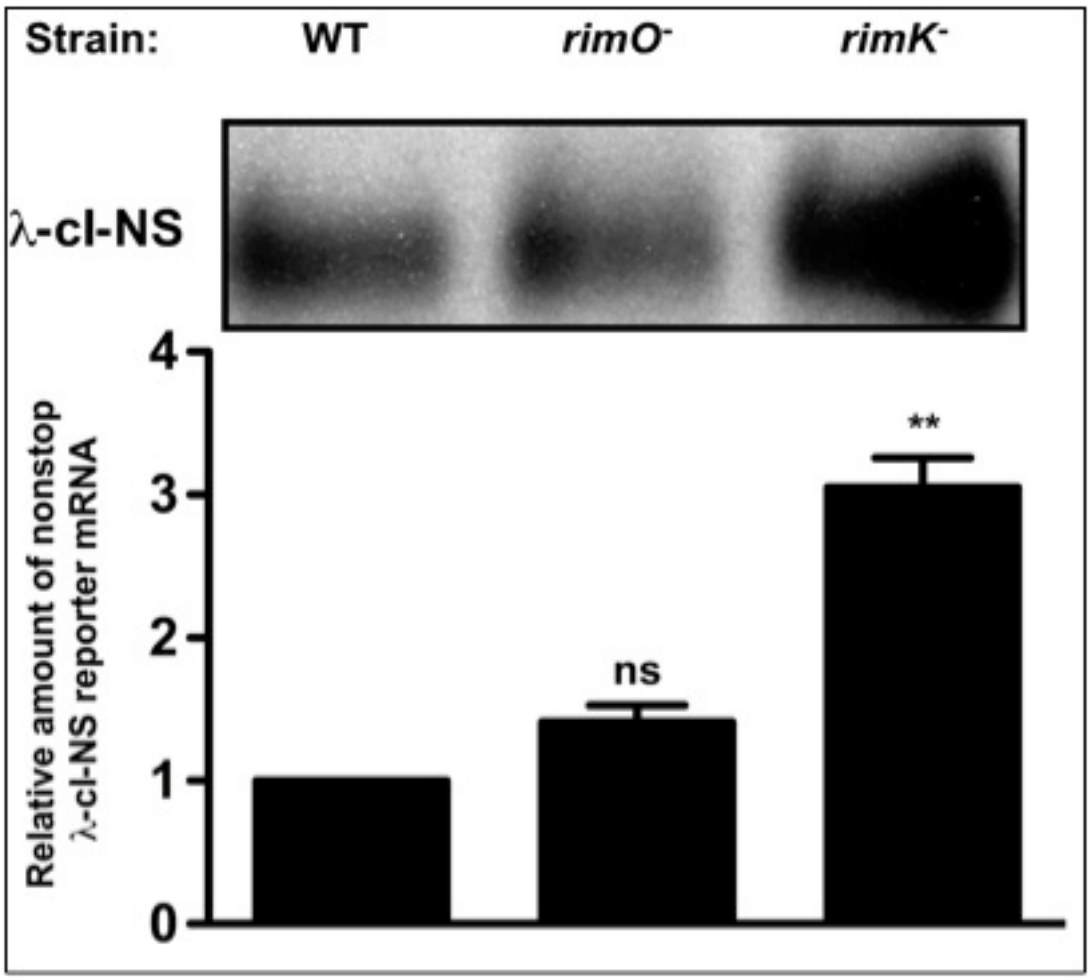

Figure 4.5B Absence of RimO does not affect steady state nonstop reporter mRNA abundance. A representative Northern blot showing the effect of *rimO* and *rimK* deletions on non-stop mRNA accumulation levels. Cells co-expressing the λ-cI-NS reporter with plasmid-borne RNase R were harvested. Total RNA samples isolated from equal number of cells were resolved by electrophoresis on denaturing formaldehyde agarose gels followed by Northern blot analysis with a probe specific for the reporter RNA. Deletion of S6 C-terminus, particular the modification of S6 by RimK hampers nonstop mRNA degradation. The data are combined from three independent experiments (MEAN ± SEM). *P*-values were calculated by performing student's *t*-test analysis on the nonstop mRNA accumulation levels between wild type and *rimO*$^{-}$ (*P* = ns) or wild type and *rimK*$^{-}$ cells (**P = 0.0024). ns = not statistically significant

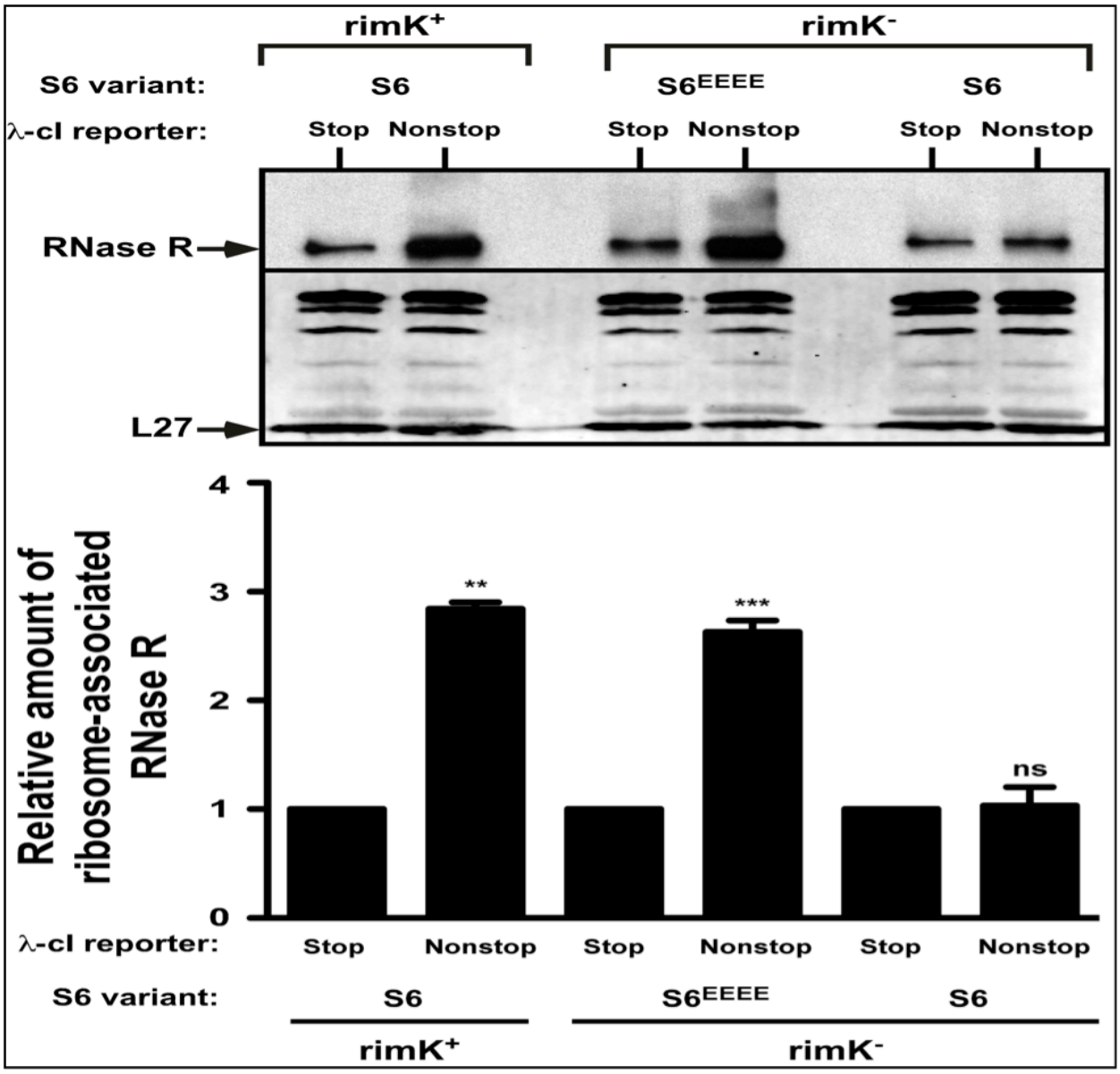

Figure 4.6A RNase R enrichment defect in *rimK* deletion background is restored upon hardcoding C-terminal glutamate residues in S6. Total ribosomes were obtained from cells of indicated strains co-expressing RNase R with the λ-cI-S or λ-cI-NS reporter mRNAs. Ribosomes translating the reporter RNAs were isolated from the total ribosomal pool using Ni^{2+}-NTA affinity chromatography. Equal numbers of ribosomes were resolved by electrophoresis on 10% SDS-polyacrylamide gels. Western blot analysis was performed to detect the presence of RNase R and ribosomal protein L27. The intensity of the band corresponding to RNase R was quantified using ImageJ. The top panel shows a representative Western blot, using an RNase R specific antibody, and the bottom panel shows a representative Western blot, using an anti-L27 serum displaying equal protein loading. The graph represents fold RNase R enrichment on ribosomes translating the λ-cI-NS reporter compared to ribosomes translating the control λ-cI-S reporter. The data are combined from three independent experiments (MEAN ± SEM). *P*-values were calculated by performing student's *t*-test analysis on the association level of RNase R with ribosomes translating stop and nonstop reporter in wild type (***P* = 0.0011), $S6^{EEEE}$/$rimK^-$ (****P*=0.0001), or $rimK^-$ (ns) cells. ns = not statistically significant

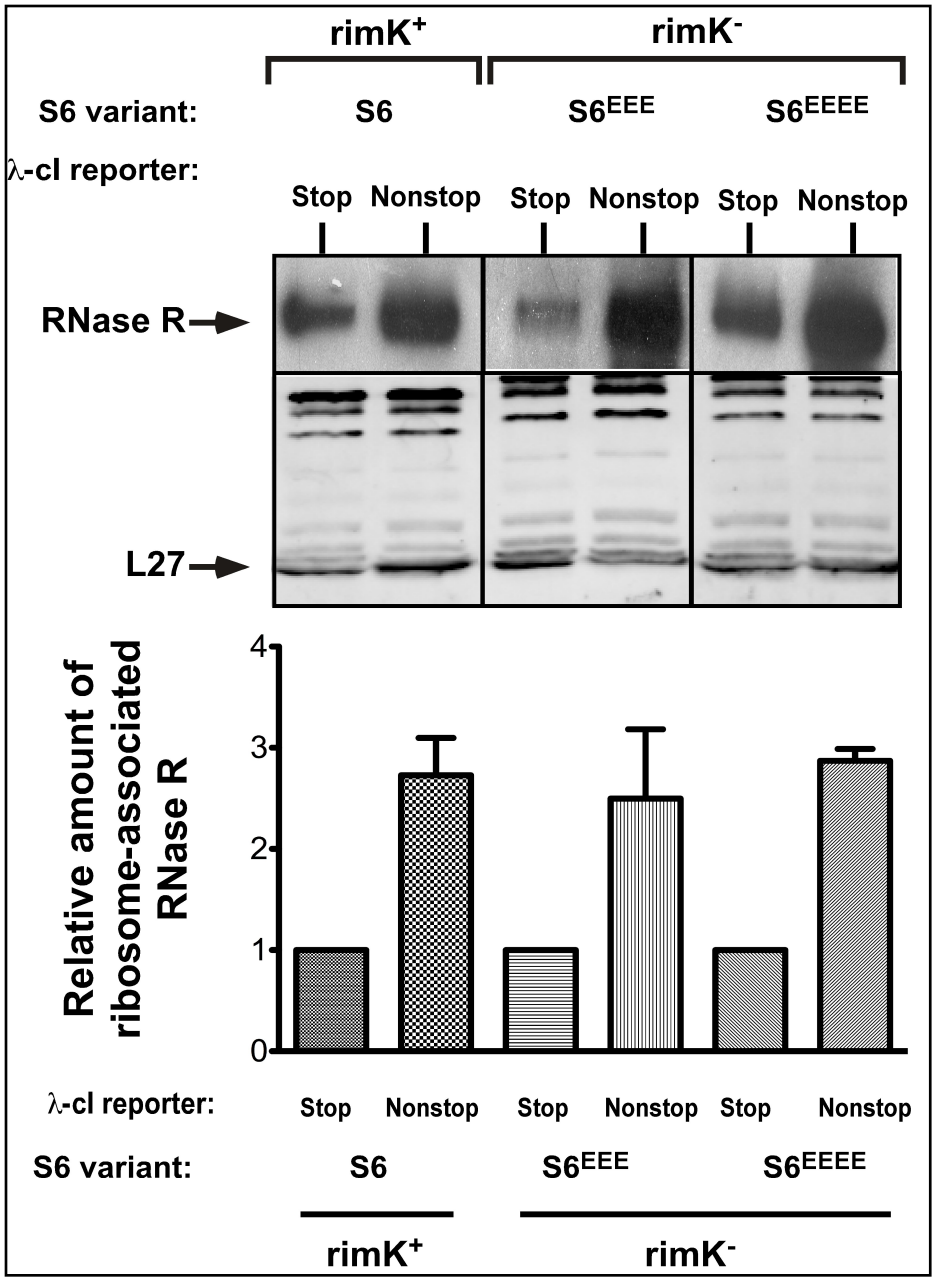

Figure 4.6B RNase R enrichment defect in *rimK* deletion background is restored upon hardcoding C-terminal glutamate residues in S6. Total ribosomes were obtained from cells of indicated strains co-expressing RNase R with the λ-cI-S or λ-cI-NS reporter mRNAs. Ribosomes translating the reporter RNAs were isolated from the total ribosomal pool using Ni^{2+}-NTA affinity chromatography. Equal numbers of ribosomes were resolved by electrophoresis on 10% SDS-polyacrylamide gels. Western blot analysis was performed to detect the presence of RNase R and ribosomal protein L27. The intensity of the band corresponding to RNase R was quantified using ImageJ. The top panel shows a representative Western blot, using an RNase R specific antibody, and the bottom panel shows a representative Western blot, using an anti-L27 serum displaying equal protein loading. The graph represents fold RNase R enrichment on ribosomes translating the λ-cI-NS reporter compared to ribosomes translating the control λ-cI-S reporter. The data are average of two independent experiments.

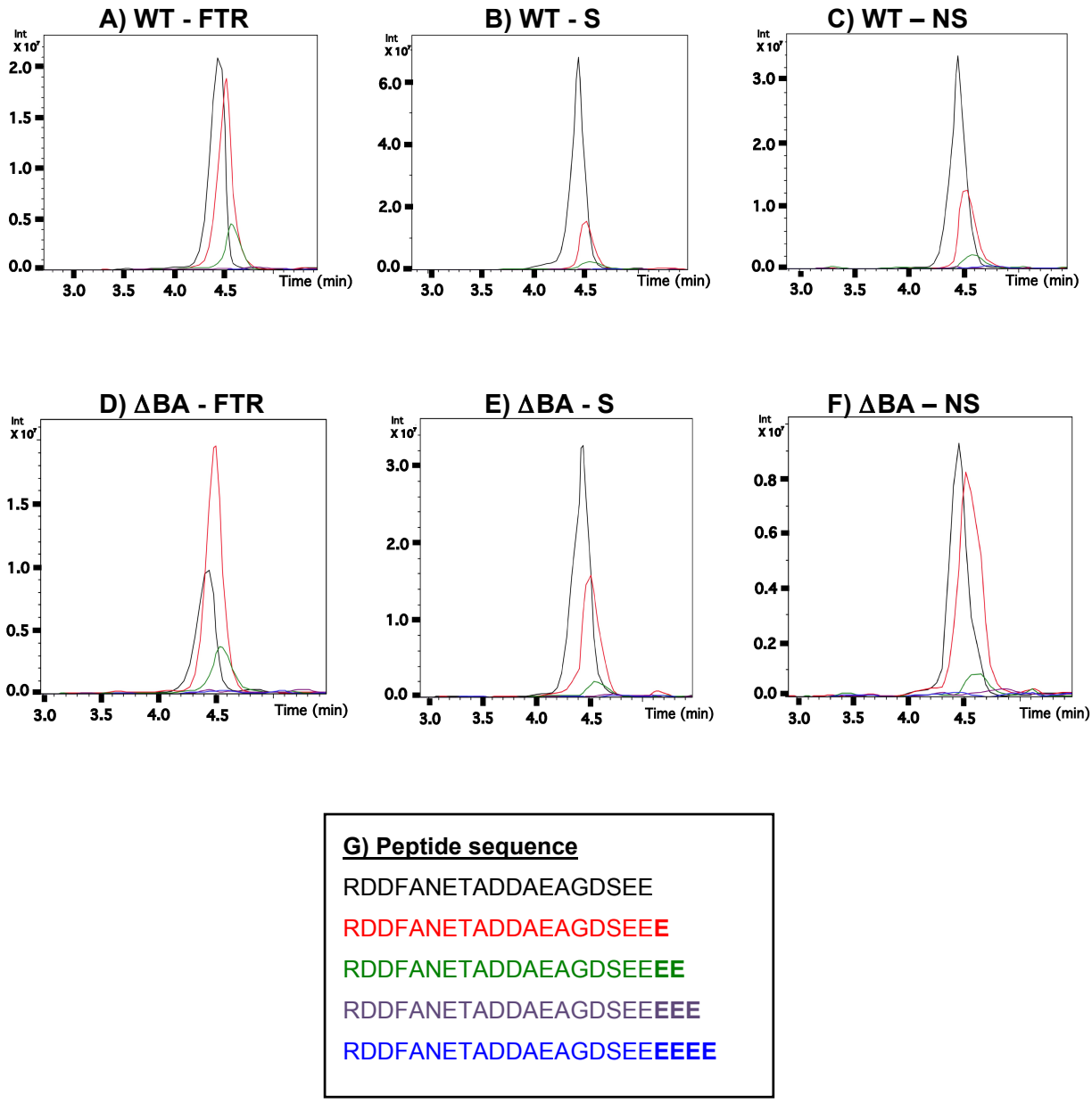

Figure 4.7 RimK-mediated modification of S6 C-terminus does not require the presence of SmpB-tmRNA. Mass spectrometric analysis of the S6 C-terminal P1 peptide forms (G) showed the presence of unmodified P1 (black), and modified P1 with one (red), two (green), three (purple), and four (blue) additional glutamate residues. Panels A, B and C show the profile of unmodified and various modified P1 forms in total (FTR), enriched ribosomes translating stop (S) and nonstop reporters (NS) respectively from wild type (WT) background. Panels D, E and F show the profile of unmodified and various modified P1 forms in total, enriched ribosomes translating stop and nonstop reporters respectively from *smpBssrA* (ΔBA) *deletion* background. The predominant modified form of P1 peptide that was observed was with one additional glutamate residue (red).

4.5 Discussion

RNase R is a highly conserved 3' to 5' exoribonuclease that is recruited by the SmpB-tmRNA complex to degrade nonstop mRNAs on stalled ribosomes. The unique lysine-rich domain of RNase R plays an essential role to productively engage with the rescued-ribosomes. Furthermore, RNase R initiates nonstop mRNA decay after ribosome switches templates to decode the tmRNA open reading frame. However, the docking site of RNase R on the ribosome, particularly the ribosomal partners required for this exclusive function have remained elusive. In this study, we provide compelling evidence to demonstrate that the RimK-dependent C-terminal tail modification of ribosomal protein S6 is crucial for RNase R-mediated nonstop mRNA degradation. We also show that RimO-catalyzed S12 modification of Asp88 residue is not required for elimination of nonstop mRNA by RNase R. From the results presented herein we conclude that RNase R binds near the mRNA exit channel on the 30S subunit, where it is positioned optimally to capture the emerging defective mRNA for selective degradation. This tightly regulated process not only requires active *trans*-translation process, but also the presence of modified form of S6 C-terminus.

The *trans*-translation system is conserved throughout the bacterial kingdom. One of the attributes of this process is the targeted elimination of nonstop mRNA by RNase R. RNase R orthologs are found in other domains of life [102]. Its importance is highlighted by the fact that it is retained even in bacteria such as *Mycoplasma* [103], with the smallest known genome. However, we noticed that the K-rich C-terminal domain of RNase R is not conserved to the same extent. This prompted us to investigate the evolutionary correlation between the retention of RNase R K-rich region and the occurrence of RimK using NCBI genome database (Figure 4.8)

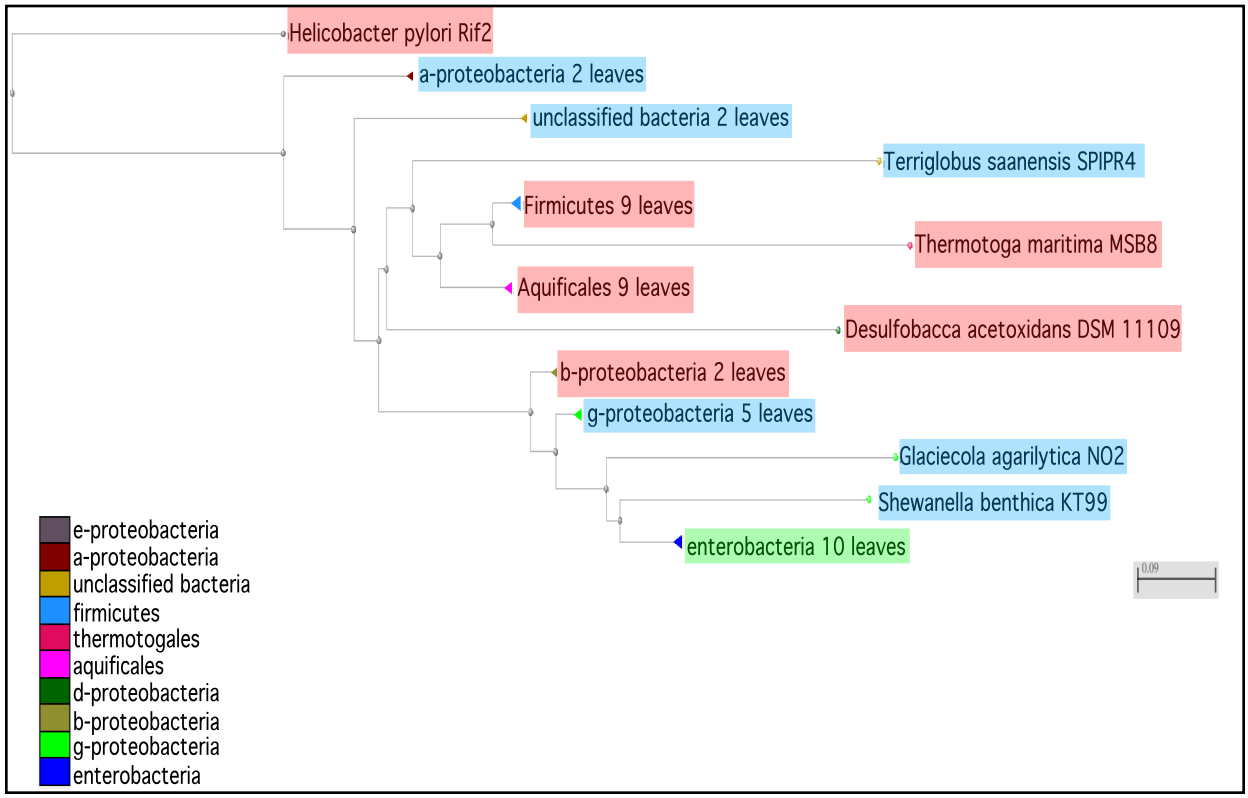

Figure 4.8 Phylogenetic analysis of co-occurrence of RNase R K-rich domain and *rimK* in bacteria. Branches highlighted in pink are phyla/genera that do not have annotated *rimK* in their genome. Although these bacteria have RNase R conserved, they do not have the K-rich domain. Branches highlighted in blue are phyla/genera that have annotated *rimK* and RNase R with K-rich domain in their genome. Enterobacteria (green) have a mix of bacteria that have both *rimK*/RNase R with K-rich and bacteria that lack *rimK* gene and K-rich domain of RNase R. The number of leaves represent the number of genera in the corresponding phyla. This figure is adapted from distance tree figure of various organisms produced by NCBI.

In a group of 20 bacteria that had varying lengths of the K-rich domain, we found that *rimK* gene was well conserved. This group included bacteria classified under phyla gamma-, alpha-, and entero- proteobacteria. Whereas, in another group of 20 bacteria that lacked RNase R K-rich domain, we did not find any annotated *rimK* gene. This group included bacteria from phyla firmicutes, aquificae, thermotogae, delta-, and beta-proteobacteria. In addition, we also found that in most cases in the latter group, the penultimate residue in the C-terminus of S6 was not glutamic acid, which suggests that RimK-like enzyme might be unable to catalyze the post-translational modification of the C-terminus. Although this is not an exhaustive search, this analysis supports our biochemical evidence that establish the functional relationship between post-

translational modification of S6 and *trans*-translation related activity of RNase R. The organisms that lack both RNase R K-rich domain and RimK might have evolved a RimK-independent approach to engage RNase R in the degradation of defective mRNA.

Interlinking of translational quality control and elimination of aberrant mRNA is a conserved mode of gene regulation in both prokaryotes and eukaryotes. However, there are key differences in the execution of this process. In eukaryotic nonstop mRNA decay pathway, the exosome complex binds near the A-site primed by the action of Ski7p, and the SKI protein complex [4]. Upon loading of the exosome, the 80S ribosomal assembly is dismantled, and the nonstop mRNA is degraded by the exosome complex in 3′ - 5′ direction. In prokaryotes, this scenario is unlikely because, intact 70S ribosomal complex is required to decode the tmRNA open reading frame. Our results have shown that RNase R is engaged on the ribosome to degrade nonstop mRNA upon successful establishment of the tmRNA ORF. In light of this, RNase R might not be positioned favorably to access the 3′ end of the message if it is bound near the A-site. Since ribosomal protein S12 is present near the decoding center, it is improbable that RNase R interacts with modified S12 to carry out *trans*-translation dependent nonstop mRNA decay. Consistent with this reasoning, we observed no defect in the enrichment of RNase R on stalled ribosomes in *rimO* deletion strain. Previous studies report that the association of RNase R on the ribosome is mediated by S12 [89]. Perhaps this interaction is required for RNase R to carry out other activities such as rRNA maturation or processing.

In this study, we have provided compelling evidence to demonstrate that RNase R binds near the mRNA exit channel to capture the defective mRNA. A preliminary phylogenetic profiling for potential interacting partners of RNase R (*rnr*) was conducted using the String database (string-db.org). This database is a repository of known and predicted protein interactions. Our analysis revealed a strong link between *rpsF* and *rnr* with a gene-neighborhood correlation confidence score of 0.766 (Figure 4.9), further supporting our results that established the requirement of S6 C-terminal tail modification for productive engagement of RNase R on the stalled ribosomes.

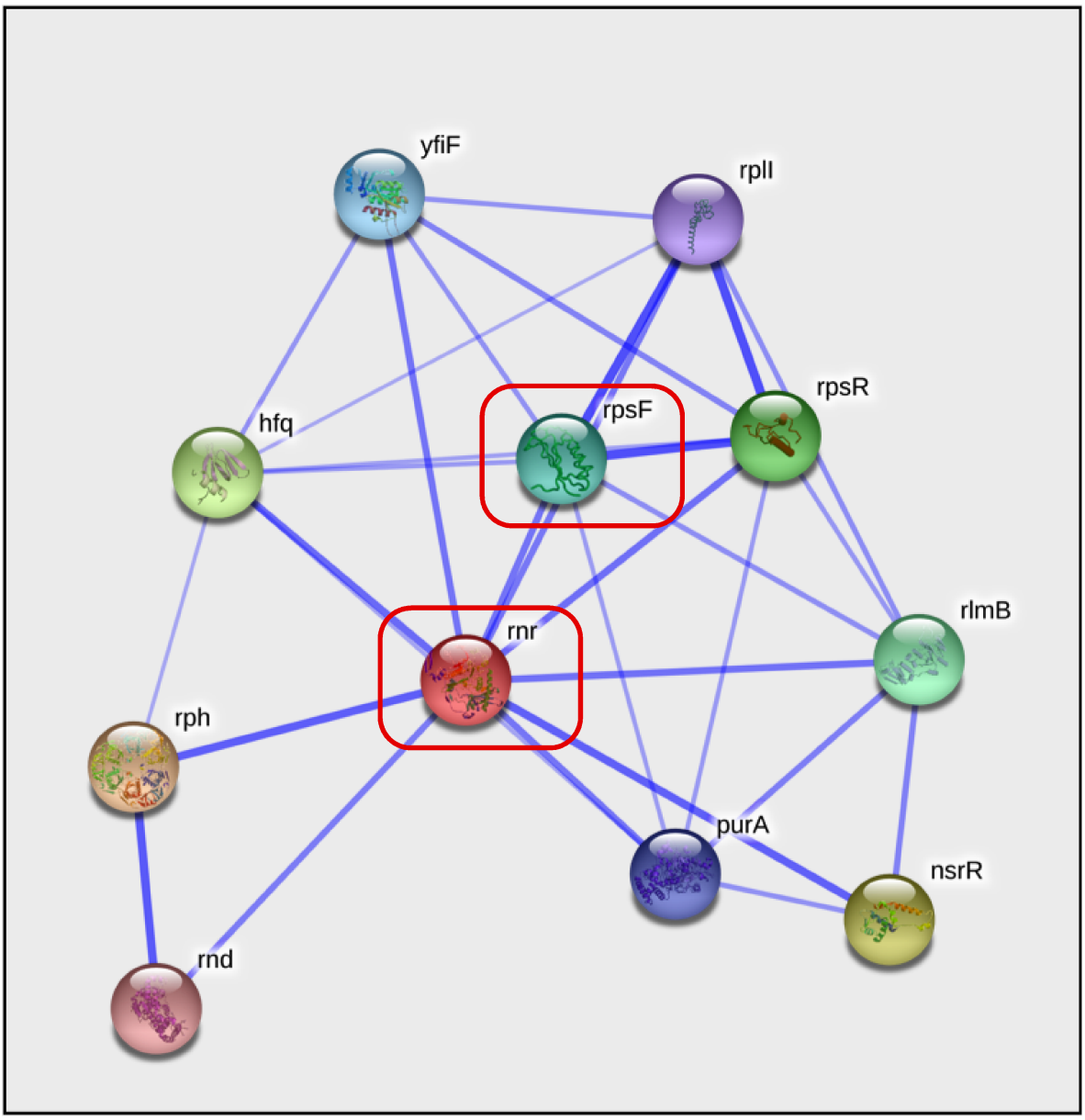

Figure 4.9 Evolutionary correlations between RNase R and ribosomal protein S6 (*rpsF*). This picture shows strong evolutionary link between *rnr* and *rpsF*. The String database search indicates the presence of genes in the neighborhood of *rnr* across several bacterial species. A confidence score of 0.766 between *rnr* and *rpsF* (red boxes) indicates high likelihood of interaction between the two genes. This picture is obtained from http://string-db.org.

The results presented herein provide the first glimpse into how a ribosomal protein and its posttranslational modification are involved in a co-translational process,

particularly in a translational quality control mechanism. Nonstop mRNA degradation on stalled ribosomes is an intricately executed event. Productive engagement of RNase R on tmRNA-rescued ribosomes occurs only when extra glutamate residues are added to the C-terminus of S6. Absence of either posttranslational modification of S6 or a fully operational SmpB-tmRNA complex does not activate RNase R on stalled ribosomes. It is interesting to note that the modification state of S6 specifically affects the nonstop mRNA degradation aspect of *trans*-translation. We also show that in order for RimK to modify S6, SmpB and tmRNA are not required. Taken together, these studies undertaken shed new light on the biological role of posttranslational modification of ribosomal protein S6 that has so far remained undefined. This exemplifies the versatility of ribosomes that serve as a platform for a variety of co-translational activities.

Chapter 5: Concluding Remarks

5.1 Summary

The overarching goal of this thesis project was to understand the mechanistic details of how defective mRNA is selectively targeted for degradation due to SmpB-tmRNA action on stalled ribosomes. I addressed this question by dividing it into three segments –

1) RNase R is the only exoribonuclease recruited by SmpB-tmRNA. What are the crucial elements within RNase R that are necessary for its response to *trans*-translation?
2) RNase R requires the presence of SmpB-tmRNA to degrade nonstop mRNA. How does SmpB-tmRNA complex effectuate nonstop mRNA decay?
3) Ribosome serves as the platform for the *trans*-translation and its associated events, particularly the targeted elimination of nonstop mRNA. What are the specific ribosomal partners of RNase R necessary to elicit nonstop mRNA decay?

In Chapter 2, I have described in detail the contributions of RNase R K-rich domain to nonstop mRNA decay. Specifically, I have identified critical residues Glu740/Lys741 and Lys749/Lys750. I have shown that mutation of these residues specifically affects *trans*-translation dependent nonstop mRNA decay *in vivo* by weakening the recruitment of RNase R variants to stalled ribosomes. Interestingly, mutation of E740/K741 and K749/K750 in the K-rich domain does not affect the catalytic activity of RNase R suggesting that these residues are involved in either intermolecular or intramolecular interactions. I attempted to obtain the crystal structure of full length *E. coli* RNase R to understand the relative positioning of K-rich domain of RNase R with

reference to the catalytic domain, but was not successful. Around the same time, a report published by the Deutscher group suggested that RNase R K-rich domain is involved in intramolecular interaction depending on the acetylation state of K544 residue. We reasoned that the disordered nature of K-rich domain in RNase R coupled with the acetylation form of K544 might contributed to heterogeneity in RNase R protein sample, which in turn might have affected ordered packing for crystal formation. Thus, we sought to obtain low-resolution SAXS-based homology model of full length *E. coli* RNase R. We found that RNase R has a trilobed structure, wherein the catalytic domain is flanked by N-terminal helix-turn-helix domain and C-terminal K-rich domain. Consistent with bioinformatics predictions, our SAXS and homology modeling data show that without binding partners K-rich domain is disordered in solution. This work provides the first glimpse of the three-dimensional orientation of various domains of RNase R.

Chapter 3 explores the roles of distinct elements in tmRNA open reading frame and SmpB C-terminal tail in nonstop mRNA decay process. Since RNase R-mediated nonstop mRNA degradation occurs only in the presence of SmpB-tmRNA-rescued ribosomes, it is conceivable that there are distinct elements present in SmpB and tmRNA that facilitate this function of RNase R. I found that RNase R degrades the defective mRNA only after tmRNA open reading frame is established as the surrogate template that enables resumption of translation by stalled ribosome. SmpB C-terminal tail is essential for enabling proper accommodation and accurate decoding of tmRNA ORF. Mere binding of SmpB-tmRNA complex to the stalled ribosomes does not result in productively engagement of RNase R. Furthermore, I have identified that the ultimate and penultimate codons of tmRNA ORF are required for facilitating nonstop mRNA decay. Based on our results and the cryo-EM structure of tmRNA-SmpB rescued ribosomes published by the Spahn group, we hypothesized that the distal portion of the tmRNA ORF makes putative contacts with the mRNA entry channel components, which results in large swivel-movement in the 30S head. In addition, RNase R might potentially bind near the mRNA exit channel. This positioning allows a spatio-temporally controlled access for RNase R to capture the aberrant mRNA for degradation.

Lastly, I sought to identify where RNase R docks on the ribosome to perform its *trans*-translation related function. It has long been known that RNase R binds to the ribosomes, and enriches in response to *trans*-translation. This gave us a clue that there is a preferred binding partner(s) of RNase R on the ribosome that allows this selective enrichment. This forms the basis of the work described in Chapters 4 and 5. From RNA CLIP and sequencing results, we noted a unique peak that mapped to the 16S rRNA region between 657 and 682 that was reproducibly found all the samples sequenced (total and enriched ribosomes translating nonstop mRNA reporter). Even though we found other peaks in the 23S rRNA, some of them were not reproducibly found apart from the intensity of the peaks being lower than the corresponding peak in the 16S rRNA. In addition, we had hypothesized that RNase R binds near mRNA exit channel. Based upon these assumptions, we set out to validate the CLIP results biochemically, by exploring the effect of the ribosomal protein S6 that is present in the vicinity of 16S rRNA region 657-682.

The biochemical evidence established that the modification of S6 C-terminus by RimK is crucial for RNase R to enrich and degrade nonstop mRNA in response to *trans*-translation. Furthermore, I have shown that hardcoding of four glutamate residues in the C-terminus of S6 in the absence of RimK is enough to restore the RNase R enrichment defects observed in *rimK* deletion strain. This suggested that the modification state of S6 C-terminus modulates RNase R activity on stalled ribosomes. This is the first demonstration of biological significance of ribosomal protein modification. S6 C-terminal tail modification by RimK plays an important role in the co-translational quality control mechanism. This underscores the capabilities of ribosomes to play a major role in processes other than protein synthesis in the cell.

Taken together, my thesis work sheds new light on the mechanism of *trans*-translation–mediated nonstop mRNA decay by RNase R. I propose that productive engagement of RNase R requires activation of two control switches – 1) tmRNA open reading frame must be accurately established, and stalled ribosomes must resume translation of the tmRNA ORF 2) ribosomal protein S6 C-terminus must be modified by

RimK in order for RNase R to enrich on stalled ribosomes. Absence of either of these features disrupts RNase R engagement on stalled ribosomes and subsequent degradation of nonstop mRNA. This two-step control of RNase R activity might have evolved to keep this robust exoribonuclease in check, thereby preventing indiscriminate degradation of messenger RNAs on the ribosomes (Figure 5.1).

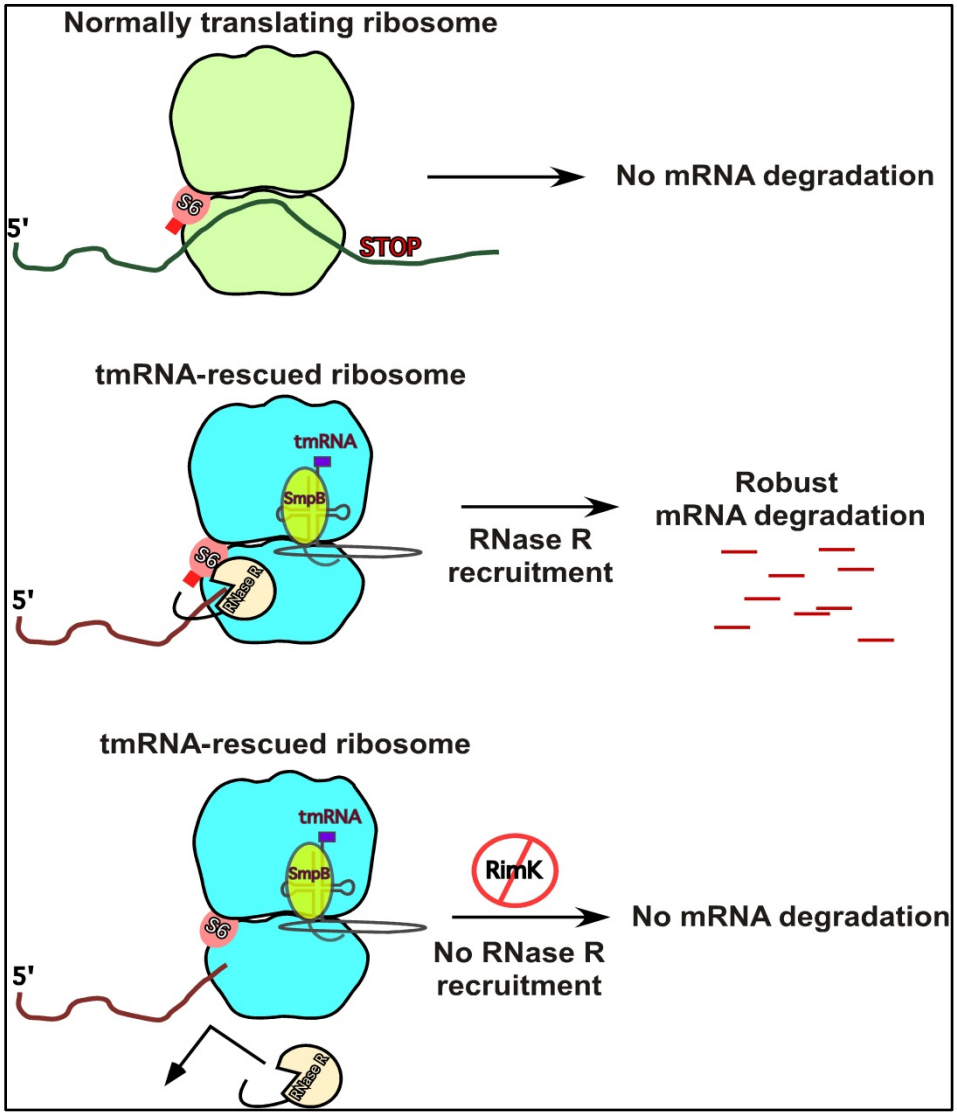

Figure 5.1 A model for RNase R-mediated nonstop mRNA decay. A normally translating ribosome (pale green) does not undergo tmRNA-mediated rescue. As a result, the mRNA is not subjected to RNase R-mediated degradation. However, when tmRNA rescues ribosomes stalled (cyan) on a defective mRNA (maroon), RNase R is specifically recruited to the ribosome to degrade the nonstop message. In the absence of RimK, S6 (salmon) does not undergo posttranslational modification (red stub). This prevents RNase R from enriching on tmRNA-rescued ribosomes due to which nonstop mRNA is stabilized.

5.2 Future directions

There are several leads based on this thesis work, some of which I have described below.

It is important to identify and characterize the precise interacting partners of E740/K741, and K749/K750, which have a significant impact on RNase R ability to degrade nonstop mRNA. It is possible that the K-rich domain of RNase R interacts with modified C-terminal tail of S6 in the context of ribosomes. Another possibility is that these residues interact with the ribosomal RNA on the 30S subunit. Conversely, crucial residues in the S6 C-terminus, other than the extra glutamate residues added by RimK should be identified to fully understand the interaction between S6 and RNase R. *In vitro* binding assays of RNase R and S6 variants might yield some answers. This study can also be done in combination with S18 and the 16S rRNA motif that was identified as the potential docking site of RNase R.

Crystallization *E. coli* full length RNase R has not been successful so far. We reasoned that the disordered nature of K-rich domain might have hindered the crystallization process. As I have identified that ribosomal protein S6 as a potential binding partner, it might be worthwhile to co-crystallize RNase R and S6 or RNase R and S6:S18 complex with the 16S rRNA motif. RNase R K-rich domain, in the presence of the binding partner, might adopt a more ordered form, which might facilitate the crystallization process. Also, from the evolutionary analysis, we have found that in certain bacteria (e.g. firmicutes, aquificales) RNase R does not have K-rich domain. Crystallization of RNase R from these organisms is likely to succeed.

Results from the mass spectrometric analysis of S6 C-terminus from Δ*smpBssrA* strain have clearly shown that RimK-mediated modification of S6 does not require the presence of SmpB and tmRNA. However, it is not clear at what stage RimK modifies S6 C-terminus. It will also be interesting to check if S6 C-terminal modification changes in response to growth phase and stress. Although S6 and S18 bind as a complex in the vicinity 16S rRNA region 657-682, I focused on characterizing the role of S6 C-terminal

modification on RNase R recruitment to stalled ribosomes. Ribosomal protein S18 and its N-terminal acetylation might play a role as well, and it is important to explore its contributions as well.

Finally, it would be interesting to test if the RimK-mediated modification of S6 C-terminus is reversible. Identification of peptidase that trims the extra glutamate residues added to S6 C-terminus by RimK might shed light on how the two antagonistic processes work in relation to *trans*-translation. Evolution of such a mechanism might function as a way to modulate RNase R ability to degrade defective mRNAs on the ribosomes.

Bibliography

1. Steitz, T.A., *A structural understanding of the dynamic ribosome machine.* Nat Rev Mol Cell Biol, 2008. **9**(3): p. 242-53.
2. Schmeing, T.M. and V. Ramakrishnan, *What recent ribosome structures have revealed about the mechanism of translation.* Nature, 2009. **461**(7268): p. 1234-42.
3. Zhang, G., M. Hubalewska, and Z. Ignatova, *Transient ribosomal attenuation coordinates protein synthesis and co-translational folding.* Nat Struct Mol Biol, 2009. **16**(3): p. 274-80.
4. Shoemaker, C.J. and R. Green, *Translation drives mRNA quality control.* Nat Struct Mol Biol, 2012. **19**(6): p. 594-601.
5. Ueda, K., et al., *Bacterial SsrA system plays a role in coping with unwanted translational readthrough caused by suppressor tRNAs.* Genes Cells, 2002. **7**(5): p. 509-19.
6. Keiler, K.C., *Biology of trans-translation.* Annu Rev Microbiol, 2008. **62**: p. 133-51.
7. Huang, C., et al., *Charged tmRNA but not tmRNA-mediated proteolysis is essential for Neisseria gonorrhoeae viability.* EMBO J, 2000. **19**(5): p. 1098-107.
8. Hutchison, C.A., et al., *Global transposon mutagenesis and a minimal Mycoplasma genome.* Science, 1999. **286**(5447): p. 2165-9.
9. Chadani, Y., et al., *Escherichia coli YaeJ protein mediates a novel ribosome-rescue pathway distinct from SsrA- and ArfA-mediated pathways.* Mol Microbiol, 2011. **80**(3): p. 772-85.
10. Chadani, Y., et al., *Ribosome rescue by Escherichia coli ArfA (YhdL) in the absence of trans-translation system.* Mol Microbiol, 2010. **78**(4): p. 796-808.
11. Camenares, D., et al., *Active and accurate trans-translation requires distinct determinants in the C-terminal tail of SmpB protein and the mRNA-like domain of transfer messenger RNA (tmRNA).* J Biol Chem, 2013. **288**(42): p. 30527-42.
12. Neubauer, C., et al., *Decoding in the absence of a codon by tmRNA and SmpB in the ribosome.* Science, 2012. **335**(6074): p. 1366-9.

13. Sundermeier, T.R., et al., *A previously uncharacterized role for small protein B (SmpB) in transfer messenger RNA-mediated trans-translation.* Proc Natl Acad Sci U S A, 2005. **102**(7): p. 2316-21.
14. Giudice, E. and R. Gillet, *The task force that rescues stalled ribosomes in bacteria.* Trends Biochem Sci, 2013. **38**(8): p. 403-11.
15. Hayes, C.S. and K.C. Keiler, *Beyond ribosome rescue: tmRNA and co-translational processes.* FEBS Lett, 2010. **584**(2): p. 413-9.
16. Keiler, K.C., P.R. Waller, and R.T. Sauer, *Role of a peptide tagging system in degradation of proteins synthesized from damaged messenger RNA.* Science, 1996. **271**(5251): p. 990-3.
17. Okan, N.A., J.B. Bliska, and A.W. Karzai, *A Role for the SmpB-SsrA system in Yersinia pseudotuberculosis pathogenesis.* PLoS Pathog, 2006. **2**(1): p. e6.
18. Okan, N.A., et al., *The smpB-ssrA mutant of Yersinia pestis functions as a live attenuated vaccine to protect mice against pulmonary plague infection.* Infect Immun, 2010. **78**(3): p. 1284-93.
19. Svetlanov, A., et al., *Francisella tularensis tmRNA system mutants are vulnerable to stress, avirulent in mice, and provide effective immune protection.* Mol Microbiol, 2012. **85**(1): p. 122-41.
20. Chadani, Y., et al., *ArfA recruits release factor 2 to rescue stalled ribosomes by peptidyl-tRNA hydrolysis in Escherichia coli.* Mol Microbiol, 2012. **86**(1): p. 37-50.
21. Garza-Sanchez, F., et al., *tmRNA regulates synthesis of the ArfA ribosome rescue factor.* Mol Microbiol, 2011. **80**(5): p. 1204-19.
22. Dulebohn, D., et al., *Trans-translation: the tmRNA-mediated surveillance mechanism for ribosome rescue, directed protein degradation, and nonstop mRNA decay.* Biochemistry, 2007. **46**(16): p. 4681-93.
23. Gagnon, M.G., et al., *Structural basis for the rescue of stalled ribosomes: structure of YaeJ bound to the ribosome.* Science, 2012. **335**(6074): p. 1370-2.
24. Repoila, F., N. Majdalani, and S. Gottesman, *Small non-coding RNAs, co-ordinators of adaptation processes in Escherichia coli: the RpoS paradigm.* Mol Microbiol, 2003. **48**(4): p. 855-61.

25. Deutscher, M.P., *Maturation and degradation of ribosomal RNA in bacteria.* Prog Mol Biol Transl Sci, 2009. **85**: p. 369-91.
26. Christensen, S.K., et al., *RelE, a global inhibitor of translation, is activated during nutritional stress.* Proc Natl Acad Sci U S A, 2001. **98**(25): p. 14328-33.
27. Carpousis, A.J., *The RNA degradosome of Escherichia coli: an mRNA-degrading machine assembled on RNase E.* Annu Rev Microbiol, 2007. **61**: p. 71-87.
28. Bandyra, K.J., et al., *The social fabric of the RNA degradosome.* Biochim Biophys Acta, 2013. **1829**(6-7): p. 514-22.
29. Bouvier, M. and A.J. Carpousis, *A tale of two mRNA degradation pathways mediated by RNase E.* Mol Microbiol, 2011. **82**(6): p. 1305-10.
30. Carabetta, V.J., et al., *The response regulator SprE (RssB) modulates polyadenylation and mRNA stability in Escherichia coli.* J Bacteriol, 2009. **191**(22): p. 6812-21.
31. Mohanty, B.K. and S.R. Kushner, *Polynucleotide phosphorylase functions both as a 3' right-arrow 5' exonuclease and a poly(A) polymerase in Escherichia coli.* Proc Natl Acad Sci U S A, 2000. **97**(22): p. 11966-71.
32. Deutscher, M.P., *Degradation of RNA in bacteria: comparison of mRNA and stable RNA.* Nucleic Acids Res, 2006. **34**(2): p. 659-66.
33. Storz, G., S. Altuvia, and K.M. Wassarman, *An abundance of RNA regulators.* Annu Rev Biochem, 2005. **74**: p. 199-217.
34. Waters, L.S. and G. Storz, *Regulatory RNAs in bacteria.* Cell, 2009. **136**(4): p. 615-28.
35. Saramago, M., et al., *The role of RNases in the regulation of small RNAs.* Curr Opin Microbiol, 2014. **18C**: p. 105-115.
36. Ge, Z., et al., *Non-stop mRNA decay initiates at the ribosome.* Molecular microbiology, 2010. **78**(5): p. 1159-70.
37. Richards, J., P. Mehta, and A.W. Karzai, *RNase R degrades non-stop mRNAs selectively in an SmpB-tmRNA-dependent manner.* Mol Microbiol, 2006. **62**(6): p. 1700-12.

38. Karzai, A.W., E.D. Roche, and R.T. Sauer, *The SsrA-SmpB system for protein tagging, directed degradation and ribosome rescue.* Nat Struct Biol, 2000. **7**(6): p. 449-55.
39. Withey, J.H. and D.I. Friedman, *A salvage pathway for protein structures: tmRNA and trans-translation.* Annu Rev Microbiol, 2003. **57**: p. 101-23.
40. Barends, S., B. Kraal, and G.P. van Wezel, *The tmRNA-tagging mechanism and the control of gene expression: a review.* Wiley Interdiscip Rev RNA, 2011. **2**(2): p. 233-46.
41. Wower, J., I.K. Wower, and C. Zwieb, *Making the jump: new insights into the mechanism of trans-translation.* J Biol, 2008. **7**(5): p. 17.
42. Karzai, A.W., M.M. Susskind, and R.T. Sauer, *SmpB, a unique RNA-binding protein essential for the peptide-tagging activity of SsrA (tmRNA).* EMBO J, 1999. **18**(13): p. 3793-9.
43. Zuo, Y. and M.P. Deutscher, *Exoribonuclease superfamilies: structural analysis and phylogenetic distribution.* Nucleic Acids Res, 2001. **29**(5): p. 1017-26.
44. Hong, S.J., Q.A. Tran, and K.C. Keiler, *Cell cycle-regulated degradation of tmRNA is controlled by RNase R and SmpB.* Mol Microbiol, 2005. **57**(2): p. 565-75.
45. Liang, W. and M.P. Deutscher, *Transfer-messenger RNA-SmpB protein regulates ribonuclease R turnover by promoting binding of HslUV and Lon proteases.* J Biol Chem, 2012. **287**(40): p. 33472-9.
46. Frazao, C., et al., *Unravelling the dynamics of RNA degradation by ribonuclease II and its RNA-bound complex.* Nature, 2006. **443**(7107): p. 110-4.
47. Zuo, Y., et al., *Structural basis for processivity and single-strand specificity of RNase II.* Mol Cell, 2006. **24**(1): p. 149-56.
48. Baba, T., et al., *Construction of Escherichia coli K-12 in-frame, single-gene knockout mutants: the Keio collection.* Mol Syst Biol, 2006. **2**: p. 2006 0008.
49. Konarev, P.V., et al., *PRIMUS: a Windows PC-based system for small-angle scattering data analysis.* Journal of Applied Crystallography, 2003. **36**(5): p. 1277-1282.

50. Guinier, A., *La diffraction des rayons X aux tres petits angles; application a l'etude de phenomenes ultramicroscopiques.* Annals of Physics, 1939. **12**: p. 161-237.
51. Semenyuk, A.V. and D.I. Svergun, *GNOM - a program package for small-angle scattering data processing.* Journal of Applied Crystallography, 1991. **24**(5): p. 537-540.
52. Putnam, C.D., et al., *X-ray solution scattering (SAXS) combined with crystallography and computation: defining accurate macromolecular structures, conformations and assemblies in solution.* Q Rev Biophys, 2007. **40**(3): p. 191-285.
53. Svergun, D.I., *Restoring low resolution structure of biological macromolecules from solution scattering using simulated annealing.* Biophys J, 1999. **76**(6): p. 2879-86.
54. Volkov, V.V. and D.I. Svergun, *Uniqueness of ab initio shape determination in small-angle scattering.* Journal of Applied Crystallography, 2003. **36**(3 Part 1): p. 860-864.
55. Liu, H., A. Hexemer, and P.H. Zwart, *The Small Angle Scattering ToolBox (SASTBX): an open-source software for biomolecular small-angle scattering.* Journal of Applied Crystallography, 2012. **45**(3): p. 587-593.
56. Petoukhov, M.V. and D.I. Svergun, *Global rigid body modeling of macromolecular complexes against small-angle scattering data.* Biophys J, 2005. **89**(2): p. 1237-50.
57. Mehta, P., et al., *Ribosome purification approaches for studying interactions of regulatory proteins and RNAs with the ribosome.* Methods Mol Biol, 2012. **905**: p. 273-89.
58. Zhang, Y., *I-TASSER server for protein 3D structure prediction.* BMC Bioinformatics, 2008. **9**: p. 40.
59. Matos, R.G., et al., *Swapping the domains of exoribonucleases RNase II and RNase R: conferring upon RNase II the ability to degrade ds RNA.* Proteins, 2011. **79**(6): p. 1853-67.

60. Sundermeier, T., et al., *Studying tmRNA-mediated surveillance and nonstop mRNA decay.* Methods Enzymol, 2008. **447**: p. 329-58.
61. Vincent, H.A. and M.P. Deutscher, *The roles of individual domains of RNase R in substrate binding and exoribonuclease activity. The nuclease domain is sufficient for digestion of structured RNA.* J Biol Chem, 2009. **284**(1): p. 486-94.
62. Cheng, Z.F. and M.P. Deutscher, *Purification and characterization of the Escherichia coli exoribonuclease RNase R. Comparison with RNase II.* J Biol Chem, 2002. **277**(24): p. 21624-9.
63. Cheng, Z.F. and M.P. Deutscher, *Quality control of ribosomal RNA mediated by polynucleotide phosphorylase and RNase R.* Proc Natl Acad Sci U S A, 2003. **100**(11): p. 6388-93.
64. Jacob, A.I., et al., *Conserved bacterial RNase YbeY plays key roles in 70S ribosome quality control and 16S rRNA maturation.* Mol Cell, 2013. **49**(3): p. 427-38.
65. Moore, S.D. and R.T. Sauer, *The tmRNA system for translational surveillance and ribosome rescue.* Annu Rev Biochem, 2007. **76**: p. 101-24.
66. Mann, B., et al., *Control of virulence by small RNAs in Streptococcus pneumoniae.* PLoS Pathog, 2012. **8**(7): p. e1002788.
67. Gottesman, S., et al., *The ClpXP and ClpAP proteases degrade proteins with carboxy-terminal peptide tails added by the SsrA-tagging system.* Genes Dev, 1998. **12**(9): p. 1338-47.
68. Choy, J.S., L.L. Aung, and A.W. Karzai, *Lon protease degrades transfer-messenger RNA-tagged proteins.* Journal of Bacteriology, 2007. **189**(18): p. 6564-71.
69. Ge, Z. and A.W. Karzai, *Co-evolution of multipartite interactions between an extended tmRNA tag and a robust Lon protease in Mycoplasma.* Mol Microbiol, 2009. **74**(5): p. 1083-99.
70. Herman, C., et al., *Degradation of carboxy-terminal-tagged cytoplasmic proteins by the Escherichia coli protease HflB (FtsH).* Genes Dev, 1998. **12**(9): p. 1348-55.

71. Ge, Z., et al., *Non-stop mRNA decay initiates at the ribosome.* Mol Microbiol, 2010. **78**(5): p. 1159-70.
72. Mehta, P., J. Richards, and A.W. Karzai, *tmRNA determinants required for facilitating nonstop mRNA decay.* RNA, 2006. **12**(12): p. 2187-98.
73. Ramrath, D.J., et al., *The complex of tmRNA-SmpB and EF-G on translocating ribosomes.* Nature, 2012. **485**(7399): p. 526-9.
74. Kurita, D., et al., *Interaction of SmpB with ribosome from directed hydroxyl radical probing.* Nucleic Acids Res, 2007. **35**(21): p. 7248-55.
75. Liang, W. and M.P. Deutscher, *A novel mechanism for ribonuclease regulation: transfer-messenger RNA (tmRNA) and its associated protein SmpB regulate the stability of RNase R.* J Biol Chem, 2010. **285**(38): p. 29054-8.
76. Cornish, P.V., et al., *Following movement of the L1 stalk between three functional states in single ribosomes.* Proc Natl Acad Sci U S A, 2009. **106**(8): p. 2571-6.
77. Qin, P., et al., *Structured mRNA induces the ribosome into a hyper-rotated state.* EMBO Rep, 2014. **15**(2): p. 185-90.
78. Zhou, J., et al., *Crystal structures of EF-G-ribosome complexes trapped in intermediate states of translocation.* Science, 2013. **340**(6140): p. 1236086.
79. Ratje, A.H., et al., *Head swivel on the ribosome facilitates translocation by means of intra-subunit tRNA hybrid sites.* Nature, 2010. **468**(7324): p. 713-6.
80. Koutmou, K.S., et al., *RF3:GTP promotes rapid dissociation of the class 1 termination factor.* RNA, 2014.
81. Lykke-Andersen, J. and E.J. Bennett, *Protecting the proteome: Eukaryotic cotranslational quality control pathways.* J Cell Biol, 2014. **204**(4): p. 467-76.
82. Isono, K. and S. Isono, *Ribosomal protein modification in Escherichia coli. II. Studies of a mutant lacking the N-terminal acetylation of protein S18.* Mol Gen Genet, 1980. **177**(4): p. 645-51.
83. Kang, W.K., et al., *Characterization of the gene rimK responsible for the addition of glutamic acid residues to the C-terminus of ribosomal protein S6 in Escherichia coli K12.* Mol Gen Genet, 1989. **217**(2-3): p. 281-8.

84. Tanaka, S., et al., *Cloning and molecular characterization of the gene rimL which encodes an enzyme acetylating ribosomal protein L12 of Escherichia coli K12.* Mol Gen Genet, 1989. **217**(2-3): p. 289-93.
85. Yoshikawa, A., et al., *Cloning and nucleotide sequencing of the genes rimI and rimJ which encode enzymes acetylating ribosomal proteins S18 and S5 of Escherichia coli K12.* Mol Gen Genet, 1987. **209**(3): p. 481-8.
86. Nesterchuk, M.V., P.V. Sergiev, and O.A. Dontsova, *Posttranslational Modifications of Ribosomal Proteins in Escherichia coli.* Acta Naturae, 2011. **3**(2): p. 22-33.
87. Arnold, R.J. and J.P. Reilly, *Observation of Escherichia coli ribosomal proteins and their posttranslational modifications by mass spectrometry.* Anal Biochem, 1999. **269**(1): p. 105-12.
88. Anton, B.P., et al., *RimO, a MiaB-like enzyme, methylthiolates the universally conserved Asp88 residue of ribosomal protein S12 in Escherichia coli.* Proc Natl Acad Sci U S A, 2008. **105**(6): p. 1826-31.
89. Liang, W. and M.P. Deutscher, *Ribosomes regulate the stability and action of the exoribonuclease RNase R.* J Biol Chem, 2013. **288**(48): p. 34791-8.
90. Agalarov, S.C., et al., *Structure of the S15,S6,S18-rRNA complex: assembly of the 30S ribosome central domain.* Science, 2000. **288**(5463): p. 107-13.
91. Isono, K. and M. Kitakawa, *A new ribosomal protein locus in Escherichia coli: the gene for protein S6 maps at 97 min.* Mol Gen Genet, 1977. **153**(2): p. 115-20.
92. Zhao, G., et al., *Structure and function of Escherichia coli RimK, an ATP-grasp fold, L-glutamyl ligase enzyme.* Proteins, 2013. **81**(10): p. 1847-54.
93. Kino, K., T. Arai, and Y. Arimura, *Poly-alpha-glutamic acid synthesis using a novel catalytic activity of RimK from Escherichia coli K-12.* Appl Environ Microbiol, 2011. **77**(6): p. 2019-25.
94. Datsenko, K.A. and B.L. Wanner, *One-step inactivation of chromosomal genes in Escherichia coli K-12 using PCR products.* Proc Natl Acad Sci U S A, 2000. **97**(12): p. 6640-5.
95. Chi, S.W., et al., *Argonaute HITS-CLIP decodes microRNA-mRNA interaction maps.* Nature, 2009. **460**(7254): p. 479-86.

96. Licatalosi, D.D., et al., *HITS-CLIP yields genome-wide insights into brain alternative RNA processing.* Nature, 2008. **456**(7221): p. 464-9.
97. Langmead, B., et al., *Ultrafast and memory-efficient alignment of short DNA sequences to the human genome.* Genome Biol, 2009. **10**(3): p. R25.
98. Li, H., et al., *The Sequence Alignment/Map format and SAMtools.* Bioinformatics, 2009. **25**(16): p. 2078-9.
99. Quinlan, A.R. and I.M. Hall, *BEDTools: a flexible suite of utilities for comparing genomic features.* Bioinformatics, 2010. **26**(6): p. 841-2.
100. Thorvaldsdottir, H., J.T. Robinson, and J.P. Mesirov, *Integrative Genomics Viewer (IGV): high-performance genomics data visualization and exploration.* Brief Bioinform, 2013. **14**(2): p. 178-92.
101. Leonhard-Melief, C. and R.S. Haltiwanger, *O-fucosylation of thrombospondin type 1 repeats.* Methods Enzymol, 2010. **480**: p. 401-16.
102. Matos, R.G., A. Barbas, and C.M. Arraiano, *RNase R mutants elucidate the catalysis of structured RNA: RNA-binding domains select the RNAs targeted for degradation.* Biochem J, 2009. **423**(2): p. 291-301.
103. Lalonde, M.S., et al., *Exoribonuclease R in Mycoplasma genitalium can carry out both RNA processing and degradative functions and is sensitive to RNA ribose methylation.* RNA, 2007. **13**(11): p. 1957-68.